# MOLECULAR MECHANISMS OF MUTAGENESIS AND LUNG TUMORIGENESIS CAUSED BY RIBONUCLEOTIDE REDUCTASE DEREGULATION

A Dissertation

Presented to the Faculty of the Graduate School

of Cornell University

In Partial Fulfillment of the Requirements for the Degree of

Doctor of Philosophy

by

Xia Xu

August 2009

# MOLECULAR MECHANISMS OF MUTAGENESIS AND LUNG TUMORIGENESIS CAUSED BY RIBONUCLEOTIDE REDUCTASE DEREGULATION

Xia Xu, Ph. D.

Cornell University 2009

Ribonucleotide reductase catalyzes the rate-liming step in deoxyribonucleotide triphosphate biosynthesis and is a major determinant of genomic integrity. Unbalanced dNTP pools can cause genetic abnormality and cell death. Although a number of elaborate regulatory mechanisms govern RNR activity, the physiological impact of RNR deregulation had not previously been examined in an animal model. The aim of this dissertation is to elucidate the physiological effect of RNR deregulation using transgenic mouse models and to further dissect the molecular mechanisms of RNR-induced mutagenesis and lung tumorigenesis.

We generated transgenic mice that broadly overexpress individual RNR genes, and found that overexpression of the small RNR subunit potently and selectively induces lung neoplasms. RNR deregulation was found to promote lung carcinogenesis through a mutagenic mechanism, as evidenced by increased mutation rates in RNR overexpressing 3T3 cells and enhanced mutagenesis and carcinogenesis when combining RNR deregulation with defects in DNA mismatch repair. Moreover, the proto-oncogene K-ras was identified as a frequent mutational target in RNR-induced lung neoplasms. Importantly, RNR-induced lung neoplasms histopathologically resemble human papillary adenocarcinoma, making RNR transgenic mice a

particularly authentic model for lung cancer.

We initially hypothesized that RNR-induced mutagenesis and carcinogenesis was due to disturbed dNTP pools. However, we observed no alteration of dNTP levels or ratios in RNR overexpressing cells, suggesting that RNR-induced mutagenesis might be independent of RNR enzyme activity. Moreover, RNR overexpression was not associated with acute transforming activity. Alternatively, excess free radical production by the small RNR subunit may account for lung specific carcinogenesis in RNR transgenic mice. To further assess the requirements for free radical production and RNR enzyme activity in RNR-induced mutagenesis, we generated Rrm2 mutants and found that Rrm2 overexpressing cells exhibited significantly higher intracellular reactive oxygen species levels and Rrm2 mutants that are defective for RNR enzyme activity still promote mutagenesis in cultured 3T3 cells and exhibited elevated reactive oxygen species levels. Our data suggest that increased ROS production, rather than increased RNR enzyme activity, is the major driving force of RNR-induced mutagenesis, and potentially lung tumorigenesis.

These studies establish a new oncogenic activity for the small subunit of RNR. RNR-induced lung tumors arose with moderate latency in a stochastic process associated with an elevated mutation rate and increased ROS production. This novel mouse lung cancer model holds great promise for providing insights into basic mechanisms in human lung cancer and developing effective strategy for prevention and therapy of lung cancer.

## BIOGRAPHICAL SKETCH

Xia Xu was born on November 2, 1975 in Inner Mongolia, China. In 1992, she graduated from Huade Middle School and entered Baotou Medical College to study Preventive Medicine. Five years later, Xia received her Medical degree in Preventive Medicine in 1997. Then she started her master degree study in the field of Health Toxicology in Chinese Academy of Preventive Medicine, Beijing, in 1999. Under the guidance of Dr. Jing Lu, Xia worked on a project related to the association of VDR and HFE gene polymorphisms with genetic susceptibility to lead toxicity in Uighur and Yi population in China. Upon completion of her Master degree in 2002, Xia came to USA to accompany her husband, Weipeng Mu. In 2004, she started her Ph.D. study in the field of Environmental Toxicology under the mentorship of Dr. Robert Weiss. She is studying the molecular mechanisms of mutagenesis and lung tumorigenesis caused by ribonucleotide reductase deregulation.

ACKNOWLEDGMENTS

I would like to acknowledge many people for helping me during my Ph.D. work. First and foremost, I would like to express my gratitude to my advisor Dr. Robert Weiss for his excellent guidance and constant encouragement throughout my Ph.D. work. He encourages me to develop independently analytical thinking, research skills and scientific writing. He trains me as an independent researcher and makes me well prepared for future career.

I am very grateful for having an exceptional committee and would like to thank Dr. Alex Nikitin, Dr. Paul Soloway, and Dr. Paula Cohen for their generous help, research expertise, and creative advise for my project. I am also grateful to Dr. Eric Alani and Dr. Jennifer Surtees for their work on the mutagenic effect of RNR deregulation in yeast.

I would like to express my gratitude to graduate students Jennifer Page and Minxing Li and undergraduate students working with me, Sarah Lagedrost and Young Lu, and former lab members Houchun Liu, Chen-Hua Zhuang, Chang-il Hwang and Joshua Levy for their help with my project. I also want to thank my lab members Stephanie Yazinski, Gabriel Balmus, and Dr. Kelly Hume for their help, suggestion and friendship.

Finally, I am very grateful to my family. I would like to thank my parents and my brother for their persistent support and encouragement. Most importantly, I am especially grateful to my husband for his companionship, full support and love.

TABLE OF CONTENTS

LIST OF FIGURES

LIST OF TABLES

CHAPTER 1

# Literature Review

## 1.1 Deoxyribonucleotide triphosphates and genome integrity

A balanced supply of deoxyribonucleotide triphosphates (dNTPs), the basic building block of DNA, is fundamental for ensuring DNA replication fidelity and efficient DNA damage repair. Imbalanced dNTP pools can cause genetic defects. Therefore, the control of dNTP concentrations is essential for the maintenance of genetic stability, and disruption of this control can cause the accumulation of mutations in oncogenes or tumor suppressor genes, resulting in tumorigenesis.

### 1.1.1 dNTP biosynthesis pathways

dNTPs are synthesized by two biosynthetic pathways, the *de novo* and the salvage pathway. In the *de novo* pathway, dNTPs are produced in multiple steps from the principle products of purine and pyrimidine, inosinic acid (IMP) and uridine monophosphate (UMP), respectively (Fig 1.1) (Kunz, 1988; Kunz et al., 1994). Except for dTTP, dNTPs are derived from the reduction of corresponding ribonucleoside diphosphates (NDPs) to deoxyribonucleoside diphosphates (dNDPs) by ribonucleotide reductase (RNR). The dNDPs are then phosphorylated to the triphosphates by nucleoside diphosphate kinase. dTTP is produced from dUMP, which is generated either from hydrolysis of dUTP by dUTPase or from deamination of dCMP by the dCMP deaminase. Then dUMP is methylated by dTMP synthase to produce dTMP, with $N^5$, $N^{10}$-methylene tetrahydrofolate (MTHF) serving as a methyl donor. Finally, dTMP kinase phosphorylates dTMP to dTDP, which is in turn phosphorylated to dTTP by nucleoside diphosphate kinase. In the salvage pathway, dNTPs are generated

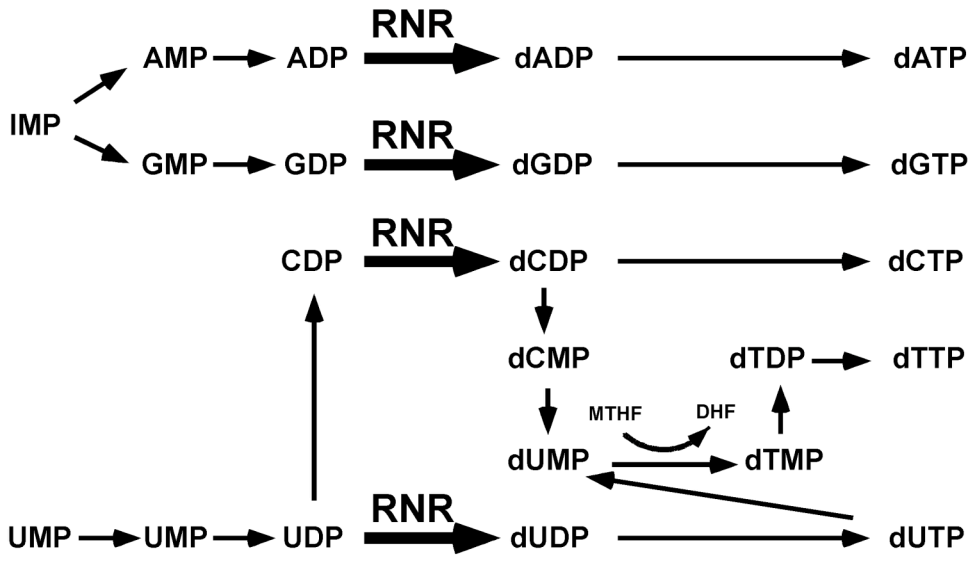


Figure 1.1 The *de novo* dNTP biosynthesis pathway.

in single steps from deoxyribonucleosides by deoxyribonucleoside kinases(Reichard, 1988). Mammalian cells have two sets of deoxyribonucleoside kinases: one is present in the cytosol, and the other in mitochondria. The cytoplasmic and mitochondrial isozymes of thymidine kinase (TK) are called TK1 and TK2, respectively, which play import roles in dTTP salvage biosynthesis. Deoxycytidine kinase (dCK), in addition to phosphorylating deoxycytidine, also plays a dominant role in salvage synthesis of dAMP and dGMP. Adenosine and guanoside kinase (dAK and dGK), also phosphorylate the resepective deoxyribonucleosides, but relatively inefficiently (Kunz et al., 1994).

### 1.1.2 Imbalanced dNTP pools and genomic instability

Biosynthesis of dNTPs is precisely regulated with respect to concentration and timing (Kunz et al., 1994). Cell cycle dependent control of dNTP pools results in periodic but coordinated changes in dNTP pool size during the cell cycle. In S phase dNTP levels are elevated to coinciding with DNA replication. In contrast, dNTP concentration is maintained at low levels for DNA repair and mitochondrial DNA replication in G1/G0, and G2/M phases. In addition to cell cycle control, the control of dNTP pool sizes is also linked to DNA damage responses (Mathews, 2006).

Loss of normal control of dNTP biosynthesis results in imbalances in dNTP pools and leads to aberrant DNA replication, enhanced mutagenesis, stimulated recombination, enhanced sensitivity to DNA damage reagents, oncogenic transformation and cell death(Kunz and Kohalmi, 1991; Mathews, 2006). Deficiency in all four dNTP pools or deprivation of any of dNTPs, such as dTTP deprivation, lead to incomplete DNA replication and defect in DNA repair, and cause mutagenesis and cell death (Reichard, 1988). Elevated dNTP pools, including unbalanced dNTP pool expansion with accumulation or depletion of one nucleotide and balanced expansion

of all four dNTP pools proportionally, are mutagenic (Kunz et al., 1994; Wheeler et al., 2005).

The mechanisms of mutagenesis caused by imbalanced dNTP pools have been extensively explored. Excess or deficient dNTPs results in non-Watson-Crick base pair and mis-insertion during DNA replication. In the presence of elevated nucleotide pools, the rate of base mis-insertion is increased during DNA replication and the efficiency of proof-reading is decreased due to the enhanced polymerization rate, termed "next-nucleotide effect". Both dNTP mis-insertion and next-nucleotide effects contribute to the mutagenicity of dNTP imbalance in *vivo* (Kunz and Kohalmi, 1991). dNTPs in excess can also form a correct base pair at a slipped or dislocated 3' terminus and lead to frameshift mutations (Bebenek et al., 1992). Furthermore, altered dNTP levels might influence the repair of damaged DNA (Kunz and Kohalmi, 1991). Hydroxyurea, an inhibitor of RNR, has been found to inhibit DNA-excision repair in human cells as a consequence of reduced dNTP levels (Snyder, 1984; Snyder, 1985). Finally, constitutively high dNTPs in inhibit cell cycle progression and leads to a defect in DNA damage checkpoint response (Chabes and Stillman, 2007).

Mutagenic effect caused by imbalanced dNTP pool size has been suggested to contribute to the carcinogenesis. Thus, dNTP pool sizes have to be tightly controlled to prevent genomic instability and cancer development. Cells utilize multilevel controls to maintain the optimal dNTP level, which ensures the replication accuracy and genome stability. Among these controls, allosteric control and genetic control of the enzymes involved in dNTP biosynthesis are major mechanisms to maintain a balanced dNTP concentration and ratios.

## 1.2 Ribonucleotide Reductase (RNR)

RNR catalyzes a crucial rate-limiting step of the *de novo* synthesis of dNTPs and is the sole enzyme responsible for reducing all four NDPs to the corresponding dNDPs, which are subsequently phosphorylated to dNTPs. Thus, RNR occupies a key position in the dNTP synthesis and plays an essential role in accurate DNA replication and repair by supplying adequate and balanced dNTPs for cells. RNR is indispensable for the survival of all living organisms. The key role of RNR in DNA synthesis, and thereby cell proliferation, makes RNR an important target for cell growth control and target of chemotherapeutic treatment of cancer.

### 1.2.1 RNR enzyme

#### 1.2.1.1 Classification of RNR

There are three main classes of RNR enzymes that depend on different metal cofactors for catalytic activity (Kolberg et al., 2004). Class I enzymes contain an oxygen-bridged dinuclear iron center, class II enzymes contain cobalamin cofactor (vitamin B12), and class III enzymes contain an iron-sulfur cluster coupled to S-adenosylmethionine (SAM). However, all three classes have a conserved cysteine residue at the active site that is converted to a thiyl radical, which initiates the substrate reduction by abstracting a hydrogen atom from the ribose ring of the substrate (Kolberg et al., 2004). The thiyl radical site is located on the tip of a protein loop in the center of a $\alpha\beta$ barrel in all three classes of RNR. In the class II, the metal cofactor may interact directly with the active site cysteine, whereas in class I and class III, a stable protein radical is generated on a separate subunit and the radical is then transferred to the catalytic site through a radical transfer pathway consisting a chain of hydrogen bonded amino acid residues (Kolberg et al., 2004). All eukaryotic RNR enzymes belong to class I and are oxygen-dependent.

#### 1.2.1.2 Overall structure of the RNR enzyme

In mammals, RNR is composed of two non-identical homodimeric subunits, the large subunit R1 and the small subunit R2 (Fig. 1.2). The large subunit R1 exists as a homodimer with a molecular weight of 170 kD (Wright et al., 1990). Each R1 monomer harbors a catalytic site, which reduces the substrate, and two allosteric regulation sites (specificity site and activity site, which will be discussed in detail later). Each R1 monomer is composed of three domains: one αβ barrel domain, an N terminal domain and one small domain (Uhlin and Eklund, 1994). The catalytic site is located in a cleft between the N-terminal domain and barrel domain. Two-monomer interaction area buries 4% of R1 surface area.

The small subunit R2 is a homodimer with a molecular weight of 88 kD and forms a heart shape. Each R2 monomer contains an oxygen-bridged dinuclear iron center and a unique tyrosyl free radical, which is transferred through a radical transfer path to produce a thiyl radical in the catalytic site of R1 subunit. This tyrosyl free radical is situated in a hydrophobic environment close to the dinuclear iron center and is deeply buried inside the R2 subunit, protected from solvent. The N-terminal of R2 is not needed for enzyme activity, but is important for cell cycle regulation of the RNR enzyme. The C-terminal of R2 is important for the formation of the holoenzyme complex with R1 (Uhlin and Eklund, 1994) (Uppsten et al., 2006). The dimer appears to be a very stable entity. Two-monomer interaction area is extensive and buries 18.5% of the accessible surface (Eklund et al., 2001).

#### 1.2.1.3 RNR catalytic mechanism

At the catalytic site of the R1 subunit, a thiyl radical initiates catalysis by abstracting the 3'-hydrogen atom from the ribose ring of the substrate ribonucleotide

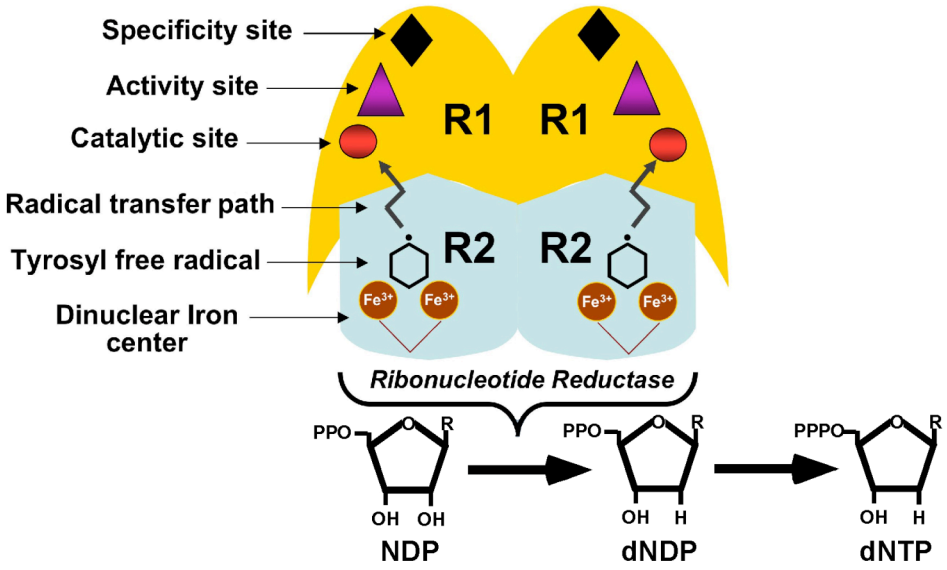


Figure 1.2 Schematic showing the structure of RNR and the reaction it catalyzes.

to generate a substrate radical (Uppsten et al., 2006). An essential redox cysteine pair at the catalytic site of R1 then reduces the substrate radical to deoxyribonucleotide by replacing the 2'-hydroxyl group on the ribose ring by a hydrogen atom. After reducing the substrate, a disulfide bond between the redox cysteine pair is formed and has to be reduced before the enzyme can be active again. Oxidized RNR can be reduced by the thioredoxin and glutaredoxin system. Oxidized thioredoxin and glutaredoxin then can be reduced by thioredoxin reductase and glutathione reductase, both depending on NADPH to provide final reducing power. Additional redox cysteine pair at the surface of the flexible C-terminus of R1 is involved in the reactivation of the enzyme by swinging out to the surface to be reduced and then swinging in again to the catalytic site to affect reduction (Eklund et al., 2001; Uhlin and Eklund, 1994).

#### 1.2.1.4 Radical formation and storage

The thiyl radical that initiates the catalysis in the R1 subunit is transiently generated by a long-range radical transfer path from a stable tyrosyl radical in the R2 subunit (Kolberg et al., 2004). The R2 subunit contains a dinuclear iron center and a stable tyrosyl radical, which is reduced and re-oxidized during each catalytic cycle (Uppsten et al., 2006).

The dinuclear iron center in the R2 subunit possesses a strong oxidation power and is responsible for generating the stable tyrosyl radical. When oxygen reacts with the diferrous R2 (Fe(II)-Fe(II)), it will spontaneously oxidize the diiron center through a series of intermediate states, leading to a oxygen-bridged diferric iron cluster (Fe(III)-Fe(III)) and oxidizing the tyrosine residue (Y177 in mouse R2) to the tyrosyl radical (Uppsten et al., 2006).

In mammals, formation of one dinuclear iron cluster in one R2 monomer can very strongly increase the formation of the second cluster in the second R2 monomer

(Kolberg et al., 2004). In addition, mammalian R2 has a low affinity to iron (II), which might be a novel regulatory mechanism utilized for preventing the formation of the tyrosyl radical when it is not needed, or under unfavorable growth conditions, such as hypoxia (Graff et al., 2002). The dinuclear iron center of mouse R2 are labile, and although the same mouse R2 dimer can carry out several redox cycles, a continuous supply of ferrous iron and oxygen is needed to keep the enzyme fully active (Kolberg et al., 2004).

When the tyrosine 177 residue in the mouse R2 subunit is mutated for another redox-active amino acid with a suitable side chain and appropriate redox potential, like tryptophan (W), this residue can be oxidized. However, despite the formation of a transient tryptophan radical, no catalytic activity could be detected in the R2-Y177W mutant (Potsch et al., 1999). Moreover, when the tyrosine 177 is mutated to phenylalanine (F), cysteine (C), or histidine (H), all these mutants also lose enzyme activity, suggesting strongly that the tyrosyl radical 177 cannot be replaced by other amino acids (Potsch et al., 1999).

#### 1.2.1.5 Radical transfer

The stable tyrosyl radical in the R2 subunit is transferred through a long-range proton-coupled radical transfer path to the thiyl radical at the catalytic site in the R1 subunit. This radical transfer path consists of a chain of conserved hydrogen-bonded residues between the catalytic site of R1 and the tyrosyl radical of R2 (Nordlund and Reichard, 2006), which involves following conserved residues: His173, Asp266, Trp103 in the R2 subunit and Tyr738, Tyr737, Cys429 in the R1 subunit (Nordlund and Eklund, 1993; Uhlin and Eklund, 1994).

In addition, a tyrosine residue (Y370 in mouse), localized in the flexible C-terminus of the R2 subunit, has been found to link the radical transfer path in the R2

subunit to the radical transfer path in the R1 subunit during the radical transfer (Rova et al., 1999). Site-directed mutagenesis of this tyrosine residue to phenylalanine or tryptophan (Y370F and Y370W) has been found to inactivate RNR enzyme activity. The Y370F mutant protein was completely inactive, whereas the Y370W mutant protein only had 1.7% of the wildtype RNR enzyme activity (Rova et al., 1999). Although this tyrosine residue localizes to the C-terminus of the R2 subunit, it is not involved in the binding of the R1 subunit (Rova et al., 1999).

### 1.2.2 RNR genes

#### 1.2.2.1 Mouse RNR genes

The genes for the mouse R1 and R2 subunits are regulated separately and are located on separate chromosomes. Three RNR genes have been identified.
The large subunit R1 is encoded by the *Rrm1* gene, which consists of 19 exons and spans 26 Kb on chromosome 7; the small subunit R2 is encoded by the *Rrm2* gene on chromosome 12 or the recently identified *p53R2* gene on chromosome 15, which shares 80% homology with *Rrm2* gene. *Rrm2* gene is 5.9 Kb and consists of 10 exons, whereas *p53R2* gene is 37 Kb and consists of 9 exons (Guittet et al., 2001; Jordan and Reichard, 1998). A heterotetrameric complex of Rrm2 and Rrm1 accounts for most RNR activity during S phase. *p53R2* was originally identified as a target gene for the p53 tumor suppressor protein and is transcriptionally induced following DNA damage (Nakano et al., 2000; Tanaka et al., 2000). Mouse p53R2 displays 81% identity to mouse Rrm2 at the amino acid level, but lacks the KEN box required for Rrm2 degradation in late mitosis. In addition to its role in stress responses, p53R2 is expressed at low levels throughout the cell cycle and complexes with Rrm1 to produce dNTPs for continuous mitochondrial DNA replication in quiescent cells (Bourdon et al., 2007; Hakansson et al., 2006b; Pontarin et al., 2007).

Several known functional domains in mouse Rrm2 are conserved in p53R2, including the iron center, tyrosine radical site, the hydrophobic pocket surrounding the tyrosyl radical site, the radical transfer pathway from the small subunit to the large subunit, and the hydrophobic channel from the surface to the interior of the protein. The major sequence difference between Rrm2 and p53R2 is that p53R2 lacks 33 amino acid residues in its N-terminus (Chabes et al., 2004; Guittet et al., 2001). The tyrosyl radical signal in the p53R2 protein is almost identical with that in Rrm2 protein. However, the reaction rate of p53R2 is lower than that of Rrm2, which may be due to its reduced binding affinity to R1(Shao et al., 2004).

#### 1.2.2.2 Yeast RNR genes

Yeast contains four RNR genes. *RNR1* and *RNR3* encode the large subunit R1, and *RNR2* and *RNR4* encode the small subunit R2. *RNR1* and *RNR3* are two highly homologous genes (Elledge and Davis, 1990). The standard large subunit R1 in yeast is a RNR1 homodimer. *RNR1* is essential for yeast. Levels of *RNR1* mRNA fluctuate during the cell cycle, being the highest during S phase, while *RNR3* mRNA is induced only after DNA damage, and is not essential. The small subunit of R2 in yeast is a heterodimer of RNR2 and RNR4, with RNR4 stabilizing an active RNR2-RNR4 complex (Chabes et al., 2000; Eklund et al., 2001).

### 1.2.3 Regulation of RNR

Due to its vital importance to cellular physiology, RNR enzyme activity is tightly controlled by a variety of elaborate regulatory mechanisms: allosteric regulation, cell cycle regulation, subcellular localization regulation, and small inhibitory protein regulation.

#### 1.2.3.1 Allosteric regulation of RNR

RNR has unique allosteric regulation mechanism through the large subunit R1 because triphosphate nucleotides regulate the substrate specificity and overall enzyme activity in such a way that a balanced supply of the different deoxynucleotides are present during DNA synthesis but also the enzyme can adapt rapidly to changes in the requirements for dNTPs (Uhlin and Eklund, 1994). Regulation involves binding of effectors to two separate allosteric sites: specificity site (S-site) and activity site (A-site). Recently, a third site, hexamerization site (H-site), has also been proposed to bind ATP to regulate RNR enzyme activity (Cooperman and Kashlan, 2003; Kashlan and Cooperman, 2003).

The S-site binds to different allosteric effectors to influences substrate choice. When dATP binds to the S-site, the RNR enzyme binds and reduces CDP to dCDP and UDP to dUDP; when dTTP binds to the S-site, the enzyme binds and reduces GDP to dGDP; when dGTP binds to the S-site, the enzyme binds and reduces ADP to dADP. The S-site does not discriminate between ATP and dATP, so ATP also promotes reduction of CDP and UDP. Furthermore, dTTP is an inhibitor of pyrimidine reduction. In addition, dGTP is a negative feedback inhibitor of GDP reduction and also inhibits reduction of pyrimidines (Jordan and Reichard, 1998; Kolberg et al., 2004; Nordlund and Reichard, 2006).

The A-site modulates enzyme activity by monitoring the ATP/dATP ratio. Binding of ATP activates RNR and binding of dATP turns the enzyme off. dATP acts as an overall negative regulator through inhibition of all four ribonucleotide reductions. Therefore, dATP has both stimulatory (S-site binding) and inhibitory (A-site binding) effect. Because dATP has higher affinity to the S-site, the inhibitory effect is only significant at very high concentration of dATP. This feedback regulation ensures that a balanced dNTP pool is supplied for DNA synthesis.

Recent studies also suggest the R1 subunit contains a third regulation site (the hexamerization site, H-site). ATP binding to the H-site promotes the formation of an $Rrm1_6$-$Rrm2_6$ hexamer. This hexamer has been suggested to be the major active form of RNR in mammalian cells(Cooperman and Kashlan, 2003; Kashlan and Cooperman, 2003). However, the presence of H-site and the $Rrm1_6$-$Rrm2_6$ hexamer is still highly controversial (Kolberg et al., 2004).

#### 1.2.3.2 Cell cycle regulation of RNR

RNR is tightly regulated during the cell cycle through transcriptional expression, mRNA stability, and protein degradation. RNR enzyme activity increases greatly during S phase. R1 and R2 are regulated differentially, with R2 being rate limiting for enzyme activity (Bjorklund et al., 1990; Eriksson et al., 1984; Mann et al., 1988).

##### 1.2.3.2.1 Transcriptional regulation of RNR during the cell cycle

During an unperturbed cell cycle, the transcription of *Rrm1* and *Rrm2* is undetectable in $G_0/G_1$ phase and reaches maximal levels in S phase (Bjorklund et al., 1990; Eriksson et al., 1984; Mann et al., 1988). However, the level of the Rrm1 subunit is nearly constant throughout the cell cycle in proliferating cells, owing to its long half-life of more than 20 hours, and it is in excess relative to the Rrm2 subunit. Therefore, the cell cycle dependent RNR activity is controlled by synthesis and degradation of the Rrm2 subunit, which has a half-life of 3 hours. *Rrm1* and *Rrm2* both contain promoter active regions (Nordlund and Reichard, 2006), which are controlled by S phase specific transcriptional machinery. Transcription of p53R2 is constant throughout the cell cycle, but is induced in response to DNA damage (Nakano et al., 2000; Tanaka et al., 2000).

The S phase specific transcription of the TATA-less mouse *Rrm1* gene is controlled by proteins that bind to four different promoter elements, β (nucleotide -189 to -167), α (-97 to -76), Inr (-4 to +16), and γ (+34 to +61) (Johansson et al., 1998). YY1, a ubiquitous transcription factor, binds to the β and α elements, which control the promoter strength. The cell cycle-specific expression of *Rrm1* is controlled by protein complexes containing TFII-I that bind to the Inr element and the downstream γ element (Johansson et al., 1998).

Although the transcription of *Rrm2* is tightly correlated to the cell cycle, less is known about the *Rrm2* promoters responsible for this cell cycle regulated transcription (Chabes et al., 2004). *Rrm2* promoters show no obvious sequence homologies with the *Rrm1* promoters that could explain the common S phase specific expression pattern. Mouse *Rrm2* promoter contains an atypical TATA –box with the sequence TTTAAA, which is not required for S –phase specific activity (Kotova et al., 2003). E2F4 binds to a repressive element of Rrm2 promoter to repress the Rrm2 transcription during G1/G0 phase. Binding of nuclear factor Y (NF-Y) to the Rrm2 promoter impedes the binding of E2F4 to this repressive site, and thus facilitates the release of E2F4 during S phase. In addition, an upstream activating region is also important for S phase specific transcription of Rrm2 gene. However, proteins binding to this activating region have not been identified (Chabes et al., 2004).

#### 1.2.3.2.2 mRNA stability

In addition to transcriptional activation of gene expression, post-transcriptional mechanisms that alter mRNA message stability also play an important role in controlling message abundance and gene expression in mammalian cells.

The *Rrm1* gene contains a *cis*-element at the 3'-UTR of the mRNA that interacts with the R1BP protein complex. The *Rrm2* gene also contains a *cis*-element

that interacts with the R2BP complex at the 3'-UTR of Rrm2 mRNA (Amara et al., 1996; Angel et al., 1987; Burton et al., 2003; Chen et al., 1994). When cells are treated with potent tumor promoter, 12-O-tetradecanoylphorbol-13-acetate (TPA), the binding of R1BP and R2BP to their respective *cis*-elements is down-regulated, which correlates with an increase in *Rrm1* and *Rrm2* mRNA stability. The *Rrm2* gene contains additional binding site at the 3'-UTR that binds to p75 in response to TGF-β stimulation and confers *Rrm2* mRNA stability. The tumor promoter TPA and a DAG (1,2, diacylglycerol) analogue can activate PKC and cause elevation of *Rrm1* and *Rrm2* mRNA levels and prolong their half-life (Amara et al., 1996; Burton et al., 2003; Chen et al., 1994). Thus, these two signaling pathways, PKC and TGF-β signaling pathways, regulate RNR message stability. Redox-sensitive mechanisms also play a role in R2BP/*Rrm2* mRNA binding activity (Amara et al., 1996). Higher oxidation potential has also been found to be associated with progression with progression toward mitosis, therefore the control of many cell cycle proteins such as RNR depend on redox-sensitive reactions (Goswami et al., 2000). Increasing oxidation during the cell cycle decreases the binding of R2BP, resulting in an increase in *Rrm2* mRNA stability, enabling the cell to increase its dNTP production for DNA synthesis (Burton et al., 2003).

#### 1.2.3.2.3 Post-translational regulation of RNR by the cell cycle

In addition to transcriptional regulation and mRNA stability, the Rrm2 subunit is also regulated by enzyme degradation during mitosis in a cell cycle dependent manner. Rrm2 has a short half-life of 3 hours. RNR enzyme activity is therefore determined in part by the Rrm2 protein levels. Rrm2 protein accumulation is periodic; the polypeptide is absent during $G_0/G_1$-phase, peaks in S–phase, and then falls in mitosis due to proteolytic degradation (Chabes and Thelander, 2000; Chabes et al.,

2003b; Eriksson et al., 1984).

The mouse Rrm2 subunit contains an N-terminally located conserved KEN box (KENXXXN), a sequence recognized and ubiquitinated by the Cdh-anaphase-promoting complex (Cdh1-APC). Cdh1-APC is an ubiquitin ligase that targets protein degradation during the mitosis and G1 phase. The overall periodicity of Rrm2 protein levels depends on this KEN box sequence. Mutating the KEN signal stabilizes the Rrm2 protein during mitosis and G1 phase (Chabes et al., 2003b). Additionally, Ser 20 at the N-terminal tail of mouse Rrm2 protein is phosphorylated by $p34^{cdc2}$ and CDK2 protein kinases, which is also important for cell cycle regulation of the enzyme but the function of this phosphorylation has not been determined (Chan et al., 1993). However, the N-terminal sequence is not needed for enzyme activity since truncation of N-terminal residues in mouse Rrm2 does not significantly affect the enzyme activity (Mann et al., 1991).

#### 1.2.3.3 Subcellular localization regulation of RNR

Translocation of RNR subunits from the cytosol to nucleus has been proposed to provide additional regulation of RNR. In mammals, it is well established that Rrm1 and Rrm2 are cytoplasmic (Engstrom and Rozell, 1988; Engstrom et al., 1984), but the location of p53R2 and the translocation of Rrm1, Rrm2 and p53R2 after DNA damage are still controversial. Nakano and Tanaka both reported that p53R2 localizes to the nucleus in genotoxin treated cells, which may facilitate the localization of nucleotides at sites of DNA damage (Nakano et al., 2000; Tanaka et al., 2000). A study in a human tumor cell line showed that both Rrm2 and p53R2 undergo translocation from the cytosol to the nucleus coincident with activation of DNA synthesis (Liu et al., 2005). In addition, translocation of Rrm1, Rrm2, p53R2 from the cytoplasm to the nucleus in response to UV irradiation is consistent with the increase in RNR activity

(Xue et al., 2003). However, a recent study found that all three RNR proteins reside in the cytosol independent of DNA damage, suggesting that dNTPs produced by RNR in the cytosol and diffuse into the nucleus or are transported into the mitochondria to support DNA replication and repair (Pontarin et al., 2008). Nuclear staining of p53R2 was probably caused by non-specific staining of polyclonal antibodies, since cytosolic localization of p53R2 was detected by using specific monoclonal antibodies or affinity chromatography purified polyclonal antibodies in Pontarin's report.

In yeast, during the normal cell cycle, RNR1 and RNR3 are localized predominantly in the cytoplasm, whereas RNR2 and RNR4 have a primarily nuclear localization. In response to DNA damage, the small subunit complex RNR2/RNR4 translocates from the nucleus to the cytoplasm, forming the active tetrameric RNR complex with the large subunit (Yao et al., 2003). Control of the nuclear localization of RNR2/RNR4 complex involves an anchor mechanism and Wtm1 is a key component of that anchor in budding yeast (Lee and Elledge, 2006; Zhang et al., 2006). In addition, *Damage regulated Import Faciliator 1 (Dif1)* has been found to directly binds to the RNR2-RNR4 complex through a Hug domain to drive nuclear import of RNR2-RNR4 complex and Dif1 is both cell-cycle and DNA-damage regulated (Lee et al., 2008; Wu and Huang, 2008). Thereby, the combination of both nuclear anchor limiting nuclear export and a regulated importer to coordinate subcellular localization of RNR has been proposed in budding yeast. In fission yeast, in addition to specifically binds and inhibit R1 (Cdc22p), inhibitory protein Spd1p can anchor the small subunit R2 in the nucleus (Hakansson et al., 2006a).

#### 1.2.3.4 Regulation of RNR by small inhibitory proteins

In some organisms, RNR activity can also be regulated by the binding of small inhibitory proteins, such as Sml1 in *S. cerevisiae* (Zhao et al., 1998) and Spd1 in *S.*

*pombe* (Hakansson et al., 2006a; Liu et al., 2003). Sml1 is a 104-residue peptide that binds the large subunit of RNR through its C-terminus and inhibit RNR enzyme activity by interfering with the regeneration of the catalytic site on the large subunit. Spd1 binds specifically to the Cdc22p (the large subunit R1 in fission yeast) to inhibit RNR activity. In addition to transcriptional induction of RNR following DNA damage, the Mec1 and Rad53 pathway also regulates RNR activity through phosphorylation and degradation of Sml1 inhibitory protein. Sml1 protein levels decrease during S phase and become undetectable after DNA damage, resulting in de-repression of RNR activity. Failure to remove Sml1 in *mec1* and *rad53* mutants results in decreased dNTP levels, incomplete DNA replication, defective mitochondrial DNA propagation, and cell death (Zhao et al., 2001). Mutant strains lacking Sml1 grow normally, exhibit increased resistance to DNA-damage agents, and have higher dNTP levels compared to wild-type strains (Zhao et al., 1998).

In mammalian cells, a *Sml1*-like mechanism for controlling the activity of RNR has not been identified. However, p53 has been found to directly interact with p53R2 and Rrm2 but not Rrm1. After exposure to UV, p53R2 and Rrm2 have been suggested to dissociate from p53 and bind to Rrm1, forming Rrm1-Rrm2 and Rrm1-p53R2 complexes to provide dNTPs for DNA repair (Xue et al., 2003).

### 1.2.4 RNR and DNA damage response

RNR plays an important role in DNA damage response and genome maintenance. In response to DNA damage and DNA replication blocks, all organisms arrest cell cycle progression at specific points and induce the expression of genes facilitating DNA repair. The largest category of DNA damage-inducible genes are those involved in DNA replication, including DNA polymerases and RNR genes.

Induction of these genes in response to stress of DNA damage is thought to produce a metabolic state that facilitates DNA replication and repair processes.

Consistent with a need for nucleotides during DNA repair, DNA damage induces transcription of the RNR genes in both yeast and mammalian cells, in a manner dependent on DNA damage checkpoint signaling pathways (reviewed in (Elledge et al., 1993) see also (Filatov et al., 1996; Guittet et al., 2001; Hakansson et al., 2006b; Nakano et al., 2000; Tanaka et al., 2000; Zhao et al., 2001). In yeast, RNR is the best-studied transcriptional target of the Mec1 and Rad53 checkpoint pathway. Dun1, a downstream kinase of the Mec1/Rad53 pathway, activates transcription of RNR genes in response to DNA damage (Chen et al., 2007b; Zhao and Rothstein, 2002; Zhou and Elledge, 1993). Dun1 was originally identified in yeast as a mutant showing a defect in the up-regulation of RNR in response to DNA damage (Zhou and Elledge, 1993). In addition to transcriptional activation of RNR, Dun1 is also responsible for phosphorylation and degradation of the RNR inhibitory protein Sml1 in response to DNA damage (Zhao and Rothstein, 2002). Dun1-dependent regulation of the localization of different RNR subunits in response to DNA damage serves as an additional mechanism for RNR activation in DNA damage response (Lee and Elledge, 2006; Zhang et al., 2006). Collectively, in yeast, DNA damage results in a substantial increase in dNTP levels. This increase in dNTP pools dramatically improves survival following DNA damage (Chabes et al., 2003a).

Like in yeast, activation of checkpoint pathways promotes the delay of cell cycle progression in mammalian cells, allowing required repair to take place before commencement of DNA replication and mitosis. DNA double-stranded breaks (DSBs) and stalled DNA replication forks prompt the activation of Atm (ataxia telangiectasia-mutated) and Atr (AT and Rad3-related) signaling pathways. Activated Atm and Atr, on one hand, recruit Mdc1, p53BP1 and Brca1 to sites of DNA damage to facilitate

repair and simultaneously propagate the checkpoint signals to Chk2/p53 and Chk1 to block G2/M transition and S phase progress. p53R2 is targeted by the p53-dependent checkpoint pathway through transcriptional activation in response to DNA damage (Nakano et al., 2000; Tanaka et al., 2000). Concomitantly, the level of Rrm2 is repressed in a p53 dependent manner (Lin et al., 2004; Tanaka et al., 2000).

It has been suggested that mammalian Rrm1 and Rrm2 are DNA damage-inducible. The Rrm1 promoter is induced up to 3-fold and the Rrm2 promoter is induced up to 10-fold by UV light at a dose-dependent manner (Filatov et al., 1996). Rrm2 protein is stabilized in response to DNA damage (Chabes and Thelander, 2000). Several studies found that Rrm2 can substitute for the function of p53R2 in providing dNTPs for DNA repair in cells lacking functional p53 (Lin et al., 2004) and excess Rrm2 protein functions coordinately with the S phase checkpoint to contend with DNA damage and alleviate replication stress (Lin et al., 2007).

The finding of the DNA damage-inducible p53R2 gene resolved the mystery of how non-proliferating cells with no detectable Rrm2 proteins would obtain dNTPs for DNA repair after DNA damage. In mammalian cells, ATM activates p53, which then induces the expression of *p53R2* by directly activating its transcription through binding of a sequence in the first intron of the *p53R2* gene(Nakano et al., 2000; Tanaka et al., 2000). P53R2 protein forms an active Rrm1-p53R2 complex with Rrm1 to provide dNTPs for DNA repair (Guittet et al., 2001; Hakansson et al., 2006b). Cells that can not make p53R2 protein are more sensitive to DNA-damaging agents (Tanaka et al., 2000; Yamaguchi et al., 2001). Recent studies found that ATM directly phosphorylates p53R2 at Ser72 in response to genotoxic stress and this modification is essential for maintaining p53R2 protein stability (Chang et al., 2008). ATM dependent p53R2 phosphorylation at Ser72 regulates cell viability and p53R2 protein stability by inhibiting p53R2 hyper-ubiquitination and degradation by MDM2 in response to DNA

damage (Chang et al., 2008). Together, transcriptional induction of p53R2 by p53 and/or phosphorylation of p53R2 by ATM are responsible for providing dNTPs by Rrm1-p53R2 complex for DNA repair following DNA damage.

It is still unclear whether dNTP levels also increase after DNA damage in mammalian cells. Mammalian cells have a more strict dATP feedback inhibition of RNR activity, so increased levels of RNR enzyme in mammalian cells might not result in a general increase in the dNTP pools (Akerblom et al., 1981). The p53-dependent induction of the p53R2 protein is important in the cellular response to DNA damage (Nakano et al., 2000; Tanaka et al., 2000), and by analogy with the yeast system, it has been assumed that mammalian cells also increase their RNR activity and dNTP pools after DNA damage (Lin et al., 2004). However, there are conflicting reports on the effect of DNA damage on dNTP pools in mammalian cells (Kunz and Kohalmi, 1991). A recent study found no major increase in the dNTP pools in logarithmically growing or resting mammalian cells after DNA damage, which is in strong contrast to the pronounced increase in dNTP pools observed in yeast after DNA damage (Hakansson et al., 2006b).

In summary, in response to DNA damage, cellular dNTP levels increase by several fold due to the elevation of RNR activity through transcriptional induction, inactivation of the RNR negative regulator sml1, and changes in subcellular translocation, as discussed above. Up-regulated RNR activity can rescue the lethality caused by mutations of essential cell cycle checkpoint genes Mec1/Rad53 in yeast (Desany et al., 1998; Zhao et al., 1998). Mammalian cells with increased RNR activity are also resistant to particular DNA damaging agents (Huang et al., 1997). In the context of DNA damage response, the increase in dNTP levels may be necessary for repair synthesis, and translesion DNA polymerases need higher concentration of

dNTPs to bypass DNA lesions (Chabes et al., 2003a). Therefore, up-regulated RNR is beneficial to cell survival following DNA damage.

## 1.3 Deregulation of RNR and genome instability

Although up-regulated RNR promotes cell survival following DNA damage, abundant evidence shows that deregulation of RNR is mutagenic, causing increased mutation rates in both yeast (Chabes et al., 2003a) and mammalian cells (Caras and Martin, 1988). Deregulation of RNR might cause genomic instability through two major different mechanisms: imbalanced dNTP pools resulting from altered RNR enzyme activity and increased oxidative DNA damage resulting from increased radical production.

### 1.3.1 Genomic instability induced by deregulated dNTP synthesis enzyme

RNR plays a dominant role in tightly regulating dNTP pool sizes and composition. Hence the control of RNR activity is important not only in regulating the kinetics of DNA replication, but also in maintaining the integrity of the genome (Herrick and Sclavi, 2007). Deregulation of RNR is mutagenic in both yeast and mammalian cells, which is largely due to elevated dNTP levels or altered dNTP ratios generated by increased RNR activity (Caras and Martin, 1988; Chabes et al., 2003a; Weinberg et al., 1981; Zhou et al., 1998a). The observation of severe mitochondrial DNA (mtDNA) depletion in humans with p53R2 mutations demonstrates that p53R2 has a crucial role in maintaining dNTP supply, especially for the synthesis of mtDNA, which constantly replicates.

As with RNR deregulation, deregulation of other enzymes involved in dNTP biosynthesis also leads to enhanced mutagenesis and genomic instability. Cdh1-APC/C not only controls RNR degradation in a cell cycle dependent manner, but also degrades thymidine kinase (TK1) and thymidylate kinase (TMPK), two enzymes

controlling dTTP synthesis, during mitosis. When these control mechanisms are shut off by mutating the KEN box in those two proteins, dTTP accumulates in a unbalanced fashion, causing an increase in spontaneous mutation rates and genomic instability (Ke et al., 2005). Thus, the tight regulation of enzymes controlling dNTP synthesis and the post-S phase shutoff of dNTP synthesis play a key role in maintaining optimal genomic stability (Mathews, 2006).

The connection between RNR deregulation and enhanced mutagenesis is still not fully understood. Allosteric regulation of RNR by dATP inhibition keeps the S phase dNTP pools at a level that is optimal for replication, which does not increase even when the limiting Rrm2 protein is overproduced. In hydroxyurea-resistant Rrm2-overproducing mouse cells having 3-15 times higher RNR activity than the parent cells, all dNTP pools were close to normal, except for a 3-4 times higher dATP pools (Akerblom et al., 1981). Furthermore, hydroxyurea-resistant, Rrm2 over-producing mouse mammary tumor TA 3 cells, containing about 40 fold higher Rrm2 protein than parent cells, had the same dNTP pools as the parent cells (Eriksson et al., 1984). In both of these cases, the cell cycle regulation of the Rrm2 protein was not disturbed (Chabes and Thelander, 2000). In contrast, in mouse cells containing Rrm1 protein with a D57N mutation in the allosteric activity site, which abolishes the dATP feedback inhibition, dNTP pools increased 3-9 fold and the spontaneous mutation rate was about 100 times higher than the parent cells (Weinberg et al., 1981). However, another study found Rrm1-D57N mutant produced mutator phenotype in mammalian cells without significant changes in dNTP pools (Caras and Martin, 1988). Therefore, whether the enhanced mutagenesis associated with RNR deregulation resulted from perturbations of dNTP pools has not been established.

Despite the well-established association between RNR and maintenance of genome integrity, the mechanisms of genomic instability caused by RNR deregulation

have not been conclusively determined. In addition to possibly altered enzyme activity and changes in dNTP pools, other mechanisms may also contribute to genomic instability associated with RNR deregulation.

### 1.3.2 RNR deregulation and oxidative DNA damage

The small subunit of RNR produces a radical for catalysis and shows dynamic carboxylate, radical, and water shifts in different redox form (Kolberg et al., 2004). The structure and function of RNR is closely linked to its redox state. Free radicals let loose in the cell can perpetrate all kinds of damage, including mutagenesis and molecular degradation (Stubbe, 1994). Similarly, cytochrome c oxidase, which has redox active tyrosine in the binuclear center, participates in reducing oxygen in respiration, suggesting that proteins containing tyrosyl radicals with a binuclear center may be reducing or oxidizing reagents (Xue et al., 2006). It has been reported that human RRM2 protein produces reactive oxygen species (ROS) *in vitro* (Xue et al., 2006). Thus, free radical-induced oxidative DNA damage might also contribute to the mutagenic effect of RNR deregulation. ROS can cause DNA damage, which has long been thought to be involved in carcinogenesis by amplifying genomic instability. However, p53R2 is indicated to play a key role in defending against oxidative stress by scavenging ROS (Xue et al., 2006).

## 1.4 RNR and cancer

Large amounts of dNTPs are required for the replication of the genome in proliferating cells during the S phase of cell cycle, whereas in the other phase the requirement is low. The level of RNR in mammalian cells is therefore closely linked with cell cycle and growth control mechanism. Elevations in RNR activity have been

reported to be linked to neoplastic properties of cells (Wright et al., 1990), malignant transformation and cancer metastasis.

### 1.4.1 **RNR and transforming activity**

Preliminary evidence had suggested that Rrm1 may function as a tumor suppressor (Bepler et al., 2002; Fan et al., 1997; Gautam et al., 2003) and has malignancy-suppressing activity. Stable expression of Rrm1 in a Ras-transfected mouse fibroblast cell line resulted in reduced anchorage-independent growth and tumor formation in syngeneic mice (Fan et al., 1997). *Rrm1* has been also found to function as a metastasis suppressor gene through induction of PTEN expression. Overexpression of *Rrm1* in human and mouse lung cancer cell lines induced PTEN expression, reduced phosphorylation of focal adhersion kinase (FAK), suppressed migration, invasion, and metastasis formation (Gautam et al., 2003).

Rrm2 has been suggested to play a direct role in determining malignant potential through cooperating with oncogenes. R2 is not only capable of acting in cooperation with a variety of oncogenes (H-ras, rac-1, v-fms, v-src, A-raf, v-fes, and c-myc) to promote anchorage-independent growth and tumor formation, but also enhances cancer invasive potential (Fan et al., 1998; Fan et al., 1996; Zhou et al., 1998b).

p53R2, on the other hand, has been proposed to have tumor suppressor activity based on its regulation by p53 and its role in the DNA damage response (Tanaka et al., 2000). Given that many human tumors contain mutations in p53, discovery of p53R2 thus created a link between one of the most important tumor suppressor and the synthesis of deoxyribonucleotides (Xue et al., 2003).

### 1.4.2 RNR and human cancer

In humans, *RRM1* is located on chromosome segment 11p15.5, a region with frequent loss of heterozygosity in non-small-cell lung cancer (NSCLC) (Bepler et al., 2002; Pitterle et al., 1999). Low levels of expression of the gene are associated with poor survival among patients with NSCLC (Bepler et al., 2004). RRM1 protein expression in NSCLC cells is nuclear, highly correlated with ERCC1 expression, and significantly associated with prolonged cancer-free and overall survival in untreated early-stage NSCLC (Zheng et al., 2007). However, *RRM1* overexpression has been linked to drug resistance in tumor chemotherapy, and is utilized as a marker for chemoresistance and poor survival in patients with advanced NSCLC (Ceppi et al., 2006; Gazdar, 2007) . Thus, RRM1 in NSCLC has been proposed to have a dual role in both cancer susceptibility and drug resistance by repairing DNA lesions during the early stage of the cancer to promote survival and by repairing the drug-DNA adducts formed after chemotherapy to cause drug resistance and poor survival during the late stage of the cancer (Gazdar, 2007).

*RRM2* expression level was correlated with both advanced breast tumor grade and stage, suggesting that RRM2 may play a dual role in supporting both rapid cell proliferation and invasive growth (Ma et al., 2003). The genomic regions containing human RRM2 (2p25-2p24) are commonly amplified in human lung cancers (Pei et al., 2001; Wong et al., 2003). Human *RRM2* gene expression levels and gene amplification have also been correlated with chemotherapy drugs (for example, docetaxel/gemcitabine) resistance and clinic outcomes of lung adenocarcinomas (Souglakos et al., 2008; Zhou et al., 2001).

*p53R2* gene is localized to chromosome 8q23.1 and several tumors have been noted to have losses of this chromosome region. A few reports have suggested potential implications of p53R2 in human squamous cell carcinomas and NSCLC

(Uramoto et al., 2006; Yanamoto et al., 2003). In addition, a number of polymorphisms in the gene encoding p53R2 have been identified in esophageal squamous cell carcinoma and in colon carcinoma (Deng et al., 2005; Smeds et al., 2001; Yamaguchi et al., 2001), but none of these mutations are associated with altered p53R2 activity (Chang et al., 2008).

The level of RNR tyrosyl radical is dependent on the oxygenation of the cells, where the radical disappears when the cells are deprived of oxygen (Probst et al., 1989). Human cancer cells with an increased level of R2 resume S phase progression faster upon re-oxygenation after exposure to moderate hypoxia than cells with a normal level of RNR (Graff et al., 2002). Cells are thus given less time for DNA repair, which would result in an increased probability of mutations. This indicates how an increased level of RNR might raise the malignant potential of tumors (Fan et al., 1998; Fan et al., 1996).

### 1.4.3 RNR as a target for cancer therapy

Tumor cells are more sensitive to the cytotoxic effect of RNR inhibition than normal cells because of the increased need for dNTPs for proliferation and decreased adaptability and low responsiveness to regulatory signals. Thus the enzyme has long been considered an excellent target for cancer chemotherapy (Shao et al., 2006). Specific inhibitors of RNR such as hydroxyurea and substrate analogues such as Gemcitabine have long been used for treatment of cancer. Hydroxyurea is a radical scavenger and it inactivates RNR by directly reducing the tyrosyl radical of the R2 subunit to a normal tyrosine residue via one-electron transfer from the drug (Shao et al., 2006). Hydroxyurea inhibits both RRM2 and p53R2 (Shao et al., 2004) and is commonly used for the treatment of chronic myelogenous leukemia and thrombocythemia. Overexpression of RRM2 increases resistance to hydroxyurea in

cancer cells and RRM2 gene amplification and alterations in transcriptional regulation are probably responsible for the mechanism of the drug resistance (Shao et al., 2006).

## 1.5 Models of RNR deregulation

Several models have been established to study the effect of RNR deregulation. In yeast, up-regulated RNR activity, through overproduction of Rnr1, inactivation of the inhibitory protein Sml1, or a mutation in allosteric activity site (*rnr1*-D57N), can rescue the lethality caused by mutations of the essential cell cycle checkpoint genes Mec1/Rad53. However, this increased survival is at the expense of increased mutagenesis due to the increase in dNTP levels. In cultured mammalian cells, expression of Rrm1-D57N mutant protein results in a mutator phenotype, with a15-25 fold increase in spontaneous mutation rates. However, no significant dNTP pool changes were observed in this study (Caras and Martin, 1988). In addition, *Rrm1* and *Rrm2* overexpressing 3T3 cells were generated and Rrm2 overexpressing cells found to have transforming activity in cooperation with variety of oncogenes. Overexpression of *Rrm1* in 3T3 cells, on the other hand, was found to have tumor suppressing activity.

In mouse models, *p53R2* knockout mice die from severe renal failure by the age of 14 weeks and show attenuated dNTP pools and higher rates of spontaneous mutation in the kidneys, suggesting that p53R2 has an essential role in maintaining dNTP levels for repair of DNA in resting cells (Kimura et al., 2003). In addition to kidney failure, p53R2 knockout mice show growth retardation, muscle atrophy and had a markedly decreased mtDNA content at 12 weeks of age, suggesting that p53R2 has a crucial role in dNTPs supply for the synthesis of mtDNA, which constantly replicates (Bourdon et al., 2007). Recently, Rrm1 transgenic mice were generated and

showed significantly suppressed carcinogen-induced lung tumor formation and higher efficiency in chemical-induced damage repair (Gautam and Bepler, 2006).

## 1.6 Summary

RNR catalyzes the rate-limiting step of dNTP biosynthesis and plays an essential role in DNA replication and DNA repair. Due to its critical role in genome maintenance, RNR activity is tightly regulated through S phase specific transcription of *Rrm1* and *Rrm2* genes, binding of allosteric effectors to Rrm1 protein, anaphase promoting complex-cdh1-mediated degradation of the Rrm2 protein during late mitosis. Deregulation of RNR has been found to cause genomic instability in both yeast and mammalian cells.

Although RNR enzyme activity has long been associated with cancer cell proliferation and RNR inhibition is an effective strategy for cancer therapy, the connection between RNR and cancer development is still unclear. It is critical to establish whether RNR deregulation will initiate and promote cancer progression. We hypothesize that deregulation of RNR, by overexpressing each RNR subunit in mice, would cause genomic instability and cancer development. The aim of this dissertation is to elucidate the physiological effect of RNR deregulation using the transgenic mouse models and to further dissect the molecular mechanisms of RNR-induced tumorigenesis.

CHAPTER 2

# Broad Overexpression of Ribonucleotide Reductase Genes in Mice Specifically Induces Lung Neoplasms

## 2.1 Abstract

Ribonucleotide reductase catalyzes the rate-limiting step in nucleotide biosynthesis and plays a central role in genome maintenance. Although a number of regulatory mechanisms govern RNR activity, the physiological impact of RNR deregulation had not previously been examined in an animal model. We demonstrate here that overexpression of the small RNR subunit potently and selectively induces lung neoplasms in transgenic mice and is mutagenic in cultured cells. Combining RNR deregulation with defects in DNA mismatch repair, the cellular mutation correction system, synergistically increased RNR-induced mutagenesis and carcinogenesis. Moreover, the proto-oncogene K-ras was identified as a frequent mutational target in RNR-induced lung neoplasms. Together, these results demonstrate that RNR deregulation promotes lung carcinogenesis through a mutagenic mechanism and establish a new oncogenic activity for a key regulator of nucleotide metabolism. Importantly, RNR-induced lung neoplasms histopathologically resemble human papillary adenocarcinomas and arise stochastically via a mutagenic mechanism, making RNR transgenic mice a valuable model for lung cancer.

## 2.2 Introduction

An adequate and balanced supply of deoxyribonucleotide triphosphates (dNTPs) is essential for accurate DNA replication and repair. The rate limiting step in *de novo* dNTP biosynthesis is catalyzed by the enzyme ribonucleotide reductase (RNR). RNR reduces ribonucleoside diphosphate (NDP) to deoxyribonucleoside diphosphate (dNDP), phosphorylation of which yields dNTP. RNR is composed of two non-identical homodimeric subunits (Nordlund and Reichard, 2006). The large R1 subunit harbors the catalytic site and is encoded by the *Rrm1* gene in mammals. The small R2 subunit contains an oxygen-bridged dinuclear iron center that generates a tyrosyl free radical that is transferred to the R1 subunit for enzyme activity. Mammalian genomes contain two independent genes, *Rrm2* and *Rrm2b* (*p53R2)*, that encode closely related R2 proteins. A complex of Rrm2 and Rrm1 accounts for most RNR activity during S phase. *p53R2* was originally identified as a target gene for the p53 tumor suppressor protein and is transcriptionally induced following DNA damage (Nakano et al., 2000; Tanaka et al., 2000). In addition to its role in stress responses, p53R2 is expressed at low levels throughout the cell cycle and complexes with Rrm1 to produce dNTPs for mitochondrial DNA replication (Pontarin et al., 2007).

Because intracellular nucleotide concentrations have a major impact on DNA replication fidelity (Mathews, 2006), RNR enzyme activity is tightly controlled by several regulatory mechanisms. During an unperturbed cell cycle, the transcription of *Rrm1* and *Rrm2* is undetectable in $G_0/G_1$ phase and reaches maximal levels in S phase cells (Bjorklund et al., 1990; Eriksson et al., 1984; Mann et al., 1988). However, owing to its long half-life, Rrm1 protein levels are nearly constant throughout the cell cycle and in excess relative to the R2 subunit. RNR enzyme activity is therefore determined in part by R2 protein levels. Rrm2 protein is absent during $G_0/G_1$-phase,

peaks in S–phase, and then falls in mitosis following ubiquitination by the anaphase promoting complex (Chabes and Thelander, 2000; Chabes et al., 2003b; Eriksson et al., 1984). Consistent with a need for nucleotides during DNA repair, DNA damage and replication stress induce RNR expression in both yeast and mammalian cells, in a manner dependent on DNA damage checkpoint pathways (Elledge et al., 1993; Hakansson et al., 2006b). While mammalian Rrm1 and Rrm2 proteins are cytoplasmic (Engstrom and Rozell, 1988), p53R2 localizes to the nucleus in genotoxin-treated cells (Nakano et al., 2000; Tanaka et al., 2000), which may facilitate the localized production of nucleotides at DNA damage sites.

RNR enzyme activity also is controlled by two allosteric sites in the R1 subunit. A specificity site regulates the relative cellular concentration of each of the four dNTPs by influencing substrate choice, while an activity site regulates the total dNTP pool size by monitoring the ATP/dATP ratio. Analysis of the mutant Rrm1-D57N, which is insensitive to feedback inhibition by dATP due to a mutation in the activity site, indicates that loss of RNR allosteric control results in a mutator phenotype in both yeast and mammalian cells (Caras and Martin, 1988; Chabes et al., 2003a; Reichard et al., 2000).

Although RNR is a major determinant of genomic integrity, the consequences of RNR deregulation in animals are unknown. We generated transgenic mice that overexpress *Rrm1*, *Rrm2,* or *p53R2* and found that overexpression of either small RNR subunit induced spontaneous lung neoplasms and was mutagenic in cultured cells. Defects in DNA mismatch repair (MMR) synergistically increased RNR-induced mutagenesis and carcinogenesis, and activating mutations in the proto-oncogene *K-ras* were identified in lung neoplasms from *Rrm2* and *p53R2* transgenic mice. These results identify mutagenic and carcinogenic effects of RNR deregulation *in vivo*.

## 2.3 Material and methods

### 2.3.1 Plasmids.

Expression plasmids encoding mouse *Rrm1*, *Rrm2*, or *p53R2* were constructed in the pCaggs expression vector (Niwa et al., 1991) as follows. The mouse *Rrm1* cDNA sequence was cloned as an XhoI fragment from clone D65 (Thelander and Berg, 1986) into XhoI-digested pCaggs plasmid, producing pCaggs-Rrm1. The *Rrm2* open reading frame was PCR amplified with primers 5'-AGAGCTCGAGCCATGCTCTCCGTCCGCAC-3' and 5'-AGAGCTCGAGTTAGAAGTCAGCATCCAAGGT-3' using clone C10 (Thelander and Berg, 1986) as a template. The resulting PCR product was digested with XhoI and cloned into XhoI-digested pCaggs plasmid, producing pCaggs-Rrm2. The *p53R2* open reading frame was PCR amplified from EST clone AA623971 with primers 5'-GCGGAATTCATGGGCGACCCGGAAAGG-3' and 5'-GCGGAATTCTTAGAAATCTGCATCCAAGGT-3'. The resulting PCR product was digested with EcoRI and cloned into EcoRI-digested pCaggs plasmid, producing pCaggs-p53R2. All PCR products were fully sequenced and confirmed to be free of mutations.

### 2.3.2 Transgenic mice.

Transgenic mice were generated by microinjection of linear plasmid DNA into the pronucleus of zygotes derived from *FVB/N* mice as previously described (Muller et al., 1988). SalI-linearized pCaggs-Rrm1, SalI/BamHI-digested pCaggs-Rrm2, and SalI/PstI-digested pCaggs-p53R2 were used. Transgenic founder mice were initially identified by Southern blot analysis using probes specific for *Rrm1*, *Rrm2*, or *p53R2*. Transgenic mice were maintained as hemizygotes on a pure *FVB/N* background by

breeding with wild-type *FVB/N* mice. Genotyping was performed by PCR with primers: 5'-ATCAGAAGGTGGTGGCTGGTGTGG-3' and 5'-GCTATGACTGGGAGTAGTCAGGAG-3' for Rrm1 and p53R2; 5'-AGAGCTCGAGCCATGCTCTCCGTCCGCAC-3' and 5'-GCTAAATCGCTCCACCAAGTTCTC-3' for Rrm2. For analysis of tumor development, cohorts of mice were aged until moribund for 15 to 21 months. As part of another study, some RNR transgenic mice were bred with mice heterozygous for a targeted deletion of the *Hus1* cell cycle checkpoint gene. $Hus1^{+/-}$ mice show no apparent phenotypes (Weiss et al., 2000) and as expected no differences in tumor incidence or any other phenotypes were noted between $Hus1^{+/-}$ (n=74) and $Hus1^{+/+}$ (n=183) mice in the cohort. Therefore, the *Hus1* genotype is not distinguished in the final data set consisting of 257 mice (Table 1). *Msh6*-null mice (Edelmann et al., 1997) were obtained from the Mouse Models of Human Cancers Consortium and bred with $Rrm2^{Tg}$ or $p53R2^{Tg}$ mice to generate $Msh6^{+/-}RNR^{Tg}$ mice. M$sh6^{+/-}RNR^{Tg}$ mice were crossed with $Msh6^{+/-}$ or $Msh6^{-/-}$ mice to produce littermates of the following genotypes: $Msh6^{-/-}RNR^{Tg}$, $Msh6^{-/-}$, $Msh6^{+/-}RNR^{Tg}$, $Msh6^{+/-}$, $Msh6^{+/+}RNR^{Tg}$ , and $Msh6^{+/+}$. Mice were aged until moribund for 6 or 17 months depending on the experiment and analyzed as noted above. All mice were maintained identically, following guidelines approved by the Cornell University Institutional Laboratory Animal Use and Care Committee.

### 2.3.3 Pathological assessment.

Mice terminated according to schedule, as well as those with visible neoplasms or showing signs of clinical disease, including hunched posture, labored breathing, poor grooming, and wasting, were euthanized by asphyxiation using carbon dioxide and necropsied. Inflated lungs and other affected tissues were fixed with 10% neutral-

buffered formalin, embedded in paraffin and 4-5 μm thick sections were stained with hematoxylin and eosin. If needed for molecular biological and biochemical studies, a part of freshly dissected tissues was snap-frozen in liquid nitrogen and kept at -80ºC. Pathological assessment was performed according to guidelines endorsed by the Mouse Models of Human Cancers Consortium (Nikitin et al., 2004).

### 2.3.4 Immunohistochemistry.

Immunohistochemistry was performed using the Vectastain ABC kit (Vector Laboratories) on 5 μm paraffin sections. Briefly, endogenous peroxidase was quenched using 3% $H_2O_2$ in distilled water. Sections were blocked for 2 h at RT in TBS containing 4% normal goat serum and 10% non-fat milk and then incubated for 2 h at 37°C in TBS containing 0.04% Triton-X100 and Anti-pro-SP-C (Chemicon International; 1:500 dilution) or anti-CC10 (Santa Cruz Biotechnology; 1:250 dilution). Sections then were washed with TBS, incubated for 30 min at RT with biotinylated anti-IgG antibody (Vector Laboratories), and incubated with ABC complex diluted in blocking solution for 30 min at RT. Staining was done with a peroxidase substrate kit (Vector Laboratories) according to manufacturer recommendations. Counterstaining of sections was performed with methyl green (Fisher Scientific).

### 2.3.5 Generation of RNR overexpressing 3T3 cell pools.

All cells were cultured in culture medium (Dulbeco's Modification of Eagles Medium supplemented with 10% bovine calf serum, 1.0 mM L-glutamine, 0.1 mM MEM non-essential amino acids, 100 μg/ml of streptomycin sulfate, and 100 U/ml of penicillin). Mouse 3T3 fibroblasts were transfected with linearized empty pCaggs vector, pCaggs-Rrm1, pCaggs-Rrm2, or pCaggs-p53R2 along with PGK-puro using

FuGENE 6 transfection reagent (Roche Diagnostics Co., Mannheim, Germany) following the procedure recommended by the manufacturer. At 48 hours, the medium was replaced with selection medium containing 1 mg/ml puromycin, which was changed every 2 days. After 2 weeks, puromycin-resistant cells were pooled and expanded for further analysis under selection conditions.

### 2.3.6 Northern blot analysis.

Total RNA was isolated from cultured cells or mouse tissues using RNA STAT-60 (Tel-Test Inc.). Approximately 2.5 μg of each RNA was resolved on a 1% agarose/formaldehyde gel and then hybridized with probes specific to mouse *Rrm1*, *Rrm2*, *p53R2*, or *Gapdh*.

### 2.3.7 Western blot analysis.

Tissue samples or cultured cells were prepared in RIPA buffer (50mM Tris-HCl [pH 8.0], 1% [vol/vol] Nonidet P-40, 0.5% sodium deoxycholate, 0.1% [wt/vol] sodium dodecyl sulfate, 150mM sodium chloride, 50mM sodium fluoride) and 1x protease inhibitor cocktail (Roche). Immunoblotting was performed on PVDF membranes using standard methods, with signal detection by enhanced chemiluminescence (Pierce). The antibodies used were mouse anti-R1 (AD203, Bio Med Tek), goat anti-R2 (sc-115, Santa Cruz Biotechnology,), rabbit anti-p53R2 (2383, ProSci-inc,) and β-actin (A5441, Sigma).

### 2.3.8 *Hprt* mutation rate assay.

Cells were maintained in HAT medium (culture medium supplemented with 0.2mM sodium hypoxanthine, 0.4μM aminopterin, 0.02μM thymidine [GIBCO]) for two weeks. Cells then were maintained in HT medium (culture medium supplemented

with 0.1mM sodium hypoxanthine, 0.016μM thymidine [GIBCO]) for one week. Subsequently, cells were seeded at a density of $5x10^5$ cells per 10cm plate (10 plates total) in culture medium containing 5μg/ml 6-thioguanine (Sigma). After 3 weeks, 6-thioguanine resistant colonies were counted, isolated, and individually expanded. RNA was extracted, and cDNA was synthesized with primer 5'-GCAGCAACTGACATTTCTAAA-3' using the Superscript™ First Strand Synthesis System (Invitrogen). The *Hprt* open reading frame was PCR amplified using primers: 5'-TTTCCGGAGCGGTAGCAG-3' and 5'-TTACTAGGCAGATGGCCACA-3'. *Hprt* mutations were identified by direct sequencing of PCR products using primers: 5'-CTTCCTCCTCAGACCGCTTT-3' and 5'-TGGCAACATCAACAGGACTC-3'. Plating efficiency was determined by plating 200 cells in medium without 6-thioguanine in triplicate for 2 weeks and counting stained colonies.

### 2.3.9 Big Blue mutation rate assay.

Big Blue *C57Bl/6* mice (Jakubczak et al., 1996), hemizygous for the lambda shuttle vector, were obtained from Stratagene (La Jolla, CA) and were bred with *Rrm1*, *Rrm2,* or *p53R2* hemizygous transgenic mice. Genomic DNA was isolated from 3-month old lung tissues by phenol-chloroform extraction using the RecoverEase DNA isolation kit protocol (Stratagene, LA Jolla, CA). The bacteriophage λ transgene was recovered from genomic DNA by incubation with *in vitro* λ packaging extract (Transpack; Stratagene) according to the manufacturer's instruction. Phage containing *cII* mutations were identified by mixing 100μl of packaged phage with 200μl of an overnight culture of *E. coli* G1250 cells. This solution was mixed with TB-1 top agar, poured onto TB1 plates, and incubated at 24°C for 48 h. To determine the total number of phage screened, 10 μl of a 1:100 dilution of packaged phage was mixed with 200μl of G1250, plated on TB1 plates in triplicate, and incubated at 37°C for 24

h. The mutant plaques were confirmed by re-plating on TB1 plates at 24°C. For *cII* sequencing, well-isolated, clear plaques (phages with cII mutants) were picked and PCR amplified (forward primer: 5'-CCGCTCTTACACATTCCAGC-3', reverse primer: 5'-CCTCTGCCGAAGTTGAGTAT-3'). Mutations in λ *cII* gene were identified by direct sequencing of the PCR products using primer 5'-CCACACCTATGGTGTATG-3'. Mutation frequencies were compared using a Maximum Likelihood Ratio test and two-way ANOVA.

### 2.3.10 Determination of mutation rates in *Saccharomyces cerevisiae*.

All yeast strains were derived from either W4069-4C (WT) or W4069-8C (*rnr1-D57N1*) (Chabes et al., 2003a). These strains are derived from the W303 strain. Mutations in the mismatch repair genes were introduced into these strain backgrounds. The *msh2D::hisG*, *msh6D::hisG* and *msh3D::hisG* alleles have complete or nearly complete disruptions of their respective genes and were introduced into these strains by single-step gene transplacement (Alani et al., 1987). The spontaneous forward mutation rate to canavanine resistance ($Can^r$) was measured in W4069-4C (WT), W4069-8C (*rnr1-D57N1*), EAY1997-2000 (*msh3*Δ), EAY2001-2003 (*rnr1-D57N msh3*Δ), EAY2004-2006 (*msh2*Δ), EAY2007-2009 (*rnr1-D57N msh2*Δ), EAY2010-2013 (*msh6*Δ), EAY2014-2019 (*rnr1-D57N msh6*Δ) as described previously (Reenan and Kolodner, 1992). Briefly, independent cultures from at least 3 independent isolates of each genotype were plated for single colonies at 30°C on YPD plates. Appropriate dilutions of cells from single colonies (~2 mm) were plated on: 1) synthetic complete (SC) medium lacking arginine to determine the number of viable cells and 2) SC-Arg plus L-canavanine (60 mg/ml) to determine the number of $Can^r$ cells per culture. The rate of mutation per generation was calculated from the median mutation frequency using the method of Lea and Coulson (Lea and Coulson, 1949).

The mutation rate and 95% confidence interval were determined from at least 22 independent measurements for each strain. To determine mutation spectra, the *CAN1* gene was PCR amplified with primers AO1863: 5'-TCAGGGAATCCCTTTTTGCA-3' and AO257: 5'-GTGAGAATGCGAAATGGCGTG-3' and sequenced with primers AO256: 5'-AGTTCTTCAGACTTCTTAACTC-3', AO1864: 5'-CCAGTGGGCGCTCTTATA-3', AO1865: 5'-TTACCGGCCCAGTTGGAT-3', AO1866: 5'-CAACCATTATTTCTGCCG-3', AO1977: 5'-CACCCAAGGACTGCGTGACAG-3'.

### 2.3.11 Sequencing of *K-ras* exons 1 and 2.

5 μm sections of lung tumor samples were microdissected with a Leica Laser Microdissection instrument and incubated in proteinase K buffer (150 μg/ml proteinase K in Taq DNA polymerase PCR buffer [MI188J, Promega]) at 50°C for 4h. The sample was heated at 100°C for 10 min to inactivate the proteinase K and then centrifuged at 4000 rpm for 2 min. The supernatant was used for PCR amplification of *K*-ras exons 1 and 2 with the following primer sets: (5'-CCATGTATTTTATTAAGTGTTGA-3' and 5'-CTCCTCGAGCAAGCGCACGCAGACTGTAGAGCA-3' for exon 1) and (5'-CTCGAATTCATCCTAATGGGTACTAATGGTGT-3' and 5'-CTCCTCGAGAGCAAAGAATCAATAAATGTAAGC-3' for exon 2). Mutations in *K*-ras exons 1 and 2 were identified by direct sequencing of the PCR products using the following primers: (5'-CTATAATGGTGAATATCTTC-3' for exon 1) and (5'-CTCTATCGTAGGGTCGTACT-3' for exon 2).

## 2.4 Results

### *2.4.1* Generation of RNR transgenic mice and analysis of transgene expression.

Deregulation of RNR is mutagenic in yeast and cultured mammalian cells (Caras and Martin, 1988; Chabes et al., 2003a). To test the consequences of RNR deregulation in an animal model, we set out to generate transgenic mice featuring broad, high level expression of the individual mouse RNR genes *Rrm1*, *Rrm2*, and *p53R2,* using pCaggs expression constructs that place the RNR genes under the control of chicken β-actin promoter and cytomegalovirus enhancer regulatory sequences. Six *Rrm1*, two *Rrm2*, and four *p53R2* transgene-positive founders were generated and subsequently maintained on a pure *FVB/N* strain background. RNR transgenic mice appeared grossly normal and were fertile. When bred with wild-type *FVB* mice, *p53R2* hemizygotes produced fewer than the expected number of transgene positive offspring (205 *p53R2* transgene positive and 349 transgene negative mice were identified among 554 mice genotyped at weaning).

Endogenous and transgenic *Rrm1*, *Rrm2* and *p53R2* mRNA expression was tested in a variety of organs by Northern blot analysis. The endogenous *Rrm1* and *Rrm2* genes were coordinately expressed, with highest expression in proliferative tissues such as testis and thymus (Fig. 2.1A, left panels). Expression of the endogenous *p53R2* gene was undetectable in all tested wild-type *FVB* tissues. Importantly, $Rrm2^{Tg}$ and $p53R2^{Tg}$ mice showed high-level transgene expression in all tissues, with overexpression being highest in muscle (Fig. 2.1A, right panels). *Rrm1* overexpression was only observed in muscle and testis of $Rrm1^{Tg}$ mice. For technical reasons, the *Rrm1* transgene included additional non-coding cDNA sequences and was microinjected as a linearized construct without removal of plasmid backbone sequences, which may contribute to the relatively poor transgene expression.

Figure 2.1. Widespread overexpression of ribonucleotide reductase genes in transgenic mice. (A) Northern blot analysis of RNR expression in wild-type and RNR transgenic mice. Total RNA was extracted from the indicated tissues from wild-type FVB mice (left panels), or RNR transgenic mice (right panels) and subjected to Northern blot hybridization with the indicated probes specific for Rrm1, Rrm2 or p53R2. Positions of endogenous and transgene-derived RNR transcripts are indicated. (B) Western blot analysis of RNR protein expression in the indicated tissues from wild type (WT) and RNR transgenic (Tg) mice, as well as lung neoplasms from the corresponding transgenic strains (Tumor 1, 2). Total protein from the indicated tissues was subjected to immunoblotting with antibodies specific to Rrm1, Rrm2 or p53R2. Duplicate membranes were immunoblotted for β-actin as a loading control.

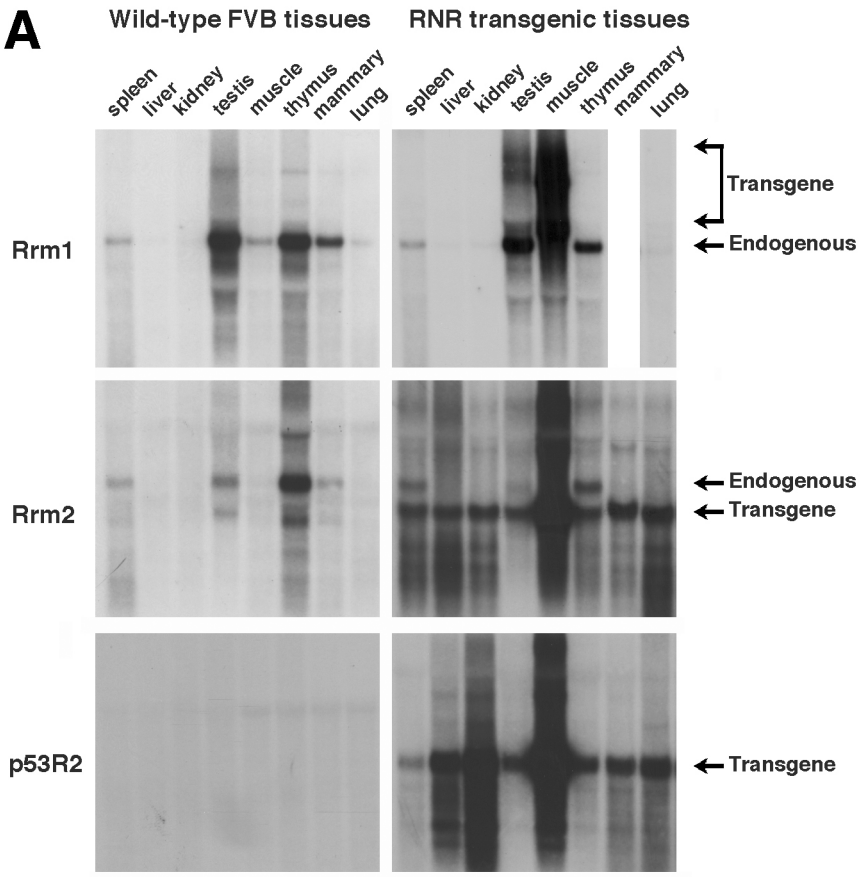
A
Wild-type FVB tissues
RNR transgenic tissues
spleen
liver
kidney
testis
muscle
thymus
mammary
lung
Rrm1
Rrm2
p53R2
Transgene
Endogenous
Endogenous
Transgene
Transgene

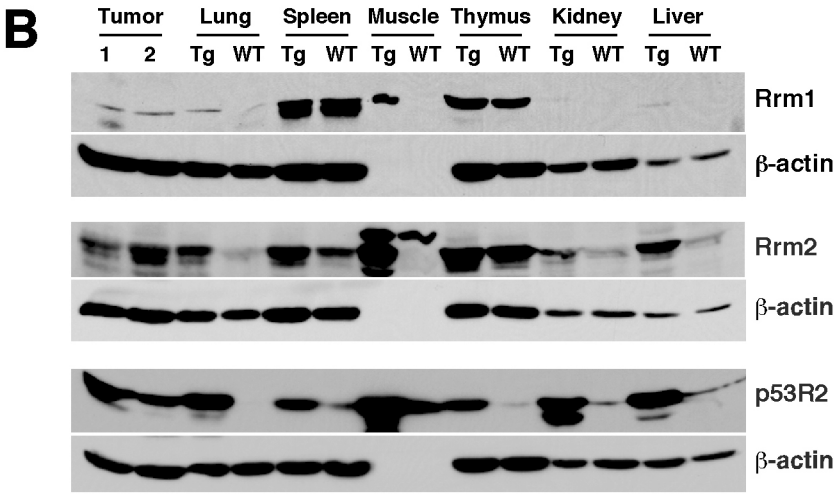
B
Tumor
Lung
Spleen
Muscle
Thymus
Kidney
Liver
1 2 Tg WT Tg WT Tg WT Tg WT Tg WT Tg WT
Rrm1
β-actin
Rrm2
β-actin
p53R2
β-actin

Consistent with results from the Northern blot analyses, immunoblotting revealed that the Rrm2 and p53R2 proteins were highly overexpressed in all tested tissues from *Rrm2*$^{Tg}$ and *p53R2*$^{Tg}$ mice (Fig. 2.1B). Although Northern blotting failed to identify *p53R2* expression in wild-type tissues (Fig. 2.1A), low levels of p53R2 protein were apparent in most wild-type *FVB* tissues. Rrm1 protein overexpression was limited to muscle and to a lesser extent lung in *Rrm1*$^{Tg}$ mice as compared to wild-type littermates. Together, these results establish the restricted overexpression of the large RNR subunit Rrm1 and the widespread, high level overexpression of the small RNR subunits Rrm2 and p53R2 in transgenic mice.

### 2.4.2 Overexpression of the small RNR subunit promotes lung carcinogenesis.

In order to identify spontaneous neoplasms and other abnormalities in RNR transgenic mice, we established a cohort consisting of 52 *Rrm1*$^{Tg}$, 75 *Rrm2*$^{Tg}$, and 81 *p53R2*$^{Tg}$ mice, as well as 49 transgene-negative control mice, and aged them until they exhibited clinical illness. Notably, a significantly increased frequency of lung neoplasms was observed in *Rrm2*$^{Tg}$ and *p53R2*$^{Tg}$ mice (Table 2.1). 72% of *Rrm2*$^{Tg}$ and 74% of *p53R2*$^{Tg}$ animals developed spontaneous lung neoplasms. By contrast, 31% of transgene-negative controls developed lung neoplasms, a frequency consistent with the reported incidence for aged wild-type *FVB* mice (Mahler et al., 1996). The lung neoplasm incidence in *Rrm1*$^{Tg}$ mice was 31%, identical to that of the control animals and significantly less than that of *Rrm2*$^{Tg}$ or *p53R2*$^{Tg}$ mice (Chi-square analysis, $p<0.05$). Lung neoplasms were observed in multiple independent *Rrm2*$^{Tg}$ and *p53R2*$^{Tg}$ lines, indicating that transgene integration site effects did not account for the neoplastic phenotype. Signs of clinical illness arose following a latency of 16-18 months for all genotypes. No differences in lung neoplasm incidence between sexes

Table 2.1 Lung neoplasm characteristics in RNR overexpressing mice

| Mouse genotype | # of animals | % of mice with lung neoplasms | % of mice with hyperplasia[§] | Average lung neoplasm size (mm)±SD | % of mice with multiple lung neoplasms | % of mice with lung adenocarcinoma |
|---|---|---|---|---|---|---|
| *WT FVB*[†] | 49 | 31% | 12% | 4.04 ± 3.98 | 8% | 6% |
| *Rrm1*$^{Tg}$ | 52 | 31% | 15% | 3.96 ± 3.59 | 8% | 10% |
| *Rrm2*$^{Tg}$ | 75 | 72%* | 44%* | 6.68 ± 4.22 | 53%* | 40%* |
| *p53R2*$^{Tg}$ | 81 | 74%* | 20% | 4.26 ± 3.44 | 47%* | 21% |

NOTE: Mice were aged until moribund for up to 21 months, euthanized by asphyxiation using carbon dioxide, and subjected to pathological examination as described in Materials and Methods.

[†]*WT FVB* refers to transgene-negative control mice.

[§]Includes mice that had both epithelial hyperplasia of alveoli and lung neoplasms.

*Statistically significant difference ($p<0.05$) relative to *WT FVB* mice. Incidences were compared by Chi-square analysis. Neoplasm sizes were compared by t-test analysis.

was noted for any of the transgenic lines. The frequency of epithelial hyperplasia of alveoli also was increased in $p53R2^{Tg}$ and especially $Rrm2^{Tg}$ mice. Other neoplasms, including papilloma, histiocytic sarcoma, mammary carcinoma, and lymphoblastic lymphoma, were observed in 13% of $Rrm1^{Tg}$, 12% of $Rrm2^{Tg}$, and 12% of $p53R2^{Tg}$ mice, but only 2% of transgene-negative mice.

The lung neoplasms in $Rrm2^{Tg}$ and $p53R2^{Tg}$ mice displayed several features consistent with a substantial lung cancer predisposition. A significantly greater lung neoplasm multiplicity was observed for $Rrm2^{Tg}$ and $p53R2^{Tg}$ mice, and the lung neoplasms in $Rrm2^{Tg}$ mice were also considerably larger than those from control animals (Table 2.1). The lung neoplasms from $Rrm2^{Tg}$ and $p53R2^{Tg}$ mice ranged from adenoma to advanced adenocarcinoma (Fig. 2.2A I-VI), and resembled human glandular pulmonary neoplasms, particularly adenocarcinomas. RNR-induced lung adenocarcinomas were primarily of the papillary subtype and exhibited pleural invasion, heterogeneous growth pattern, nuclear atypia, high mitotic index, and blood vessel invasion (Fig. 2.2A III-VI). A greater frequency of adenocarcinoma was observed in $Rrm2^{Tg}$ and $p53R2^{Tg}$ mice as compared to $Rrm1^{Tg}$ or transgene-negative mice (Table 2.1), with *Rrm2* overexpression in particular eliciting pathologically advanced neoplasms. Together, these data indicate that overexpression of either small RNR subunit in mice promotes lung neoplasm formation, with *Rrm2* being more potent than *p53R2* with respect to tumor size, multiplicity, and malignancy.

To investigate the possible cell type of origin for RNR-induced lung neoplasms, we performed immunohistochemistry using antibodies against Clara cell antigen (CC10) and surfactant apoprotein-C (SP-C), markers that distinguish Clara and alveolar type II cells, respectively. Eight of eight lung neoplasms from $Rrm2^{Tg}$ and $p53R2^{Tg}$ mice were positive for SP-C (Fig. 2.2A VII), while none was positive for CC10 (Fig. 2.2A VIII). Adjacent bronchioles, on the other hand, were positive for

Figure 2.2 Histopathological and molecular analysis of lung neoplasms from RNR transgenic mice. (A) (I) Lungs from a *Rrm2*$^{Tg}$ mouse with multiple independent neoplasms affecting several lobes. (II-VI) H&E-stained sections of lung neoplasms. (II) Solid adenoma from a *p53R2*$^{Tg}$ mouse. (III-VI) Papillary adenocarcinomas from *Rrm2*$^{Tg}$ or *p53R2*$^{Tg}$ mice showing pleural invasion (arrow) (III), regional variation in growth pattern (IV), multiple mitotic figures (arrows) (V), and blood vessel invasion (arrow) (VI). (VII, VIII) Immunohistochemical staining of RNR-induced lung neoplasms for Pro-SP-C (VII) or CC10 (VIII) by the ABC method, with methyl green counterstain. Inserts show higher magnification views of the boxed regions. Calibration bar: II, IV: 50 μm; III: 241 μm; V: 10 μm; VI: 25 μm; VII, VIII: 100 μm. (B) Northern blot analysis of lung neoplasms from RNR transgenic mice. Total RNA was prepared from lung neoplasms (Tumor 1, Tumor 2, Tumor 3) or normal lung tissue (Lung) from RNR transgenic mice, as well as from wild-type *FVB* lung tissue (WT FVB). Northern blotting was performed with the indicated radiolabeled probes. (C) Western blot analysis of Rrm1 expression in lung neoplasms (Tumor 1, Tumor 2) or normal lung tissues (lung) from RNR transgenic mice as well as normal lung from wild-type FVB lung tissue (WT FVB) . Total protein was subjected to immunoblotting with antibody specific to Rrm1 or α-tubulin as a loading control.

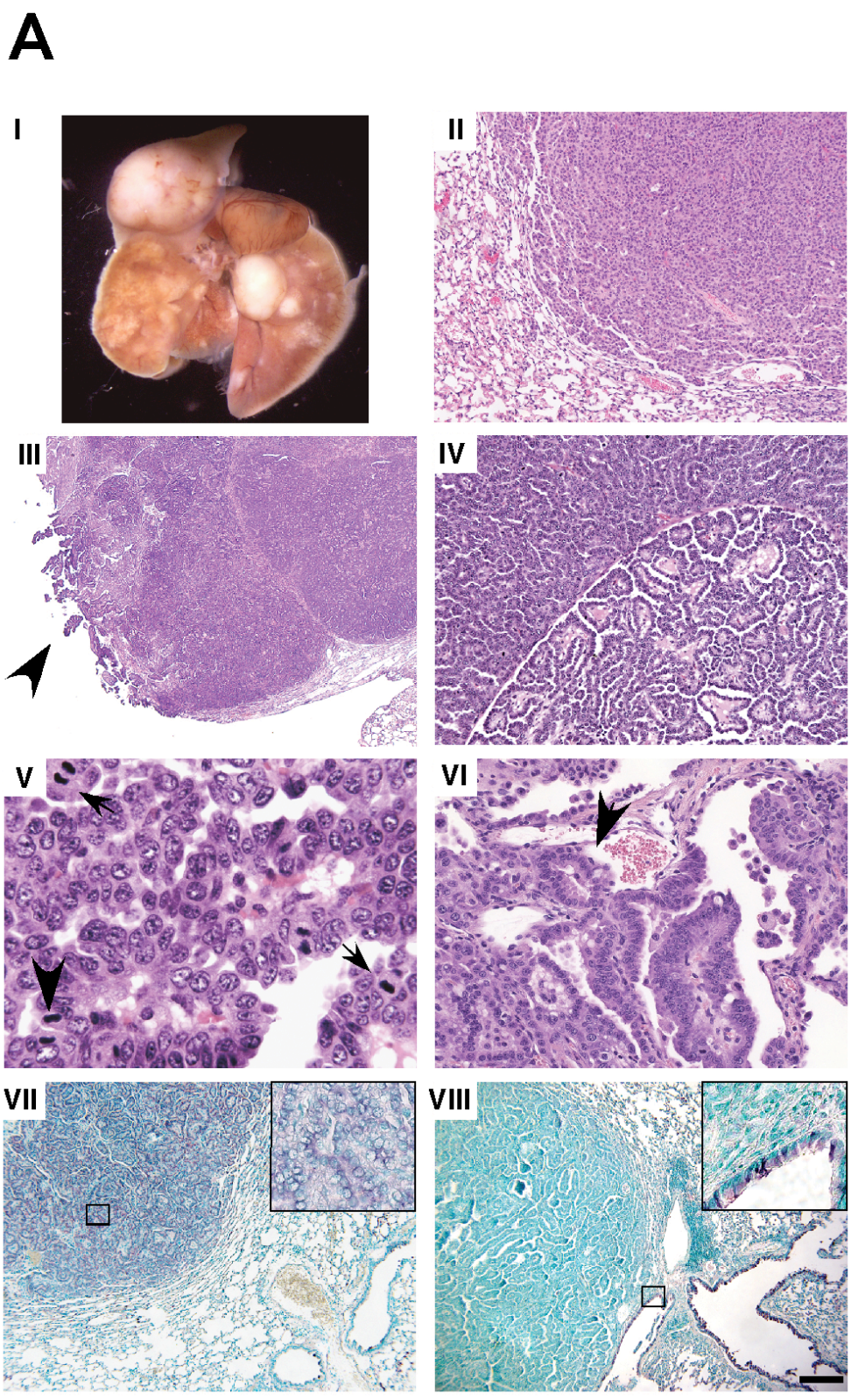
A
I
II
III
IV
V
VI
VII
VIII

Figure 2.2 (continued)

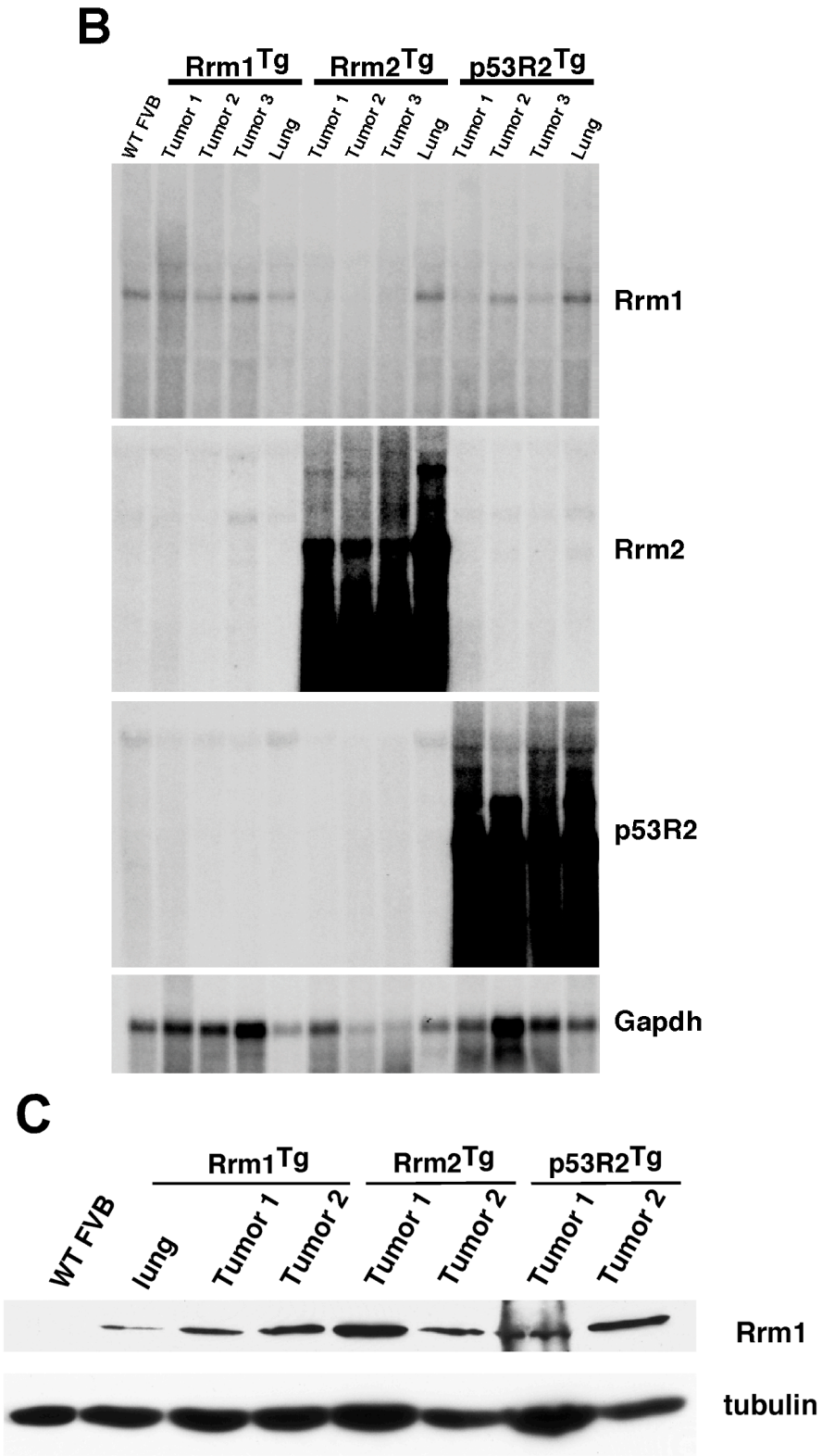

CC10 and negative for SP-C as expected. These results suggest that RNR-induced lung neoplasms arose from alveolar type II cells or their progenitors.

To confirm a causative role for RNR overexpression in lung carcinogenesis, we analyzed the expression of *Rrm1*, *Rrm2,* and *p53R2* in lung neoplasms by Northern (Fig. 2.2B) and Western (Fig. 2.1B) blotting. Lung neoplasms from $Rrm2^{Tg}$ and $p53R2^{Tg}$ animals showed prominent RNR overexpression, consistent with a causative role for RNR in the genesis of these lung lesions. By contrast, lung neoplasms from $Rrm1^{Tg}$ mice did not display high level transgene expression, providing further evidence that carcinogenesis in $Rrm2^{Tg}$ and $p53R2^{Tg}$ mice is highly specific. Overall, these data identify a novel oncogenic activity for the small RNR subunit.

Previous studies suggest that Rrm1 has tumor suppressor activity (Bepler et al., 2002; Fan et al., 1997; Gautam et al., 2003). Lung neoplasms in $Rrm2^{Tg}$ and $p53R2^{Tg}$ mice showed slightly lower *Rrm1* mRNA expression levels compared to normal lung tissues from these transgenic mice in Northern blot analysis (Fig 2.2B). In order to test whether enhanced lung tumorigenesis in $Rrm2^{Tg}$ or $p53R2^{Tg}$ mice is associated the down-regulation of Rrm1, we analyzed Rrm1 protein levels in lung neoplasms from RNR transgenic mice by western blotting. As shown in Fig. 2.2C, there was no difference in the expression of Rrm1 protein in these lung lesions induced by small RNR subunit overexpression, suggesting that lung tumorigenesis in $Rrm2^{Tg}$ and $p53R2^{Tg}$ mice is not due to down-regulated Rrm1 protein levels.

$Rrm1^{Tg}$ mice did not show increased lung carcinogenesis, which might be due to the fact that the R2 subunit is the limiting component of the enzyme. To test whether overexpression of the large subunit Rrm1 would enhance lung tumorigenesis induced by Rrm2 or p53R2 overexpression, we crossed $Rrm1^{Tg}$ mice to $Rrm2^{Tg}$ or $p53R2^{Tg}$ mice to generate RNR bi-transgenic mice. We established a cohort consisting of 14 $Rrm1^{Tg}Rrm2^{Tg}$, 9 $Rrm1^{Tg}p53R2^{Tg}$, 13 $Rrm1^{Tg}$ , 4 $Rrm2^{Tg}$, and 6 $p53R2^{Tg}$ mice, as

well as 9 transgene negative controls, and aged them until they exhibited clinical illness up to about 17 months. As shown in table 2.2, 93% (13/14) of *Rrm1*$^{Tg}$*Rrm2*$^{Tg}$ bi-transgenic mice developed spontaneous lung neoplasms, which was not significantly different than the lung tumor incidence in *Rrm2*$^{Tg}$ mice (100%, 4/4); similarly, 56% (5/9 ) of *Rrm1*$^{Tg}$*p53R2*$^{Tg}$ bi-transgenic mice exhibited lung neoplasms, which was not significantly different with lung tumor incidence of *p53R2*$^{Tg}$ mice (67% ; 4/6). Consistent with the data from the cohort of mice with the individual RNR transgenes, 22% (2/9) transgene negative control mice and 8% (1/13) *Rrm1*$^{Tg}$ transgenic mice developed spontaneous lung neoplasms. In addition, compared to *Rrm2*$^{Tg}$ mice, *Rrm1*$^{Tg}$*Rrm2*$^{Tg}$ bi-transgenic mice showed no differences in the frequency of multiple lung neoplasms and adenocarcinomas. Similarly, when compared to *p53R2*$^{Tg}$ mice, *Rrm1*$^{Tg}$*p53R2*$^{Tg}$ bi-transgenic mice showed no difference in lung tumor multiplicity. In addition, we did not observed an increased incidence of other tumor in these *Rrm1*$^{Tg}$*Rrm2*$^{Tg}$ and *Rrm1*$^{Tg}$*p53R2*$^{Tg}$ bi-transgenic mice as compared to either *Rrm2*$^{Tg}$ or *p53R2*$^{Tg}$ mice. These data suggest that the overexpression of the large RNR subunit does not enhance lung tumorigenesis induced by the small RNR subunit.

### 2.4.3 Increased mutation frequency following RNR overexpression in cultured 3T3 cells.

We hypothesized that RNR overexpression induced lung neoplasms through a mutagenic mechanism because defects in RNR allosteric control result in increased mutation frequencies in yeast and mammalian cells (Caras and Martin, 1988; Chabes et al., 2003a). To determine if RNR overexpression was similarly mutagenic, we generated *Rrm1*, *Rrm2*, or *p53R2* overexpressing 3T3 cell pools using the same expression constructs as used to generate the transgenic mice. Overexpression of

Table 2.2 Lung neoplasm characteristics in RNR bi-transgenic mice

| Mouse genotype | # of animals | Age (days) | % of mice with lung neoplasms | Average lung neoplasm size (mm)±SD | % of mice with multiple lung neoplasms | % of mice with lung adenocarcinoma | % of mice with other neoplasms[§] |
|---|---|---|---|---|---|---|---|
| *WT FVB*[†] | 9 | 508 | 22% | 8.0 ± 8.5 | 0% | 11% | 11% |
| $Rrm1^{Tg}$ | 13 | 466 | 8% | 6.00 ± 0 | 0% | 8% | 0% |
| $Rrm2^{Tg}$ | 4 | 489 | 100%* | 5.3 ± 3.3 | 100%* | 50%* | 25% |
| $p53R2^{Tg}$ | 6 | 516 | 67%* | 1.6 ± 1.1 | 50%* | 0% | 0% |
| $Rrm1^{Tg}$ $Rrm2^{Tg}$ | 14 | 427 | 93%* | 6.4 ± 2.9 | 100%* | 57%* | 21% |
| $Rrm1^{Tg}$ $p53R^{Tg}$ | 9 | 461 | 56%* | 4.7 ± 2.9 | 40%* | 30% | 33% |

NOTE: Mice were aged until moribund for about 500 days, euthanized by asphyxiation using carbon dioxide, and subjected to pathological examination as described in Materials and Methods.

[†]*WT FVB* refers to transgene-negative control mice.

*Statistically significant difference ($p<0.05$) relative to *WT FVB* mice. Incidences were compared by Chi-square analysis. Neoplasm sizes were compared by t-test analysis.

[§] Other neoplasms including lymphoma, ovary tumor, urinary bladder tumor.

individual RNR genes in these cell pools was confirmed by Northern and Western blotting (Fig. 2.3A and B). We then measured mutation frequency using the *Hprt* mutation detection assay, which identifies cells harboring *Hprt* mutations by virtue of their resistance to 6-thioguanine (6-TG) (Fenwick, 1985). In a representative experiment (Fig. 2.3C), a significantly increased mutation frequency was observed in a *Rrm2* overexpressing cell pool ($9.0 \times 10^{-6}$) as compared to *Rrm1* overexpressing or empty plasmid vector cell pools (less than $0.7 \times 10^{-6}$ and $0.8 \times 10^{-6}$, respectively). Three independent *Rrm2* overexpressing cell pools showed a consistently increased mutation frequency that was 9.9- to 16.0-fold greater than that observed for vector control cells. A *p53R2* overexpressing cell pool showed a more modestly but nevertheless significantly increased mutation frequency of $3.0 \times 10^{-6}$ (Fig. 2.3C). However, mutation frequency in *p53R2* overexpressing cells varied, with three *p53R2* overexpressing cell pools showing an elevated mutation frequency that was 4.2- to 11.2-fold greater than that for vector control cells while two other *p53R2* overexpressing cell pools displayed no increase in mutation frequency. Whether this variability is due to differences in expression levels between individual cell pools, or to the fact that the mutation frequencies measured were near the lower end of sensitivity for this assay, has not been determined. However, three independent *Rrm1* overexpressing cell pools and another five empty plasmid vector cell pools showed no detectable increase in mutation frequency.

Figure 2.3 Increased mutation frequency in RNR overexpressing NIH/3T3 cell pools. (A) Northern blot analysis of RNR expression in stable 3T3 cell pools transfected with either pCaggs empty vector or pCaggs RNR genes. Total RNA was extracted from the indicated cell lines and subjected to Northern blot hybridization with probes specific for Rrm1, Rrm2, p53R2, or Gapdh. (B) Western blot analysis of RNR protein expression in RNR overexpressing 3T3 cells. Total protein was extracted from the indicated cell lines and subjected to immunoblotting with antibodies specific to Rrm1, Rrm2, or p53R2. Duplicate membranes were immunoblotted for b-actin as a loading control. Samples in (A) and (B) were run on single blots, which were then cropped to remove extraneous lanes. (C) Mutation frequency at the Hprt locus in Rrm1, Rrm2 and p53R2 overexpressing 3T3 cells. Mutation frequency was determined by Hprt assay.

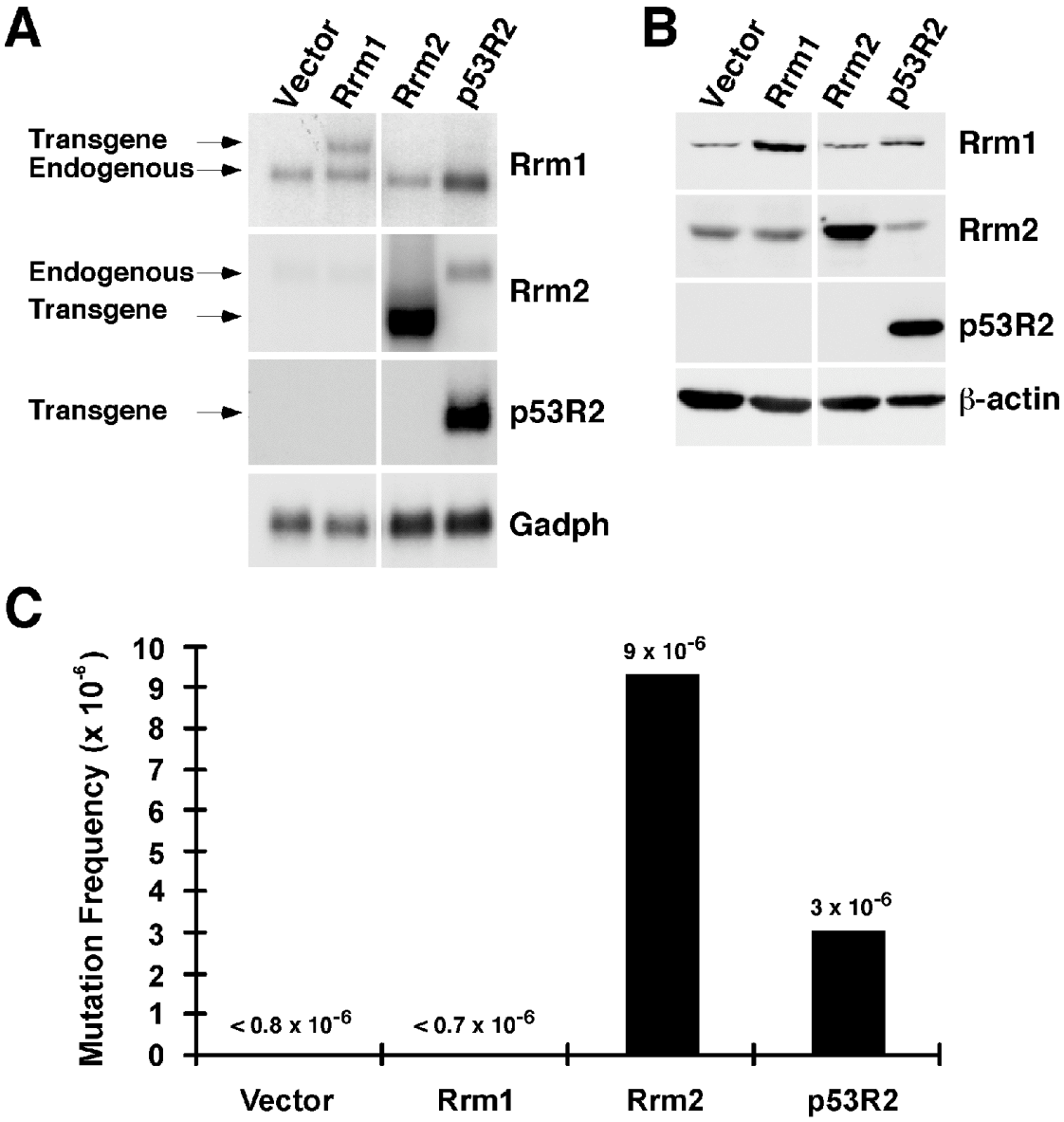
A
Vector
Rrm1
Rrm2
p53R2
Transgene
Endogenous
Rrm1
Endogenous
Transgene
Rrm2
Transgene
p53R2
Gadph
B
Vector
Rrm1
Rrm2
p53R2
Rrm1
Rrm2
p53R2
β-actin
C
Mutation Frequency (x 10-6)
10
9
8
7
6
5
4
3
2
1
0
9 x 10-6
3 x 10-6
< 0.8 x 10-6
< 0.7 x 10-6
Vector
Rrm1
Rrm2
p53R2

To determine the nature of the mutations conferring 6-TG resistance, we sequenced the *Hprt* gene from individual colonies (Wijnhoven et al., 2000). Interestingly, four of seven *Hprt* mutations from the *Rrm2* overexpressing cell pool shown in Fig. 2.3C were G→T substitutions (Table 2.3), which are relatively rare among reported spontaneous *Hprt* mutations (Zhang et al., 1992). Similar results were obtained in a separate experiment with an independent *Rrm2* overexpressing cell pool (Table 2.3). One of six mutations from the *p53R2* overexpressing cell pool shown in Fig. 2.3C also was a G→T mutation, but no G→T mutations were observed among six 6-TG resistant clones from a second independent experiment (Table 2.3). Collectively, the results indicate that overexpression of the small RNR subunit causes a mutator phenotype.

### 2.4.4 Combined defects in RNR regulation and MMR result in synergistic increases in mutagenesis and carcinogenesis.

To further evaluate a role for mutagenesis in RNR-induced lung carcinogenesis, we investigated whether combining RNR deregulation with a defect in MMR, the repair system that suppresses mutation accumulation, would cause a synergistic increase in mutagenesis and carcinogenesis. In eukaryotes, a complex of Msh2-Msh6 is responsible for recognizing base-base mispairs and single base insertion/deletions, while a Msh2-Msh3 complex detects larger insertion/deletion loops (Modrich, 2006). We first tested this hypothesis in *S. cerevisiae* by measuring the mutation rate by canavanine resistance assay in strains with deregulated RNR activity and mutations in MMR genes. To deregulate budding yeast RNR, we utilized the rnr1-D57N mutant in which a single amino acid change in the R1 activity site makes the enzyme insensitive to feedback inhibition by dATP

Table 2.3 Mutational spectrum at the *Hprt* locus in RNR overexpressing cell pools

| Cell pool | Clone ID | Mutation[†] | Amino acid change |
|---|---|---|---|
| Rrm2-A | 1 | 355 G>T | G>Stop codon |
| | 2 | 106 del G | Stop codon |
| | 3[§] | 568 G>T | G>Stop codon |
| | 4 | 602 A>G | D>G |
| | 5 | 403 ins AG | stop codon |
| Rrm2-B | 1 | 403-404 GA>TT[‡] | D>F |
| | 2 | 584 A>C | Y>S |
| | 3 | 613 G>T | V>F |
| | 4[§] | 403-404 GA>TT[‡] | D>F |
| | 5[§] | 389 T>G | V>G |
| | 6[§] | 584 A>C | Y>S |
| | 7 | 403-404 GA>TT[‡] | D>F |
| p53R2-A | 1 | 643 A>G | K>E |
| | 2 | 581 A>T | D>V |
| | 3[§] | 542 T>C | F>S |
| | 4 | 581 A>T | D>V |
| | 5 | 530 A>G | D>G |
| | 6 | 542 T>C | F>S |
| p53R2-B | 1[§] | 586 A>G | N>D |
| | 2 | 586 A>G | N>D |
| | 3 | 635 G>A | G>E |
| | 4 | 409 A>T | I>F |
| | 5[§] | 609-626 del | Stop codon |
| | 6 | 544 G>T | E>Stop codon |

NOTE: 6-thioguanine resistant colonies were isolated and expanded from the indicated cell pools. RNA was extracted for cDNA synthesis and the *Hprt* gene coding region was amplified by PCR. Mutations in the *Hprt* cDNA were identified by directly sequencing PCR products. These data represent results from two independent experiments done with independent RNR overexpressing cell pools (A and B). The mutation frequencies shown in Fig. 1C are for cell pools Rrm2-B and p53R2-B.

[†]The numerical value indicates the position of the mutated nucleotide followed by the specific sequence change.

[§]Additional, independent colonies on the same plate had the same mutation as these clones and were excluded as clonal events.

[‡]These clones also expressed low levels of a smaller transcript that had a deletion of nucleotides 403-470.

(Caras and Martin, 1988). Consistent with published reports (Chabes et al., 2003a), *rnr1-D57N* yeast exhibited a 3.4-fold increase in mutation rate relative to the wild-type strain, which had a mutation rate of 1.5 X $10^{-7}$ (Fig. 2.4). MMR defective strains also displayed elevated mutation rates (*msh2Δ*: 28.4-fold; *msh3Δ*: 2.9-fold; *msh6Δ*: 9.8-fold), similar to previous reports (Lau et al., 2002). Notably, *rnr1-D57N msh2Δ* and *rnr1-D57N msh6Δ* double mutants displayed approximately multiplicative increases in mutation rate relative to the single mutants (61.4-fold and 23.8-fold, respectively). Multiplicative increases in mutagenesis are seen for mutations that affect factors acting in series in a common pathway (Morrison et al., 1993), suggesting that the Msh2-Msh6 complex corrects DNA mismatches induced by RNR deregulation. By contrast, combining *rnr1-D57N* with *msh3Δ* resulted in only an additive increase in mutation rate (*rnr1-D57N msh3Δ:* 3.9-fold). The spectrum of mutations arising in *WT*, *rnr1-D57N, msh2Δ*, and *msh6Δ* strains was consistent with previous publications (Chabes et al., 2003a; Lau et al., 2002; Marsischky et al., 1996) and included primarily base substitutions, as well as frameshift mutations for *msh2Δ* (Table 2.4). The frequency of frameshift mutations involving single nucleotide insertions or deletions was substantially increased in *rnr1-D57N msh2Δ* and *rnr1-D57N msh6Δ* strains relative to the single mutants.

The synergistic effects of RNR deregulation and MMR deficiency on mutation rates in yeast prompted us to further test genetic interactions between RNR and MMR in mice, by crossing RNR transgenic mice with *Msh6*-null mice (Edelmann et al., 1997). If RNR overexpression induces lung carcinogenesis through a mutagenic mechanism, *Msh6* deficiency would be predicted to accelerate lung carcinogenesis in RNR transgenic mice. A cohort of $Msh6^{-/-}$, $Msh6^{+/-}$, or $Msh6^{+/+}$ mice that also carried either the *Rrm2* or *p53R2* transgene was established and examined for survival and cancer susceptibility. Interestingly, the median lifespan for $Msh6^{-/-}p53R2^{Tg}$ mice (136

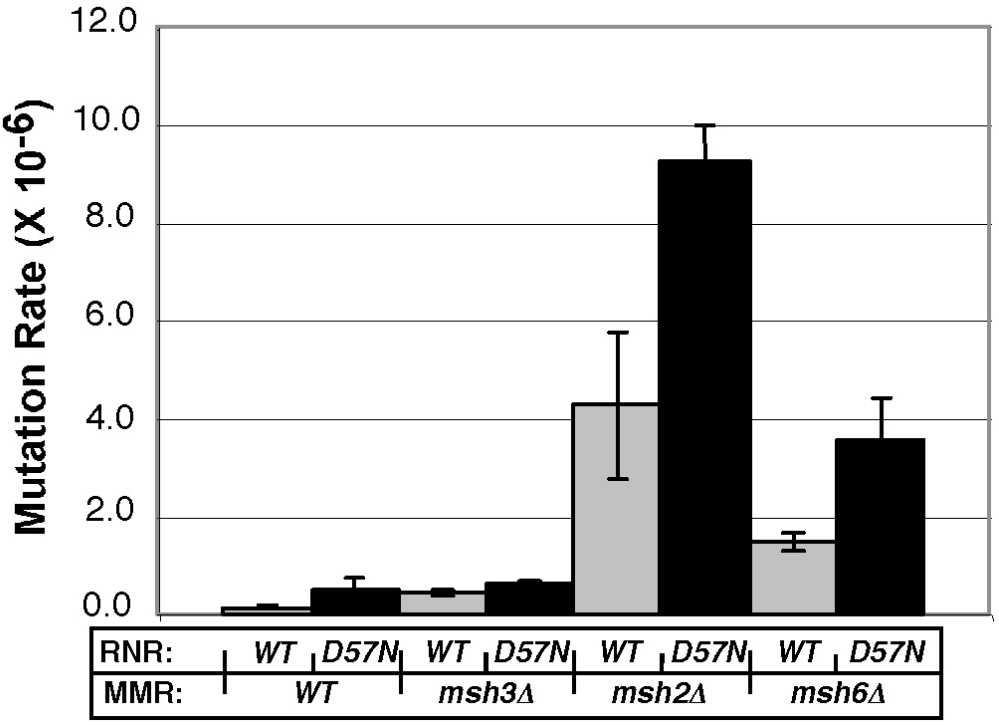


Figure 2.4 Genetic interactions between RNR and mismatch repair in yeast. Canavanine mutation rate assay for *RNR1(WT)* and *rnr1-D57N* strains on MMR-deficient backgrounds (*msh3Δ*, *msh2Δ*, *msh6Δ*, or WT) of *S. cerevisiae*. The forward mutation rate (per generation) to canavanine resistance was measured for the indicated single and double mutant combinations. Error bars show the 95% confidence interval.

Table 2.4. Mutational spectrum at the *CAN1* locus in *wild-type* and *rnr1-D57N* yeast strains that vary in mismatch repair status

| Type of mutation | *WT* (4C) | | *rnr1-D57N* (8C) | | *msh2Δ* (4C/98) | | *msh6Δ* (4C/108) | | *rnr1-D57N msh2Δ* (8C/98) | | *rnr1-D57N msh6Δ* (8C/108) | |
|---|---|---|---|---|---|---|---|---|---|---|---|---|
| | # | % | # | % | # | % | # | % | # | % | # | % |
| Base substitution | | | | | | | | | | | | |
| GC pair | 6 | 55% | 10 | 63% | 4 | 31% | 15 | 68% | 3 | 18% | 14 | 37% |
| AT pair | 3 | 27% | 3 | 19% | 2 | 15% | 3 | 14% | 0 | 0% | 8 | 21% |
| Frame shift | | | | | | | | | | | | |
| Deletion | 1 | 9% | 1 | 6% | 6 | 46% | 1 | 5% | 4 | 24% | 12 | 32% |
| Insertion | 0 | 0% | 2 | 12% | 1 | 8% | 3 | 14% | 10 | 59% | 4 | 11% |
| Large deletion | 1 | 9% | 0 | 0% | 0 | 0% | 0 | 0% | 0 | 0% | 0 | 0% |
| Total | 11 | 100% | 16 | 100% | 13 | 100% | 22 | 100% | 17 | 100% | 38 | 100% |

NOTE: The *CAN1* gene was PCR amplified from Can$^r$ colonies and directly sequence.

days) was significantly reduced compared to that of transgene-negative *Msh6*$^{-/-}$ mice (258 days; $p<0.05$; logrank test) (Fig. 2.5). The reduced survival of *Msh6*$^{-/-}$*p53R2*$^{Tg}$ mice was associated with early onset lymphomagenesis (Table 2.5). Because these *Msh6*$^{-/-}$*p53R2*$^{Tg}$ mice died at a young age, we could not evaluate whether *Msh6* deficiency cooperated with *p53R2* overexpression in inducing lung neoplasms. The survival rate for *Msh6*$^{-/-}$*Rrm2*$^{Tg}$ and transgene negative *Msh6*$^{-/-}$ mice was not significantly different ($p=.975$; logrank test), suggesting that *Rrm2* overexpression, unlike *p53R2* overexpression, did not enhance lymphomagenesis (Fig. 2.5). However, that 90% of *Msh6*$^{-/-}$*Rrm2*$^{Tg}$ mice had developed lung neoplasms despite their shortened lifespan of approximately 10 months was suggestive of a synergistic genetic interaction (Table 2.5). To directly test whether lung carcinogenesis was accelerated in *Msh6*$^{-/-}$*Rrm2*$^{Tg}$ mice, we sacrificed a cohort of *Msh6*$^{-/-}$*Rrm2*$^{Tg}$ mice and littermate controls at 6 months of age. 3 of 18 *Msh6*$^{+/+}$*Rrm2*$^{Tg}$ mice and 3 of 17 *Msh6*$^{+/-}$*Rrm2*$^{Tg}$ mice had developed lung neoplasms by 6 months, while no lung neoplasms were observed in transgene-negative *Msh6*$^{+/+}$ or *Msh6*$^{+/-}$ littermates (Table 2.6). Lung neoplasms were also observed in 2 of 13 *Msh6*$^{-/-}$ mice. *Msh6* deficiency strongly accelerated *Rrm2*-induced lung carcinogenesis, as 13 of 13 *Msh6*$^{-/-}$*Rrm2*$^{Tg}$ mice developed lung neoplasms by 6 months of age, with 9 of these mice carrying multiple lung neoplasms.

To determine whether combining RNR overexpression with MMR deficiency would increase mutation frequency *in vivo*, we analyzed the mutation frequency at the λ phage *cII* locus in lung tissue from 3 month old *RNR*$^{Tg}$ mice, with or without *Msh6* deficiency, using the Big Blue transgene system (Jakubczak et al., 1996). There was no difference in mutation frequency in RNR transgenic mice as compared to wild-type mice (Fig. 2.6A and Table 2.7), possibly because the Big Blue system is relatively insensitive due to a high background mutation frequency. However, the mutation

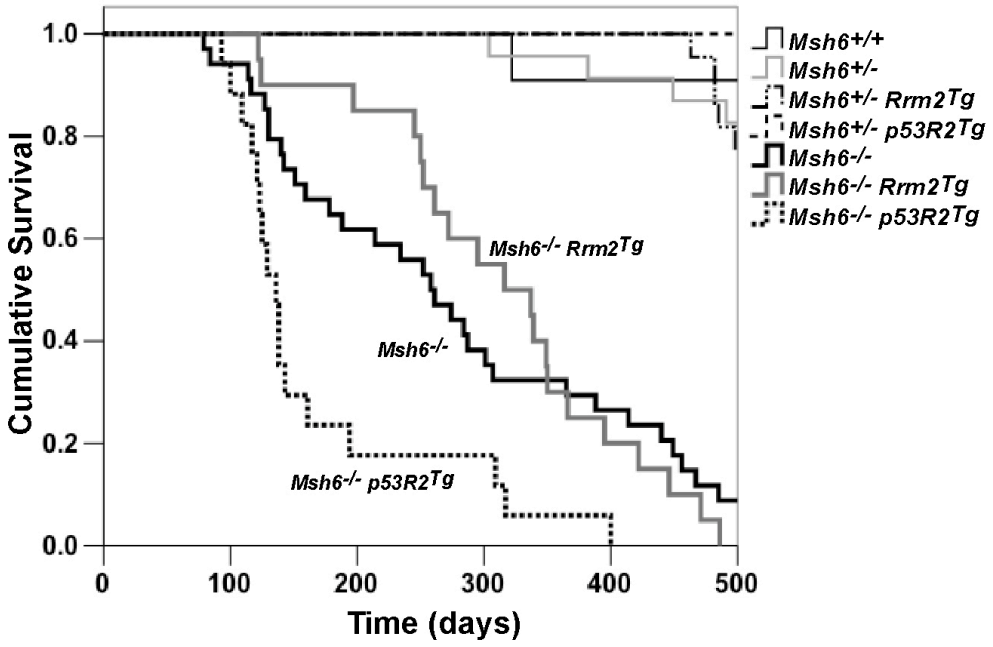


Figure 2.5 Genetic interactions between RNR and mismatch repair in mice. Survival curves for *Msh6*$^{-/-}$*RNR*$^{Tg}$ *(Rrm2*$^{Tg}$ *or p53R2*$^{Tg}$*)* mice. Mice were aged until moribund for up to 17 months. Survival curves were generated using SPSS software. The following number of animals was analyzed for each genotype: *Msh*$^{+/+}$ (11), *Msh6*$^{+/-}$ (23), *Msh6*$^{+/-}$ *Rrm2*$^{Tg}$ (22), *Msh6*$^{+/-}$*p53R2*$^{Tg}$ (11), *Msh6*$^{-/-}$ (34), *Msh6*$^{-/-}$*Rrm2*$^{Tg}$ (20), *Msh6*$^{-/-}$ *p53R2*$^{Tg}$ (17).

Table 2.5 Combining RNR overexpression with mismatch repair deficiency results in a synergistic increase in tumorigenesis

| Mouse genotype | Number of animals | Median age of death | Number of mice with lung neoplasms (%) | Number of mice with lymphoma (%) | Number of mice with other neoplasms[†] (%) |
|---|---|---|---|---|---|
| *Msh6*$^{-/-}$ *p53R2*$^{Tg}$ | 17 | 136 | 4 (24%) | 16 (94%) | 2 (12%) |
| *Msh6*$^{-/-}$ *Rrm2*$^{Tg}$ | 20 | 316 | 18 (90%) | 15 (75%) | 7 (35%) |
| *Msh6*$^{-/-}$ | 34 | 258 | 12 (35%) | 29 (85%) | 8 (24%) |
| *Msh6*$^{+/-}$ *p53R2*$^{Tg}$ | 11 | 519 | 4 (36%) | 0 (0%) | 1 (9%) |
| *Msh6*$^{+/-}$ *Rrm2*$^{Tg}$ | 22 | 510 | 21 (96%) | 1 (5%) | 2 (9%) |
| *Msh6*$^{+/-}$ | 23 | 518 | 6 (26%) | 3 (13%) | 0 (0%) |
| *Msh6*$^{+/+}$ *p53R2*$^{Tg}$ | 4 | 519 | 2 (50%) | 0 (0%) | 1 (25%) |
| *Msh6*$^{+/+}$ *Rrm2*$^{Tg}$ | 2 | 503 | 2 (100%) | 0 (0%) | 0 (0%) |
| *Msh6*$^{+/+}$ | 11 | 518 | 3 (27%) | 0 (0%) | 2 (18%) |

NOTE: Mice were aged for up to 17 months, euthanized by asphyxiation using carbon dioxide, and subjected to pathological examination as described in Materials and Methods.

[†]Other neoplasms include gastrointestinal, liver, skin, and uterine neoplasms.

Table 2.6. Combining RNR overexpression with mismatch repair deficiency results in a synergistic increase in lung carcinogenesis

| Mouse genotype | # of animals | % of mice with lung neoplasms | % of mice with multiple lung neoplasms | # of lung neoplasms per mouse† ±SD | Average lung neoplasm size (mm)±SD | % of mice with lymphoma |
|---|---|---|---|---|---|---|
| *Msh6*$^{-/-}$*Rrm2*$^{Tg}$ | 13 | 100%* | 69%* | 2.9 ± 1.99 | 1.30 ± 0.54 | 31% |
| *Msh6*$^{-/-}$ | 13 | 15% | 0% | 1.0 ± 0 | 1.25 ± 1.06 | 8% |
| *Msh6*$^{+/-}$*Rrm2*$^{Tg}$ | 17 | 18% | 0% | 1.0 ± 0 | 0.73 ± 0.68 | 12% |
| *Msh6*$^{+/-}$ | 10 | 0% | 0% | N/A | N/A | 0% |
| *Msh6*$^{+/+}$*Rrm2*$^{Tg}$ | 18 | 17% | 6% | 1.33 ± 0.58 | 1.23 ± 0.25 | 0% |
| *Msh6*$^{+/+}$ | 14 | 0% | 0% | N/A | N/A | 0% |

NOTE: Mice were aged for 6 months, euthanized by asphyxiation using carbon dioxide, and subjected to pathological examination as described in Materials and Methods. Only mice that lived to 6 months were included. Four *Msh6*$^{-/-}$*Rrm2*$^{Tg}$ mice died before 6 months due to lymphoma, one of which also had a lung neoplasm. Four *Msh6*$^{-/-}$ mice died before 6 months due to lymphoma.

†Values refer to the average number of lung neoplasms per mouse among tumor-bearing animals only.

*Statistically significant difference ($p<0.01$) relative to *Msh6*$^{-/-}$, *Msh6*$^{+/-}$*Rrm2*$^{Tg}$, or *Msh6*$^{+/+}$*Rrm2*$^{Tg}$ mice as determined by Fisher's Exact test.

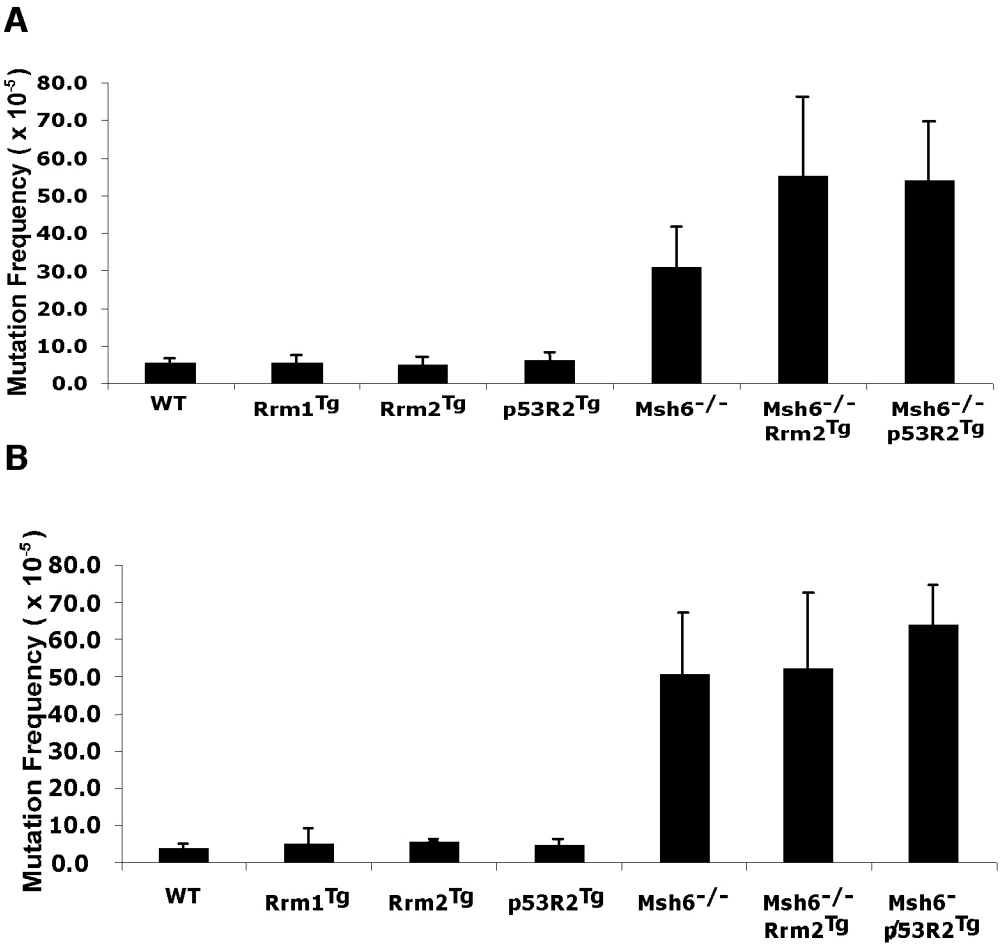


Figure 2.6 Synergistic effect on mutagenesis when combining RNR and mismatch repair defects in mice. Mutation frequency at the λ cII locus in lung (A) or spleen (B) tissues from RNR overexpressing and control mice. Genomic DNA was isolated from 3-month old mice of the indicated genotypes and packaged into infectious phage. Mutation frequency was determined based on the ratio of the number of mutant phage obtained to the total number of phage analyzed.

Table 2.7. Analysis of mutation frequencies at the *cII* locus of a bacteriophage l transgene in lung tissue from Msh6$^{-/-}$ RNR$^{Tg}$ and control mice

| Stain | Animal ID | Age (days) | Sex | Total number of plaques | Number of mutants | Mutation frequency | Mutation frequency (Avg ± SD) |
|---|---|---|---|---|---|---|---|
| *WT* | 6378 | 90 | F | 341550 | 16 | 4.7 | 5.5±1.3 |
| | 6394 | 98 | M | 366948 | 23 | 6.2 | |
| | 6469 | 102 | M | 579466 | 25 | 4.3 | |
| | 6793 | 92 | F | 264000 | 20 | 7.6 | |
| | 6830 | 91 | M | 269500 | 11 | 4.1 | |
| | 6864 | 93 | F | 363000 | 17 | 4.7 | |
| | 3682 | 95 | M | 286000 | 18 | 6.3 | |
| *Rrm1*$^{Tg}$ | 6380 | 90 | F | 260000 | 10 | 3.8 | 5.4±1.9 |
| | 6468 | 102 | M | 332133 | 23 | 6.9 | |
| | 6470 | 102 | M | 341000 | 9 | 2.6 | |
| | 6465 | 133 | F | 284715 | 21 | 7.4 | |
| | 6466 | 133 | F | 264000 | 16 | 6.1 | |
| | 6832 | 91 | M | 260333 | 15 | 5.8 | |
| *Rrm2*$^{Tg}$ | 6395 | 98 | M | 247250 | 14 | 5.7 | 5.0±2.0 |
| | 6397 | 98 | M | 173600 | 14 | 8.1 | |
| | 6895 | 93 | M | 418000 | 29 | 6.9 | |
| | 6896 | 93 | M | 286000 | 11 | 3.8 | |
| | 6900 | 93 | F | 82830 | 4 | 4.8 | |
| | 3681 | 95 | M | 363000 | 11 | 3.0 | |
| | 3463 | 96 | M | 341667 | 10 | 2.9 | |
| *p53R2*$^{Tg}$ | 6359 | 57 | F | 463833 | 23 | 4.9 | 6.5±1.6 |
| | 6790 | 93 | F | 402800 | 35 | 8.7 | |
| | 6862 | 92 | F | 198000 | 13 | 6.6 | |
| | 3378 | 91 | F | 423333 | 24 | 5.7 | |
| *Msh6*$^{-/-}$ | 3676 | 95 | F | 357500 | 78 | 21.8 | 31.3±1.4 |
| | 3750 | 96 | F | 455000 | 133 | 29.2 | |
| | 3752 | 96 | M | 220000 | 92 | 41.8 | |
| *Msh6*$^{-/-}$ *Rrm2*$^{Tg}$ | 3163 | 102 | M | 363000 | 156 | 43.0 | 55.2±20.9 |
| | 3461 | 96 | F | 223333 | 189 | 84.6 | |
| | 3467 | 96 | M | 671667 | 256 | 38.1 | |
| | 3677 | 95 | F | 263333 | 145 | 55.1 | |
| *Msh6*$^{-/-}$ *p53R2*$^{Tg}$ | 3321 | 102 | F | 352000 | 128 | 36.4 | 54.0±15.4 |
| | 3749 | 96 | F | 290000 | 176 | 60.7 | |
| | 3751 | 96 | F | 315000 | 204 | 64.8 | |

NOTE: Genomic DNA was isolated from the lungs of 3-month old mice and l vector was then packaged into phage. The number of mutants was derived from raw counts of mutant plaques.

frequency in *Msh6*$^{-/-}$*Rrm2*$^{Tg}$ (55.2 ± 20.9 x $10^{-5}$) and *Msh6*$^{-/-}$*p53R2*$^{Tg}$ (54.0 ± 15.4 x $10^{-5}$) lung tissues was consistently higher than that in *Msh6*$^{-/-}$ lung tissue (31.1 ± 10.4 x $10^{-5}$), although these differences were not statistically significant. By contrast, the mutation frequency was similar in spleen tissue from *Msh6*$^{-/-}$*Rrm2*$^{Tg}$ (52.0 ± 20.1 x $10^{-5}$) and *Msh6*$^{-/-}$ (50.5 ± 16.3 x $10^{-5}$) mice, but slightly elevated in *Msh6*$^{-/-}$*p53R2*$^{Tg}$ (63.7 ± 10.7 x $10^{-5}$) animals (Fig. 2.6B and Table 2.8). Together, these results indicate that MMR deficiency synergizes with RNR overexpression in a tissue specific manner to increase mutagenesis and carcinogenesis.

### 2.4.5 RNR-induced lung neoplasms display a unique signature of *K-ras* activating mutations.

A mutagenic mechanism implies that RNR overexpression triggers additional genetic alterations while promoting tumor development. Because mutations in codons 12 and 61 of the *K-ras* proto-oncogene are often observed in human and mouse lung cancers (Mills et al., 1995; You et al., 1989), we examined the frequency of *K-ras* mutations in microdissected lung neoplasms from the RNR cohort. 100% of *Rrm2*-induced lung neoplasms and 79% of *p53R2*-induced lung neoplasms carried *K-ras* activating mutations (Table 2.9), indicating that RNR-induced lung carcinogenesis frequently involves *K-ras* activating mutations. 56% and 100% of the rare lung neoplasms from transgene-negative control and *Rrm1*$^{Tg}$ mice, respectively, also had *K-ras* mutations.

Sequence analysis revealed that the lung neoplasms from *Rrm2*$^{Tg}$ and *p53R2*$^{Tg}$ mice exhibited distinct mutation spectra relative to those from transgene-negative and *Rrm1*$^{Tg}$ mice (Table 2.10). In particular, 50% of the *K-ras* codon 12 mutations from *Rrm2*-induced lung neoplasms were G→T transversions (GGT→GTT, G12V), as were 30% of those from *p53R2*-induced lung neoplasms. By contrast, lung neoplasms

Table 2.8. Analysis of mutation frequencies at the *cII* locus of a bacteriophage l transgene in spleen tissue from Msh6$^{-/-}$ RNR$^{Tg}$ and control mice

| Stain | Animal ID | Age (days) | Sex | Total number of plaques | Number of mutants | Mutation frequency | Mutation frequency (Avg ± SD) |
|---|---|---|---|---|---|---|---|
| *WT* | 6378 | 90 | F | 173844 | 8 | 4.6 | 3.8 ± 0.9 |
| | 6394 | 98 | M | 599500 | 24 | 4.0 | |
| | 4020 | 101 | M | 108333 | 3 | 2.8 | |
| *Rrm1*$^{Tg}$ | 6380 | 90 | F | 292230 | 5 | 1.7 | 4.9 ± 3.9 |
| | 6468 | 102 | M | 270000 | 25 | 9.3 | |
| | 6470 | 102 | M | 373000 | 14 | 3.8 | |
| *Rrm2*$^{Tg}$ | 6395 | 98 | M | 225500 | 13 | 5.8 | 5.6 ± 0.3 |
| | 6397 | 98 | M | 198000 | 11 | 5.6 | |
| | 3463 | 96 | M | 226667 | 12 | 5.3 | |
| *p53R2*$^{Tg}$ | 3754 | 96 | M | 335000 | 9 | 2.7 | 4.4± 1.5 |
| | 3378 | 91 | F | 350000 | 20 | 5.7 | |
| | 6790 | 92 | F | 165000 | 8 | 4.8 | |
| *Msh6*$^{-/-}$ | 3676 | 95 | F | 261750 | 78 | 29.8 | 50.5 ± 16.3 |
| | 3750 | 96 | F | 111000 | 65 | 58.6 | |
| | 2431 | 100 | M | 135000 | 91 | 67.4 | |
| | 3752 | 96 | M | 216667 | 100 | 46.2 | |
| *Msh6*$^{-/-}$ *Rrm2*$^{Tg}$ | 3163 | 102 | M | 335000 | 114 | 34.0 | 52.0 ± 20.1 |
| | 3461 | 96 | F | 116000 | 45 | 38.8 | |
| | 3467 | 96 | M | 149667 | 117 | 78.2 | |
| | 3677 | 95 | F | 198333 | 113 | 57.0 | |
| *Msh6*$^{-/-}$ *p53R2*$^{Tg}$ | 3321 | 102 | F | 138350 | 80 | 57.8 | 63.7 ±10.7 |
| | 3749 | 96 | F | 136667 | 104 | 76.1 | |
| | 3751 | 96 | F | 141667 | 81 | 57.9 | |

NOTE: Genomic DNA was isolated from the spleen of 3-month old mice and λ vector was then packaged into phage. The number of mutants was derived from raw counts of mutant plaques.

Table 2.9. Mutations in *K-ras* codons 12 and 61 in lung tumors from RNR transgenic mice

| Mouse genotype | # of neoplasms analyzed | # of mutations in *K-ras* | | |
|---|---|---|---|---|
| | | Codon 12 (%) | Codon 61 (%) | Total (%) |
| *WT FVB*[†] | 9 | 2 (22%) | 3 (33%) | 5 (56%) |
| $Rrm1^{Tg}$ | 4 | 4 (100%) | 0 (0%) | 4 (100%) |
| $Rrm2^{Tg}$ | 12 | 6 (50%) | 6 (50%) | 12 (100%) |
| $p53R2^{Tg}$ | 14 | 7 (50%) | 4 (29%) | 11 (79%) |

NOTE: DNA was extracted from lung neoplasm tissue isolated by laser microdissection. *K-ras* exons 1 and 2 were amplified by PCR and then directly sequenced.

[†]*WT FVB* refers to transgene-negative control mice.

Table 2.10. Mutational spectrum at *K-ras* codons 12 and 61 in RNR-induced and control lung neoplasms

| Genotype | Tumor | Mutations in codon 12 | Mutations in codon 61 |
|---|---|---|---|
| *WT FVB* (N=9) | 1234 | G12D, GGT>GAT | None |
| | 4738 | G12D, GGT>GAT | None |
| | 3427 | None | Q61R, CAA>CGA |
| | 3855 | None | Q61R, CAA>CGA |
| | 1579 | None | Q61R, CAA>CGA |
| | 3352 | None | None |
| | 4741 | None | None |
| | 1417 | None | None |
| | 1575 | None | None |
| *Rrm1*$^{Tg}$ (N=4) | 4737 | G12D, GGT>GAT | None |
| | 5804 | G12D, GGT>GAT | None |
| | 984 | G12D, GGT>GAT | None |
| | 1416 | G12D, GGT>GAT | None |
| *Rrm2*$^{Tg}$ (N=12) | 6956 | G12D, GGT>GAT | None |
| | 791 | G12D, GGT>GAT | None |
| | 1577 | G12V, GGT>GTT | None |
| | 5485 | G12R , GGT>CGT | None |
| | 792 | G12V, GGT>GTT | None |
| | 1164 | G12V, GGT>GTT | None |
| | 1162 | None | Q61R, CAA>CGA |
| | 1166 | None | Q61R, CAA>CGA |
| | 1161 | None | Q61H, CAA>CAT |
| | 6071 | None | Q61H, CAA>CAT |
| | 1322 | None | Q61L, CAA>CTA |
| | 3892 | None | Q61L, CAA>CTA |
| *p53R2*$^{Tg}$ (N=14) | 3114 | G12D, GGT>GAT | None |
| | 1233 | G12D, GGT>GAT | None |
| | 3428 | G12D, GGT>GAT | None |
| | 3432 | G12D, GGT>GAT | None |
| | 908 | G12R, GGT>CGT | None |
| | 909 | G12V, GGT>GTT | None |
| | 905 | G12V, GGT>GTT | None |
| | 4817 | None | Q61R, CAA>CGA |
| | 3117 | None | Q61R, CAA>CGA |
| | 3353 | None | Q61R, CAA>CGA |
| | 1225 | None | Q61H, CAA>CAT |
| | 904 | None | None |
| | 3113 | None | None |
| | 907 | None | None |

NOTE: DNA was extracted from lung neoplasm tissue isolated by laser microdissection. *K-ras* exons 1 and 2 were amplified by PCR and then directly.

from transgene-negative and *Rrm1*$^{Tg}$ mice showed exclusively G→A transitions (GGT→GAT, G12D) in *K-ras* codon 12. We conclude that *K-ras* activating mutations, common events in lung carcinogenesis, are central to *Rrm2*- and *p53R2*-induced lung carcinogenesis and arise through a mechanism that appears distinct from that underlying spontaneous lung tumor development in wild-type animals. Alterations in the *p53* tumor suppressor gene are also common in human lung cancer (Chiba et al., 1990). The majority of these alterations are missense mutations that result in the accumulation of high levels of mutant p53 protein. Other mutations in p53 gene confer the loss of p53 expression. To investigate whether aberrant expression of p53 is associated with these RNR-induced lung neoplasms, we analyzed p53 expression levels in lung neoplasms by western blotting. As shown in Fig 2.7, there was no difference in p53 expression levels in these RNR-induced lung neoplasms compared to normal lung from *RNR*$^{Tg}$ or transgene negative control mice. This result suggests that p53 mutations may not be a common event in RNR-induced lung tumorigenesis.

**2.5 Discussion**

RNR enzyme activity has long been positively correlated with cancer cell division (Elford et al., 1970), and RNR inhibition is an effective strategy for suppressing tumor proliferation and survival (Shao et al., 2006). Yet, investigation of the effects of RNR deregulation in animal models has been incomplete. We report that overexpression of *Rrm2* or *p53R2* specifically induces lung but not other neoplasms at high frequency in transgenic mice. Previous studies indicated that human RRM2 has transforming activity in cultured cells (Fan et al., 1996), while p53R2 has been suggested to have tumor suppressor activity based on its regulation by p53 and its role in the DNA damage response (Tanaka et al., 2000). RNR may be an example of a

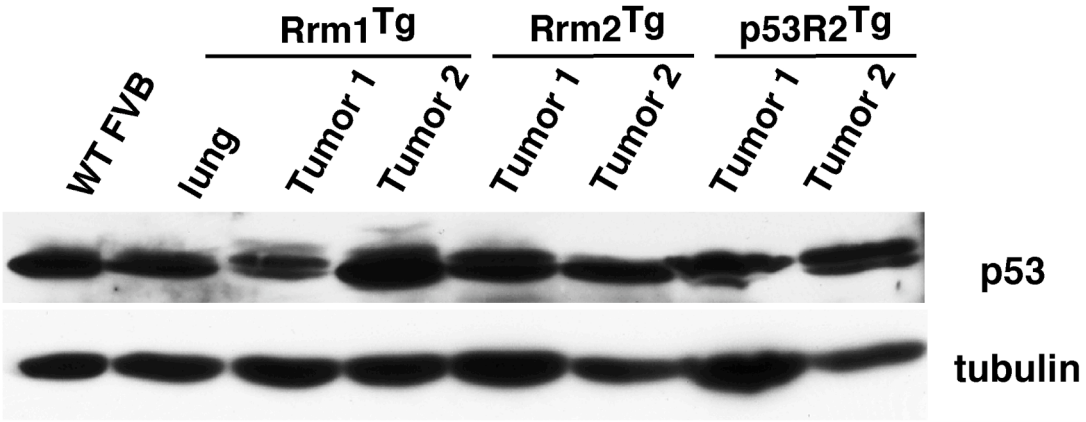


Figure 2.7 p53 expression in RNR-induced lung neoplasms. Western blotting analysis of p53 expression in lung neoplasms (Tumor 1, Tumor 2) or normal lung tissues (lung) from RNR transgenic mice as well as normal lung from wild-type FVB mice (WT FVB). Total protein was subjected to immunoblotting with antibody specific to p53 or α-tubulin as loading control.

growth regulator that has dual roles both as a tumor suppressor and oncogene. While impaired RNR function can trigger genomic instability by limiting nucleotide availability for DNA replication and repair purposes, RNR hyperactivity may be equally detrimental due to its mutagenic effects. Interestingly, the genomic regions containing human *RRM2* (2p25-2p24) and *p53R2* (8q23.1) are commonly amplified in human lung cancers (Goeze et al., 2002; Lui et al., 2001; Pei et al., 2001; Wong et al., 2003), raising the possibility that RNR deregulation might have a causative role in human lung carcinogenesis. Because RNR is a DNA damage-inducible enzyme, our results also suggest that increased RNR levels due to chronic DNA damage in the lungs of smokers may contribute to tumor development.

In contrast to $Rrm2^{Tg}$ and $p53R2^{Tg}$ mice, $Rrm1^{Tg}$ mice did not show increased lung carcinogenesis. In addition, $Rrm1^{Tg}Rrm2^{Tg}$ and $Rrm1^{Tg}p53R2^{Tg}$ mice did not show enhanced lung carcinogenesis compared to $Rrm2^{Tg}$ and $p53R2^{Tg}$ mice. This might be due to the relatively limited overexpression of the *Rrm1* transgene. or the fact that the R2 subunit is the limiting component of the enzyme (Engstrom et al., 1985; Mann et al., 1988). However, Rrm1 demonstrates tumor suppressor activity both in cultured cells and human lung cancer patients (Fan et al., 1997; Gautam et al., 2003; Zheng et al., 2007). Consistent with our findings, *Rrm1* overexpression in another mouse model also did not result in any overt spontaneous phenotypes and instead was reported to suppress chemical carcinogenesis in the lung (Gautam and Bepler, 2006). Thus, lung tumor induction might be specific to the small RNR subunit and independent of RNR enzyme activity.

We determined that RNR-induced lung tumorigenesis proceeded through a mutagenic mechanism. Overexpression of *Rrm2* or *p53R2*, but not *Rrm1*, in 3T3 cells resulted in a significant increase in mutation frequency. Additional experiments in

budding yeast indicated that MMR normally corrects base mispairs that arise due to RNR deregulation, as multiplicative increases in mutation rate were observed when the allosteric site mutant *rnr1-D57N* was combined with MMR gene mutations. A similar genetic interaction between RNR and MMR was observed in mice. *Msh6*-null mice develop primarily lymphoma (Edelmann et al., 1997), and *p53R2* overexpression cooperated with *Msh6*-deficiency to cause an earlier onset of lymphomagenesis and shortened lifespan in $Msh6^{-/-}p53R2^{Tg}$ mice as compared to $Msh6^{-/-}$ controls. We also observed that *Msh6* deficiency strongly accelerated *Rrm2*-induced lung carcinogenesis, with 100% of $Msh6^{-/-}Rrm2^{Tg}$ mice developing lung neoplasms by 6 months of age. The accelerated lung carcinogenesis in $Msh6^{-/-}Rrm2^{Tg}$ mice was associated with increased mutation frequency in lung tissue, while the accelerated lymphomagenesis in $Msh6^{-/-}p53R2^{Tg}$ mice correlated with a modestly elevated mutation frequency in spleen tissue. The synergy observed between these pathways raises the possibility that aberrant RNR expression may be selected for in MMR-deficient cancers.

A key question arising from this study is the molecular basis for mutagenesis and lung tumor induction by *Rrm2* and *p53R2* overexpression. One possibility is that increased RNR expression leads to dNTP level alterations that impair replication fidelity and trigger mutations in growth regulatory genes. Abnormal nucleotide levels result in increased base misinsertion during DNA replication as well as decreased proof-reading due to enhanced polymerization rates (Mathews, 2006). Consistent with the notion that regulators of nucleotide biosynthesis can influence cell transformation, overexpression of another enzyme involved in dNTP biosynthesis, thymidylate synthase, transforms cultured cells (Rahman et al., 2004) and promotes tumor formation in transgenic mice (Chen et al., 2007a).

Alternatively, carcinogenesis due to R2 subunit overexpression could be

independent of nucleotide metabolism. One possibility is that free radical production by Rrm2 and p53R2 contributes to cell transformation. During each catalytic cycle the small RNR subunit generates a tyrosyl radical that normally is transferred to the active site in Rrm1 for use in NDP reduction (Nordlund and Reichard, 2006). R2 protein overexpression might lead to increased radical generation and the formation of reactive oxygen species (ROS), which cause oxidative DNA damage and are mutagenic. ROS also have mitogenic effects and can play a direct role in neoplastic transformation (Droge, 2002). Notably, human RRM2 protein generates ROS *in vitro*, although recombinant p53R2 was reported in the same study to have antioxidant activity, despite the fact that both RRM2 and p53R2 generate tyrosyl free radicals (Xue et al., 2006). G→T transversions, a signature of oxidative DNA damage, were detected at *K-Ras* codon 12 in lung neoplasms from $Rrm2^{Tg}$ and $p53R2^{Tg}$ mice, and also at the *Hprt* locus in *Rrm2* and *p53R2* overexpressing 3T3 cells. Because MMR corrects mismatches arising from both replication errors (Modrich, 2006) and oxidative DNA damage (Slupphaug et al., 2003), the multiplicative increases in mutagenesis and carcinogenesis observed when combining RNR overexpression with MMR deficiency are compatible with both dNTP level alterations and increased ROS production as possible mechanisms of action.

The possibility that R2 subunit overexpression induces mutagenesis and tumorigenesis through excessive free radical production may account for the observation that RNR transgenic mice, despite broad RNR overexpression, develop lung but not other neoplasms at high frequency. The lung is an oxygen-rich environment with a high basal level of ROS (Rahman, 2003) and thus may be more susceptible to increased free radical production. Alternatively, it could be that the mutational targets of RNR dictate the tissue specificity. Indeed, activated *K-ras* preferentially induces lung neoplasms in mice (Johnson et al., 2001). Other more

trivial explanations for the lung specific carcinogenesis, such as subtle transgene expression level differences or varying DNA repair efficiencies among tissues, also cannot be ruled out.

Although *Rrm2* and *p53R2* encode related R2 proteins, they did not give identical results in our experiments. While overexpression of either was capable of inducing lung neoplasms, *Rrm2* overexpression elicited larger and more malignant tumors. *p53R2* overexpression, on the other hand, significantly accelerated lymphomagenesis in *Msh6*-null mice, suggesting a broad effect of *p53R2* overexpression. *Rrm2* also was more mutagenic than *p53R2* in cultured cells, and induced a greater proportion of G→T transversions in both the *Hprt* and *K-ras* genes. One possible explanation for the partially distinct phenotypes associated with *Rrm2* and *p53R2* is that both dNTP alterations and ROS production can contribute to neoplastic transformation, and that these activities differ between Rrm2 and p53R2. The distinct subcellular localizations of Rrm2 and p53R2 (Nakano et al., 2000; Tanaka et al., 2000) could contribute to such differing effects on dNTP biosynthesis or ROS production.

Mouse models hold great promise for facilitating the development of diagnostic tools, prognostic markers, and therapeutics for lung cancer, the leading cause of cancer death world-wide. Like human lung adenocarcinomas (Linnoila et al., 1992), the RNR-induced lung neoplasms expressed SP-C, a marker of type II alveolar cells. Furthermore, RNR-induced lung neoplasms arose with moderate latency in a stochastic process associated with an elevated mutation rate, suggesting that this may be a particularly authentic model for lung cancer. A mutagenic mechanism for RNR-induced lung carcinogenesis implies that several genetic alterations are required for lung carcinogenesis. Consistent with this model, we observed activating *K-ras* mutations at very high frequency in RNR-induced lung neoplasms. *K-ras* has been

reported to be mutated in 90% of mouse lung neoplasms and as many as 25% of human lung adenocarcinomas (Mills et al., 1995; You et al., 1989). That G→T transversions in *K-ras* codon 12 were detected in RNR-induced lung neoplasms further validates this lung cancer model, as G→T transversions are the most common mutations at *K-ras* codon 12 in human lung cancers and correlate with a poorer prognosis (Keohavong et al., 1996; Rodenhuis et al., 1988). Continued use of the RNR lung cancer model has great potential for revealing additional genetic alterations that contribute to lung tumor initiation and progression.

**2.6 Acknowledgment**

We thank Dr. Phil Leder for his support of this project, Dr. Lars Thelander for Rrm1 and Rrm2 cDNA clones, Dr. Andrei Chabes for yeast strains 4069-4C and 4069-8C, Charlene Manning and Dr. Jianrong Lu for assistance with plasmid cloning, Nick Fuda for contributions to the yeast mutation rate analyses, Anne Harrington for performing transgene microinjections, and Dr. Ruth Collins and Dr. Sylvia Lee for helpful discussions.

The majority data of this chapter was published.

Xu, X., Page, J.L., Surtees, J.A., Liu, H., Lagedrost, S., Lu, Y., Bronson, R., Alani, Eric., Nikitin, A. Yu., and Weiss, R.S. (2008) Broad overexpression of ribonucleotide reductase genes in mice specifically induces lung neoplasms. Cancer Research, 68 (8): 2652-60.

Fig. 2.1A was done by R. Weiss.

Partial of Fig. 2.1B (Rrm1 and p53R2 western) was done by J. Page.

Panel VII and VIII of Fig. 2.2A was done by H. Liu.

Fig. 2.4 and table 2.4 was done by J. Surtees.

CHAPTER 3

# RNR-induced Mutagenesis and Lung Tumorigenesis through an Oxidative Mechanism

## 3.1 Abstract

Ribonucleotide reductase plays a central role in maintaining genomic stability by catalyzing the rate-limiting step of dNTP biosynthesis for DNA replication and repair. Its activity is tightly regulated through allosteric mechanism and control of expression levels throughout the cell cycle. Recent studies showed that overexpression of the small subunit of RNR promoted lung tumorigenesis through a mutagenic mechanism and established a novel oncogenic activity for RNR. We initially hypothesized that RNR-induced mutagenesis and carcinogenesis might be caused by altered dNTP pools due to increased RNR activity. However, RNR-induced mutagenesis was not associated with altered dNTP levels or ratios. In addition, RNR overexpression was not associated with acute transforming activity, which has been suggested by previous studies. Alternatively, we hypothesized that excess free radical production by the small RNR subunit may result in mutation accumulation and account for lung specific tumorigenesis. Indeed, Rrm2 overexpression was associated with elevated reactive oxygen species (ROS) levels. Rrm2 mutants, defective for RNR enzyme activity but still capable of producing free radicals, were able to promote mutagenesis and enhance ROS production. Our data indicate that the mechanism of RNR-induced mutagenesis and lung tumorigenesis may be independent of RNR enzyme activity and instead may be caused by increased oxidative stress associated with overexpression of the small radical generating RNR subunit.

## 3.2 Introduction

Cancer arises due to stepwise accumulation of mutations that produce oncogenes with dominant gain of function and tumor suppressor genes with recessive loss of function. Therefore, genomic instability, due to either aging or inherited defects in carekeeper genes, has been thought to be the driving force of aggressive transformation of normal cells into highly malignant cancer cells. To maintain the integrity of the genome, cells employ multi-level safeguards: DNA replication, gene transcription, DNA repair, and cell cycle checkpoints (Hoeijmakers, 2001). Among these mechanisms, maintaining homeostasis of deoxyribonucleotide (dNTP) levels is fundamental for ensuring the replication fidelity and efficient repair of DNA lesions. Ribonucleotide reductase (RNR) is an essential enzyme that controls the homeostasis of dNTP levels and thereby maintains genomic integrity.

RNR catalyzes the rate-limiting step in the production of deoxyribonucleotide triphosphates (dNTPs) for DNA replication and DNA repair. Mammalian RNR is composed of two non-identical homodimeric subunits: the large subunit R1 and the small subunit R2 (Nordlund and Reichard, 2006). The R1 subunit contains allosteric regulation and catalytic sites to provide sufficient and balanced dNTP pools; the R2 subunit contains a dinuclear iron center and a tyrosyl free radical that is essential for enzyme catalytic activity. A proton-coupled electron transfer chain composed of hydrogen-bonded residues is responsible for radical transfer between the tyrosyl radical site of R2 and the catalytic site of R1. In mammals, the *Rrm1* gene encodes the large subunit R1, and the *Rrm2* gene encodes the small subunit R2 which together form the Rrm1-Rrm2 complex that provides dNTPs for normal cell proliferation during S phase. The *p53R2* gene encodes another small subunit and forms the Rrm1-p53R2 complex that supplies dNTPs for mitochondrial DNA replication and DNA

repair throughout the cell cycle (Nakano et al., 2000; Pontarin et al., 2007; Tanaka et al., 2000).

Due to its essential role in maintaining genome integrity, RNR activity is tightly regulated through allosteric mechanism and control of expression levels throughout the cell cycle (Bjorklund et al., 1990; Chabes and Thelander, 2000; Chabes et al., 2003b; Elledge et al., 1993). The Rrm1 protein level is constant and in excess throughout the cell cycle, whereas Rrm2 is limiting and only expressed during the S phase owing to transcriptional induction in the late G1 phase and degradation by Cdh-APC ubiquitination during the G2/M phase. p53R2 is expressed at a low level throughout the cell cycle and is induced after DNA damage in a p53 dependent manner (Nakano et al., 2000; Tanaka et al., 2000).

Deregulation of RNR has been found to cause genomic instability in both yeast and cultured mammalian cells (Caras and Martin, 1988; Chabes et al., 2003a; Reichard et al., 2000). In yeast, upregulation of RNR by abolishing feedback inhibition at the activity site of R1 subunit leads to improved survival after DNA damage and increased mutagenesis associated with altered dNTP pools (Chabes et al., 2003a; Zhao et al., 1998). In cultured mammalian cells, deregulation of RNR by mutating the activity site responsible for feedback inhibition resulted in increased mutagenesis, although no dNTP pool alterations were detected (Caras and Martin, 1988). Recently, we generated mouse models of RNR deregulation and identified a novel causative role of RNR in the etiology of spontaneous lung neoplasms through a mutagenic mechanism (Xu et al., 2008). Overexpressing the small subunits of RNR, Rrm2 and p53R2, is mutagenic in cultured 3T3 cells and in transgenic mouse tissues. More strikingly, widespread overexpression of the small subunit of RNR in transgenic mice specifically promotes lung carcinogenesis. Studies in human cancers suggest that RRM1 is a putative tumor suppressor gene (Pitterle et al., 1999) and loss

of heterozygosity at the chromosome region containing RRM1 has been correlated with poor survival in non-small cell lung cancer patients (Bepler et al., 2002). However, *RRM1* overexpression has been linked to drug resistance in tumor chemotherapy, and is utilized as a marker for chemoresistance and poor survival in patients with advanced NSCLC (Ceppi et al., 2006; Gazdar, 2007). Thus, RRM1 in NSCLC has been proposed to have a dual role in both cancer susceptibility and drug resistance (Gazdar, 2007). There is limited information concerning the effect of RRM2 expression in tumors. Overexpression of RRM2 in human oral carcinoma cells enhanced invasive potential (Zhou et al., 1998b). Polymorphisms of the p53R2 gene have also been found to correlate to esophageal squamous cell carcinomas and colon carcinoma. More interestingly, the genome regions containing human RRM2 and P53R2 are frequently amplified in lung cancer patients (Goeze et al., 2002; Lui et al., 2001; Pei et al., 2001).

Studies in human patients and our RNR transgenic mouse model may provide new insights into the role of RNR in cancer development. Rather than functioning only as a downstream effector of transformation by providing high dNTP levels for cancer cell proliferation, RNR deregulation also may have a direct role in initiation of cancer development by promoting mutagenesis, leading to mutations in oncogenes or tumor suppressor genes. However, the molecular mechanisms of RNR-induced mutagenesis and lung tumorigenesis are still unclear.

The simplest explanation for RNR-induced mutagenesis is that deregulation of RNR causes altered dNTP pools, which are mutagenic. Mutagenesis induced by RNR deregulation in budding yeast is associated with altered dNTP levels (Chabes et al., 2003a). However, there has been conflicting reports on whether altered dNTP levels are associated with mutagenesis caused by RNR deregulation in mammalian cells (Caras and Martin, 1988; Weinberg et al., 1981). One possible explanation for this

discrepancy is that changes in dNTP levels in subnuclear compartments are undetectable by measurement of total dNTP levels. Alternatively, other mechanisms that control dNTP homeostasis, such as the control of enzymes in the salvage pathway, may play a role in keeping dNTP levels undisturbed when RNR is deregulated. It also remains possible that RNR-induced mutagenesis could be independent of RNR enzyme activity.

Previous studies suggest that Rrm2 has transforming activity since Rrm2 can enhance transforming potential in combination with activated oncogenes in cultured mammalian cells. However, Rrm2 alone has not been found to have any direct transforming activity (Fan et al., 1998; Fan et al., 1996). Interestingly, p53R2 has previously been suggested to have tumor suppressor activity, since it is induced transcriptionally after DNA damage in a p53 dependent manner. p53R2 directly participates in DNA damage repair by providing dNTPs and p53R2 deficient cells are more sensitive to DNA damage agents (Nakano et al., 2000; Tanaka et al., 2000). However, p53R2 transgenic mice were also highly prone to spontaneous lung tumorigenesis and cells overexpressing p53R2 exhibited enhanced mutagenesis (Xu et al., 2008). Thus, the role of p53R2 in genomic stability and cancer is still unclear.

Since the small subunit of RNR contains a tyrosyl radical essential for enzyme activity, another potential mechanism for RNR-induced mutagenesis and lung carcinogenesis is that free radical production due to the overexpressed small subunit and leads to oxidative DNA damage that drives RNR-induced mutagenesis and carcinogenesis. Recently, studies found that human RRM2 recombinant protein can function as an oxidant reagent due to its ability to produce free radicals (Xue et al., 2006), although p53R2 has been proposed to have anti-oxidative property, despite the fact that both RRM2 and p53R2 generate tyrosyl radicals. ROS generating property of human RRM2 raises the possibility that elevated RNR expression might cause

increased oxidative stress, leading to genomic instability and lung cancer development.

There has been abundant evidence for involvement of ROS in lung carcinogenesis in both human lung cancer studies and mouse lung cancer models. It is well known that tobacco smoke contains DNA oxidants and causes an increase in 8-oxo-deoxyguanine (8-oxo-dG) in the human lung. 8-oxo-dG is the most prevalent oxidative DNA damage, and can base pair with adenine and cytosine with equal efficiency during DNA replication, resulting in G to T transversions (Nakabeppu et al., 2004). Lung cancer patients had higher levels of 8-oxo-dG than in non-lung cancer patients (Inoue et al., 1998). Lung cancer risk is reduced by consumption of anti-oxidant containing fruits and vegetables (Miller et al., 2004; Riboli and Norat, 2003). Increased levels of MnSOD and decreased levels of catalase, two key players in regulation of intracellular ROS levels, have been found in human lung cancer patients. A polymorphic variant in OGG1, a protein that excises 8-oxo-dG from DNA, causes reduced enzyme activity and the increased risk of lung cancer (Le Marchand et al., 2002). Mth1 hydrolyzes the 8-oxo-dGMP, avoiding the incorporation of 8-oxo-dG into DNA during DNA synthesis, and Ogg1 glycosylase removes 8-oxo-dG from DNA (Nakabeppu et al., 2004). In mouse models, deficiency in either the *Ogg1* gene or the *Mth*1 gene in knockout mice is associated with an increased incidence of lung tumors. *Ogg1* knockout mice accumulated high levels of 8-oxo-dG (Minowa et al., 2000; Sakumi et al., 2003; Tsuzuki et al., 2001; Xie et al., 2004). This evidence supports ROS as a causative agent in lung cancer development (Maciag and Anderson, 2005).

We previously found that widespread overexpression of RNR in transgenic mice specifically promotes spontaneous lung tumorigenesis through a mutagenic mechanism (Xu et al., 2008). Notably, we found increased signature mutations of

oxidative DNA damage at *K-ras* codon 12 from these RNR-induced lung neoplasms and at the *Hprt* gene locus in RNR overexpressing 3T3 cells. Mismatch repair corrects mismatches from replication error and oxidative DNA damage (Modrich, 2006; Slupphaug et al., 2003). We observed multiplicative increase in mutagenesis and lung tumorigenesis when combining RNR overexpression with mismatch repair deficiency in our previous study, a finding that is compatible with increased ROS production as possible mechanism for RNR-induced mutagenesis. The lung is an oxygen-rich environment with high basal level of ROS (Rahman, 2003) and thus may be more susceptible to free radical production. This evidence strongly suggests that RNR-induced lung tumorigenesis might involve oxidative DNA damage in a highly tissue specific manner. This may be related to the redox property of the small subunit of RNR.

In this study, we investigated the molecular mechanisms of RNR-induced mutagenesis and lung tumorigenesis and obtained results suggesting that RNR overexpression drives mutagenesis and lung tumorigenesis through an oxidative mechanism. First, we did not observe detectable alterations in dNTP levels or ratios in lung cells from RNR transgenic mice or in RNR overexpressing 3T3 cells. Second, we did not observe acute transforming activity of RNR. However, Rrm2 overexpressing cells consistently show increased ROS levels. Interestingly, cells overexpressing Rrm2 mutants, which are defective for RNR enzyme activity but can still produce the initial tyrosyl radical or a transient tryptophan radical, exhibited enhanced mutagenesis and increased oxidative stress. Our results indicate that RNR-induced mutagenesis may be independent of RNR enzyme activity, and instead could act through elevated oxidative stress due to free radical overproduction.

### 3.3 Materials and Methods

#### 3.3.1 Cells.

All cells were cultured in culture medium (Dulbeco's Modification of Eagles Medium supplemented with 10% bovine calf serum, 1.0 mM L-glutamine, 0.1 mM MEM non-essential amino acids, 100 μg/ml of streptomycin sulfate, and 100 U/ml of penicillin). Mouse 3T3 cells overexpressing Rrm1, Rrm2, p53R2, Rrm2-Y177W, Rrm2-Y370W, Rrm2-Y177F, Rrm2-Y370F, or empty vector were generated as described in Material and Methods section in Chapter 2.

#### 3.3.1 Measurement of intracellular dNTP pool size.

$10^6$ RNR over-expressing *3T3* cells were plated on 100mm tissue culture dishes in DMEM supplemented with 10% dialyzed bovine calf serum on the day before the experiment. 24 h after plating, cells were harvested by trypsinization and 5x $10^5$ cells were centrifuged for 3 min at 1300g. The supernatant was aspirated and the cell pellet was extracted with 100 μl of cold 0.4N perchloric acid for 20 min on ice. After centrifugation (1 min at 16,000g), the supernatant was neutralized by mixing with 100 μl 0.5N trioctylamine (Sigma) in 1, 1, 2-trichlorotrifluoroethane (Sigma). The phases were separated by centrifugation (2 min at 16,000g) and the upper aqueous phases were fast frozen in dry ice-ethanol and stored at –80°C until analyzed. dNTP pool size was measured according to methods described by Sherman and Fyfe (Sherman and Fyfe, 1989). The reaction mixture (40 μl) contained 100mM HEPES buffer (pH 7.3) and 10mM $MgCl_2$, 1 U of E. coli DNA polymerase I klenow fragment (Fermentas), 0.25μM (for dATP and dTTP) or 0.05μM (for dCTP or dGTP) oligonucleotide template, 8 μl of dNTP extract, and 1.25 μM $^3$H-dATP(18 Ci/mmol, Moravek Biochemicals) (for dTTP, dCTP, and dGTP) or $^3$H-dTTP(60 Ci/mmol,

Moravek Biochemicals) ( for dATP). Following is the sequence of oligonucleotide template for measuring:

dTTP:5'ATTATTATTATTATTAGGCGGTGGAGGCGG 3'

3' CCGCCACCTCCGCC 5'

dCTP:5' TTTGTTTGTTTGTTTGTTTGGGCGGTGGAGGCGG 3'

3' CCG CCACCTCCGCC 5'

dGTP:5' TTTCTTTCTTTCTTTCTTTCGGCGGTGGAGGCGG 3'

3' CCGCCACCTCCGCC 5'

dATP:5' AAATAAATAAATAAATAAATGGCGGTGGAGGCGG 3'

3'CCGCCACCTCCGCC 5'

Reactions were started by addition of the enzyme and were carried out for 60 min at room temperature. After incubation, 20 μl aliquots were removed and spotted onto Whatman DE81 paper. The papers were dried, washed (3x 10 min) with 5% $Na_2HPO_4$, and rinsed once each with distilled water and 95% ethanol. After drying, the radioactivity on the paper was measured in a liquid scintillation counter.

### 3.3.2 Lung cell isolation and preparation.

3-month old wildtype *FVB, Rrm1, Rrm2* and *p53R2* transgenic mice were euthanized and lung cells were isolated. Briefly, perfused and lavaged lungs were digested with elastase (4.3U/ml, Worthington, Lakewood, NJ) for 25 min at 37°C, then minced sequentially filtered through nylon meshes (160, 37, 10μm pore size), and plated on mouse IgG (Polysciences, Inc ) coated cell culture dishes for 1h at 37°C in a humidified incubator with 6% $CO_2$ in air (Bates et al., 2002). Cells were then trypsinized and harvested for dNTP measurement. To make IgG coated plates, put 1.5 ml 0.5mg/ml IgG in 50mM Tris (pH=9.5) to cover 60mm culture dish and rock for 3 hrs at room temperature.

### 3.3.4 Focus formation assay.

$1x10^6$ *3T3* cells were plated on 100mm dishes with DMEM supplemented with 10% bovine calf serum the day before the experiment. 24 hrs later, cells were fed with fresh DMEM supplemented with 10% bovine calf serum. Cells were then transfected by calcium phosphate precipitation using 20μg of each construct plasmid DNA. 48 hrs post transfection, cells were trypsinized and 1/3 of cells were passed into new 100mm cultured dishes and fed with DMEM supplemented with 10% bovine calf serum every 3 days for 3 weeks. Cells were then fixed in 95% methanol for 1 h, stained with 10% Giemsa, and foci were scored. Ras and Myc plasmids have been described previously (Kelekar and Cole, 1987; Parada et al., 1982).

### 3.3.5 Construction of expression plasmids and site-directed mutagenesis.

Rrm2-Y177W, Rrm2-Y177F, Rrm2-Y370W and Rrm2-Y370F mutant constructs were generated by overlap extension PCR of pCaggs-Rrm2 plasmid where the required mutation was introduced as described previously (Ho et al., 1989). The internal primers that hybrids at the site of mutations for site-directed mutagenesis were:

Y177W forward: 5'-GGAAAACATACACTCTGAAATGTGGAGTCTCCTTATTGACACTTAC-3';

Y177W reverse: 5'-GTAAGTGTCAATAAGGAGACTCCACATTTCAGAGTGTATGTTTTCC-3';

Y370W forward: 5'-GCGAGTAGGCGAGTGGCAGAGGAGGGGAGTCATG-3';

Y370W reverse: 5'-CATGACTCCCATCCTCTGCCACTCGCCTACTCGC-3';

Y177F forward: 5'-GGAAAACATACACTCTGAAATGTTCAGTCTCCTTATTGACACTTAC-3';

Y177F reverse: 5'-GTAAGTGTCAATAAGGAGACTGAACATTTCAGAGTGTATGTTTTCC-3';
Y370F forward: 5'-TTGAGAAGCGAGTAGGCGAGTTTCAGAGGATGG-3';
Y370F reverse: 5'-CCATCCTCTGAAACTCGCCTACTCGCTTCTCAA -3'(underlined letters denote the mutated codon);
The upstream flanking primer containing the *xhoI* site used for PCR extension is: 5'-AAA**CTCGAG**CCATGCTCTCCGTCCGCACCCC-3' and the downstream flanking primer containing the *xhoI* site is : 5'-AGAG**CTCGAG**TTAGAAGTCAGCATCCAAGGT-3' (boldface letters denote the *xhoI site)* ;

To synthesize overlapping fragments, two separate PCR reactions were performed. In the first PCR reaction, the universal upstream flanking primer and reverse site-specific internal primer for each mutant were used to generate upstream overlapping fragment; in the second reaction, forward site-specific internal primer for each mutant and the universal downstream flanking primer were used to amplify downstream overlapping fragment. Synthesized upstream and downstream overlapping fragments were then fused by denaturing and annealing them in a subsequent extension reaction. The fused products were then PCR amplified using the universal upstream flanking primer and the universal downstream flanking primer. The fragments containing the mutations were then ligated into the pCaggs-Rrm2 plasmid digested with *xhoI* to replace the original wildtype Rrm2 fragment. Whole Rrm2 cDNA was sequenced for all plasmids to confirm the mutated codons and to ensure the absence of other mutations.

### 3.3.6 Generation of mutant Rrm2 overexpressing 3T3 cell pools.

Mouse 3T3 fibroblasts were transfected either with the empty pCaggs vector (1.35 μg) as a control or with the pCaggs-Rrm2, pCaggs-Rrm2-Y177W, pCaggs-Rrm2-Y370W, pCaggs-Rrm2-Y177F, or pCaggs-Rrm2-Y370F expression vector (1.35 μg) along with PGK-puro (0.15 μg) using FuGENE 6 Transfection Reagent (Roche Diagnostics Co., Mannheim, Germany) following the procedure recommended by the manufacturer. The medium was replaced by selection medium containing 1.25 μg/ml puromycin every 2 days. After 3 weeks, puromycin-resistant cells were pooled and expanded for further analysis under selection conditions.

### 2.5.1 Western blot analysis.

Cultured cells were prepared in RIPA buffer (50mM Tris-HCl [pH 8.0], 1% [vol/vol] Nonidet P-40, 0.5% sodium deoxycholate, 0.1% [wt/vol] sodium dodecyl sulfate, 150mM sodium chloride, 50mM sodium fluoride) and 1x protease inhibitor cocktail (Roche). Immunoblotting was performed on PVDF membranes using standard methods, with signal detection by enhanced chemiluminescence (Pierce). The antibodies used were goat anti-R2 (sc-115, Santa Cruz Biotechnology,) and α-tubulin (A5441, Sigma).

### 2.5.2 Cell proliferation assay.

Cells were cultured and passed according to the 3T3 protocol. In brief, $10^6$ cells were plated on a 100 mm culture dish; after 3 days, cells were counted and $10^6$ cells were replated. Population Doublings were calculated using the formula $\Delta PDL=\log(n_f/n_0)/\log 2$, where $n_0$ is the initial number of cells and $n_f$ is the final number of cells at each passage(Blasco et al., 1997).

### 2.5.3 *Hprt* mutation rate assay.

Cells were cultured in HAT medium (culture medium supplemented with 0.2mM sodium hypoxanthine, 0.4μM aminopterin, 0.02μM thymidine [GIBCO]) for two weeks. Cells then were cultured in HT medium (culture medium supplemented with 0.1mM sodium hypoxanthine, 0.016μM thymidine [GIBCO]) for one week. Subsequently, cells were seeded at a density of $5x10^5$ cells per 10cm plate (10 plates total) in culture medium containing 5μg/ml 6-thioguanine (Sigma) for 3 weeks. Then plates were fixed in methanol for 1 hour and stained with crystal violet overnight, then rinsed with water and dried. Number of 6-thioguanine resistant colonies were then counted. Plating efficiency was determined by plating 200 cells in medium without 6-thioguanine in triplicate for 2 weeks and counting stained colonies (Fenwick, 1985).

### 3.3.7 ROS measurement.

Intracellular ROS levels were measured by quantifying carboxyl-2,7-dichlorodihydrofluorescin diacetate ( $CH_3$-DCFDA) fluorescence. Briefly, $1x\ 10^6$ Rrm2 over-expressing 3T3 cells were plated per 100mm tissue culture dish in DMEM supplemented with 10% bovine calf serum two days before the experiment. 48 hrs after plating, cells were trypsinized and washed twice with warm PBS. $1x\ 10^6$ cells were then resuspended in 10μM freshly prepared $CH_3$- DCFDA ( Molecular Probe ) at $1x\ 10^6$ cells/ml and incubated at 37°C in the dark for 20 min. Cells were then filtered through 40 micron nylon mesh and analyzed immediately by flow cytometry at 488 nm excitation and 530 nm emission on a FACs-Calibur flow cytometer (Beckman). Ten thousands cells were routinely collected and data were analyzed with Flowjo software (Radisky et al., 2005).

## 3.4 Results

### 3.4.1 No detectable alterations in dNTP levels or ratios in RNR overexpressing 3T3 cells and RNR transgenic lung tissues.

RNR deregulation by abolishing feedback inhibition at the activity site of R1 subunit in yeast causes altered dNTP levels and enhanced mutagenesis (Chabes et al., 2003a). We hypothesized that the mutagenic effects of RNR overexpression would also involve altered dNTP pool size due to an increased RNR activity, which is manifested by enhanced mutagenesis in RNR overexpressing cells and by lung tumorigenesis in RNR transgenic mice (Xu et al., 2008). To test this hypothesis, we first measured intracellular dNTP levels in logarithmically growing RNR overexpressing 3T3 cells. There were no significant differences detected in dATP, dTTP, dCTP and dGTP pools in Rrm1, Rrm2 and p53R2 overexpressing cells compared to those in empty plasmid vector cells (Fig. 3.1A). Each dNTP pool size was consistent with previously reported results for logarithmically growing 3T3 cells, with dTTP being highest and dGTP being lowest (Ke et al., 2005). To further test this *in vivo*, we analyzed intracellular dNTP levels in lung cells from 3-month old RNR transgenic mice. Compared to lung cells from wildtype control mice, lung cells from *Rrm1*, *Rrm2* and *p53R2* transgenic mice exhibited similar levels of dATP, dTTP, dCTP and dGTP pools (Fig. 1B). The individual dNTP levels in these adult lung cells were consistent with the reported dNTP levels in muscle tissue, with dCTP pool being highest and dTTP pool being the lowest (Hakansson et al., 2006b). In summary, RNR overexpression was not associated with detectable changes in dNTP levels or ratios in RNR overexpressing 3T3 cells and transgenic lung cells, suggesting that RNR overexpression induced mutagenesis and lung tumorigenesis might not involve altered dNTP levels or ratios.

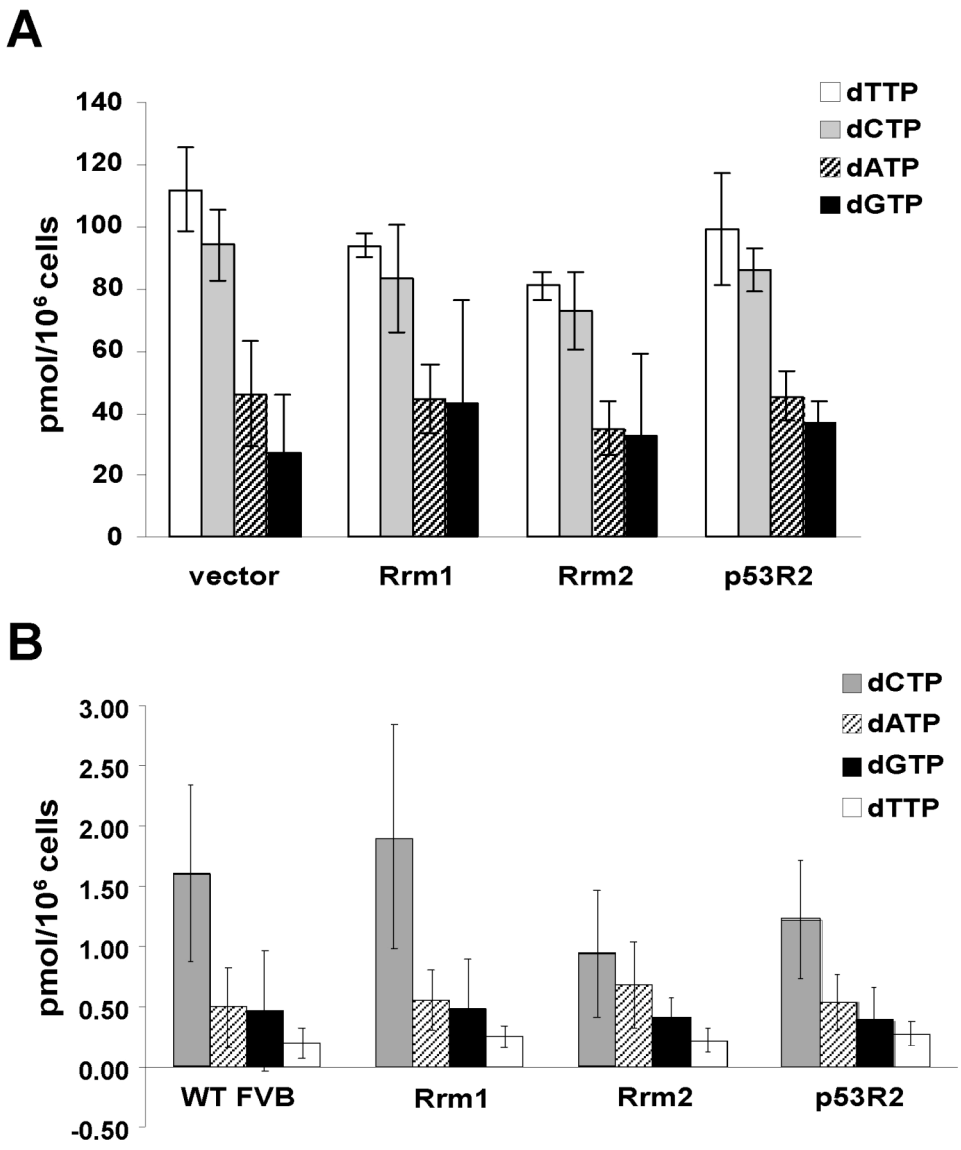


Figure 3.1 Intracellular dNTP pools in logarithmically growing RNR over-expressing 3T3 cells or RNR transgenic lung tissues. Intracellular dNTPs were extracted and quantified from (A) logarithmically growing 3T3 cells overexpressing Rrm1, Rrm2, p53R2, or containing the empty plasmid vector and (B) RNR transgenic lung tissues, using an enzymatic assay as described in Materials and Methods. Each data point represents the mean of three independent experiments, with error bars representing the standard deviation.

### 3.4.2 RNR has no detectable acute transforming activity.

Previous studies suggest that Rrm2 has transforming potential in cooperation with a variety of oncogenes (Fan et al., 1998; Fan et al., 1996). To determine whether lung tumorigenesis caused by *Rrm2* and *p53R2* overexpression involves acute transforming activity of the small RNR proteins, we transfected *Rrm1*, *Rrm2*, *p53R2* and control vector into 3T3 cells and scored formation of transformation foci 3 weeks posttransfection. As shown in Fig. 3.2.A, introduction of any of the RNR genes alone did not result in the focus formation, suggesting that overexpression of individual RNR genes is not sufficient to transform 3T3 cells, which is consistent with previous reports (Fan et al., 1998; Fan et al., 1996). Previous studies suggest that Rrm2 increased focus formation in *H-ras* transfected 3T3 cells. To further test whether RNR cooperate with the *H-ras* gene in focus formation and explore the role of transforming activity in RNR-induced tumorigenesis, we introduced *Rrm1, Rrm2, p53R2* and control vector into 3T3 cells along with *H-ras* gene to assess focus formation. We observed that Rrm1, Rrm2, and p53R2 did not cooperate with H-ras to transform 3T3 cells, since they exhibited a similar number of foci with cells co-transfected with vector and *H-ras* (Fig 3. 2.B, C). However, consistent with previous studies that *c-Myc* can cooperate with *H-ras* in focus transformation, *c-Myc* and *H-ras* co-transfected cells exhibited significantly increased foci formation. Our data suggest that RNR-induced lung carcinogenesis might not involve direct transforming activity of RNR.

### 3.4.3 Generating *Rrm2-Y177W* and *Rrm2-Y370W* mutant overexpressing 3T3 cells.

We did not observe altered dNTP levels and ratios in RNR overexpressing cells. Although cannot rule out the possibility that alterations in dNTP levels within

Figure 3.2. Focus formation in 3T3 cells transfected with either individual RNR genes or RNR genes with *H-ras* genes. (A) 3T3 cells were transfected with *Rrm1, Rrm2, p53R2* or empty plasmid vector using Calcium phosphate coprecipitation methods. Transfected cells were fed every 3 days for 3 weeks, then fixed and stained with Giemsa. (B) 3T3 cells were co-transfected with *H-ras* gene with *Rrm1, Rrm2, p53R2* or empty plasmid vector using Calcium phosphate coprecipitation methods. Transfected cells were fed every 3 days for 3 weeks, then fixed and stained with Giemsa. Cells co-transfected with *c-Myc* and *H-ras* were used as positive control. (C) The number of foci formation in three independent experiments was plotted. Each data point is the mean with error bars representing the standard deviation.

**A**

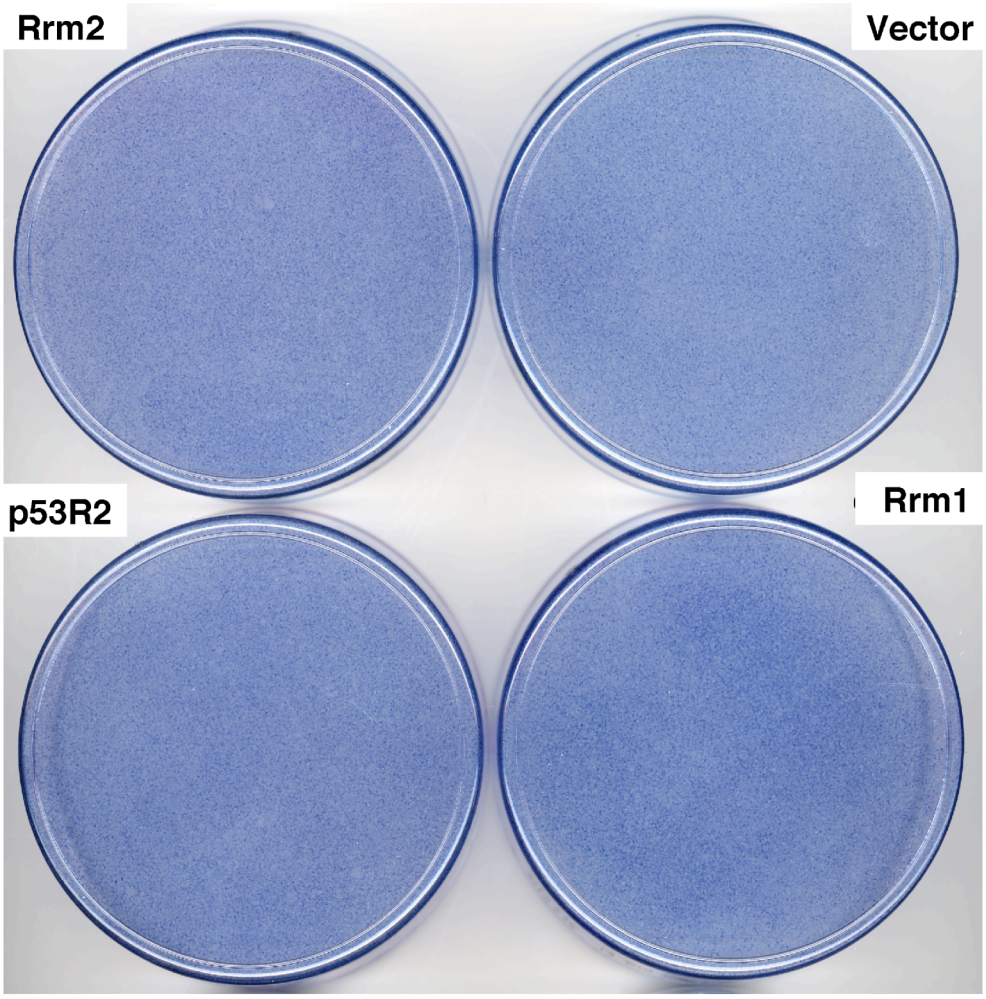

Figure 3.2 (continued)

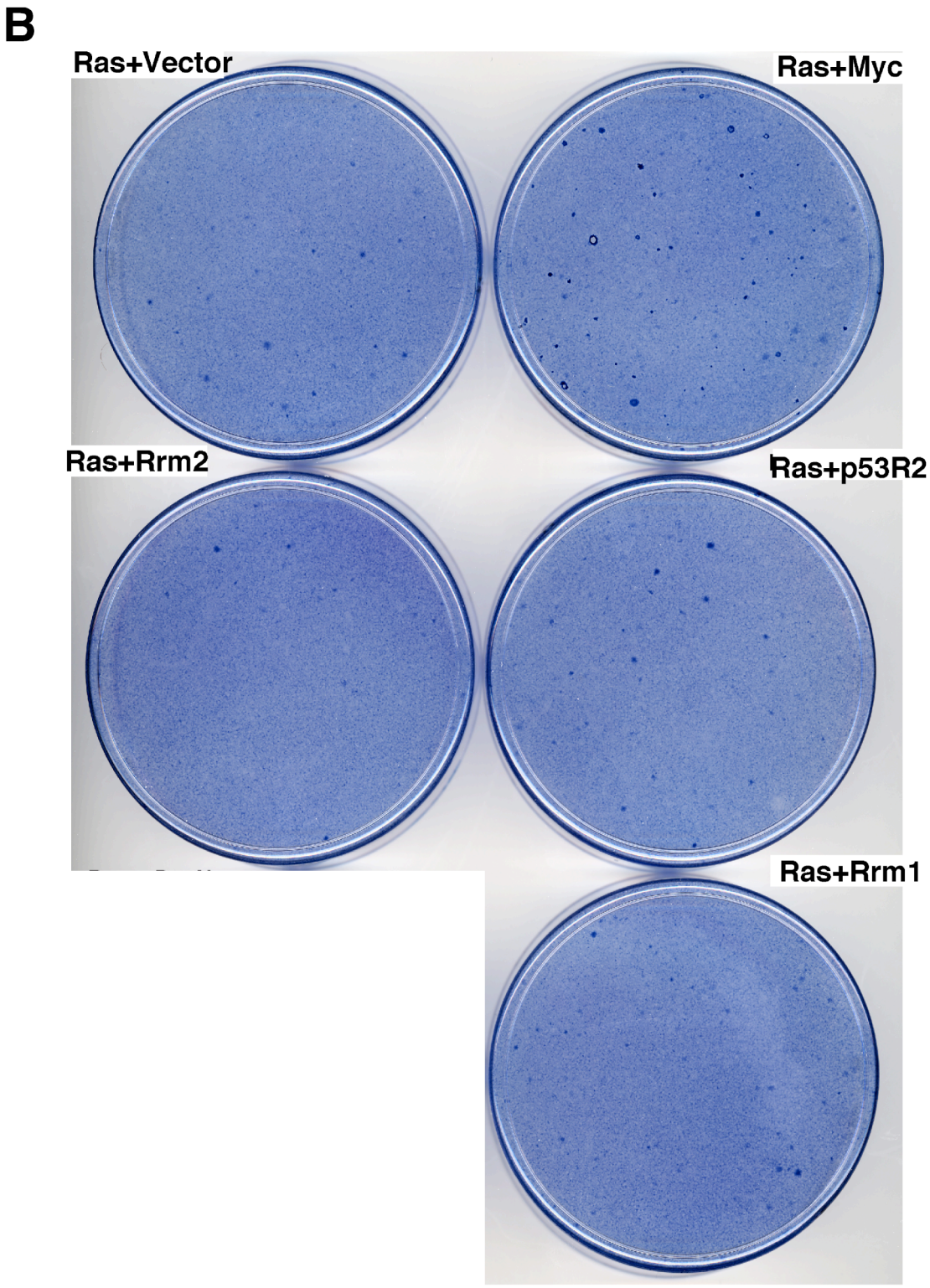

Figure 3.2 (continued)

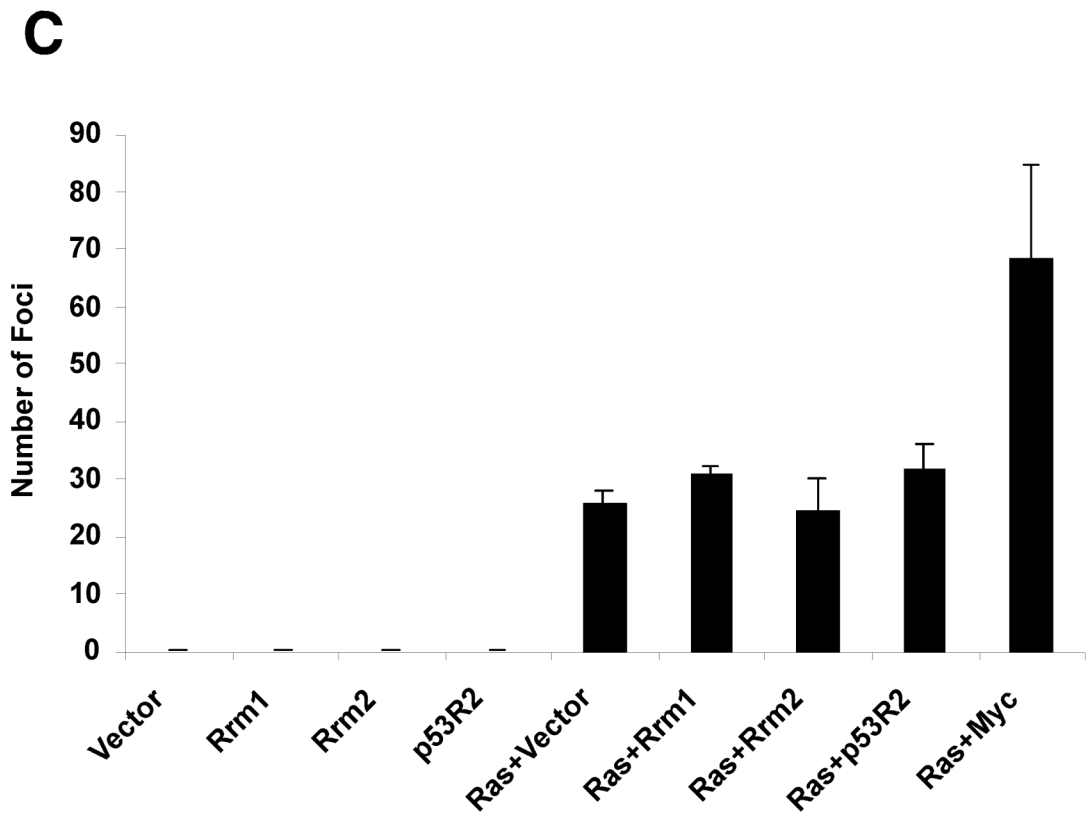

subcellular compartments are undetectable when measuring total dNTP levels, our data suggest that mutagenic and lung tumorigenic effects caused by RNR overexpression might involve other RNR activities beside reduction of NDP. One such mutagenic activity could be radical production, since both the mutator phenotype and lung cancer development were specific to small subunit overexpression. We hypothesized that RNR induced mutagenesis and lung tumorigenesis might involve increased reactive oxygen species due to elevations in free radical production associated with small subunit overexpression. To test whether enzyme activity or free radical formation is required for RNR-induced mutagenesis and lung tumorigenesis, we generated *Rrm2* mutants defective for these functions (Fig. 3.3).

The Rrm2-Y177W mutant, with a mutation at the initial tyrosyl radical site, has been shown to only produce a transient tryptophan radical and to be defective for enzyme activity (Potsch et al., 1999). The Rrm2-Y370W mutant, carrying a mutation in the radical transfer path between the Rrm2 and Rrm1 subunits, can still produce the initial tyrosyl radical but only has a 1.7% of RNR enzyme activity compared to the wildtype Rrm2 protein (Rova et al., 1999). To test whether these Rrm2 mutants, which are unable to support RNR enzyme activity but can still produce radicals, are also mutagenic, we generated *Rrm2-Y177W* and *Rrm2-Y370W* mutant constructs using site-directed mutagenesis and cloned them into the same pCaggs expression vector used for generating RNR overexpressing 3T3 cells and RNR transgenic mice. Then we generated *Rrm2-Y177W* mutant and *Rrm2-Y370W* mutant overexpressing 3T3 cell pools as described in Material and Methods. Overexpression of individual *Rrm2* mutant genes in these cells was confirmed by Western blot (Fig. 3.4A). The cells overexpressing wildtype Rrm2, Rrm2-Y177W or Rrm2-Y370W mutants had similar proliferation rates as compared to cells expressing empty vector (Fig. 3.4B)

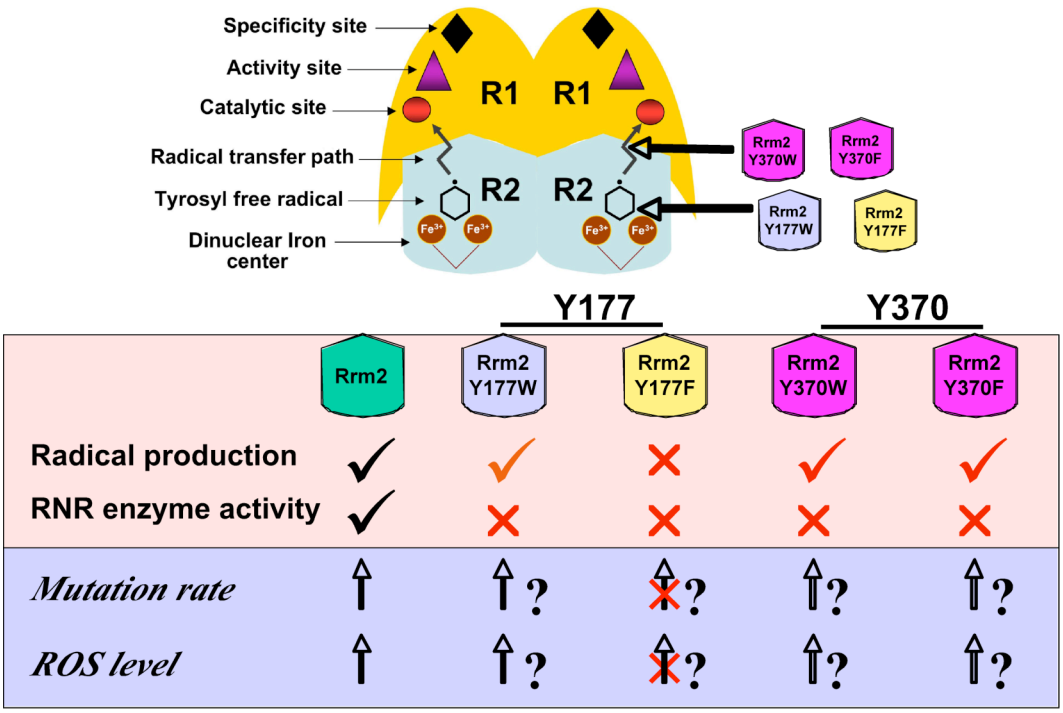


Figure 3.3 Schematic showing Rrm2 mutants and predicted results. Rrm2 mutants defective for either radical production or enzyme activity were generated to assess their importance in RNR-induced mutagenesis. Rrm2-Y177W mutant can produce a transient tryptophan radical and is defective for enzyme activity. Rrm2-Y370W and Rrm2-Y370F mutant are unable to support enzyme activity due to a mutation at a residue required for radical transfer, but can still produce initial tyrosyl radical at Y177. Rrm2-Y177F mutant is defective for both radical generation and enzyme activity.

Figure 3.4 Increased mutation frequency in Rrm2 mutant overexpressing 3T3 cell pools. (A) Western blot analysis of Rrm2 protein expression in 3T3 cells overexpressing *Rrm2-Y177W* and *Rrm2-Y370W* mutants. Total protein was extracted from the indicated cell lines and subjected to immunoblotting with antibodies specific to Rrm2. The membrane was re-probed for α-tubulin as a loading control. (B) Accumulated population doublings (PDL) of 3T3 cells overexpressing *Rrm2, Rrm2-Y177W, Rrm2-Y370W* or empty plasmid vector. Cells were cultured following a 3T3 protocol as described in Material and Methods. Plot shows the number of PDL. (C) Mutation frequency at the *Hprt* locus in 3T3 cells overexpressing *Rrm2, Rrm2-Y177W, Rrm2-Y370W* or empty plasmid vector. Mutation frequency was determined by *Hprt* assay as described in Material and Methods.

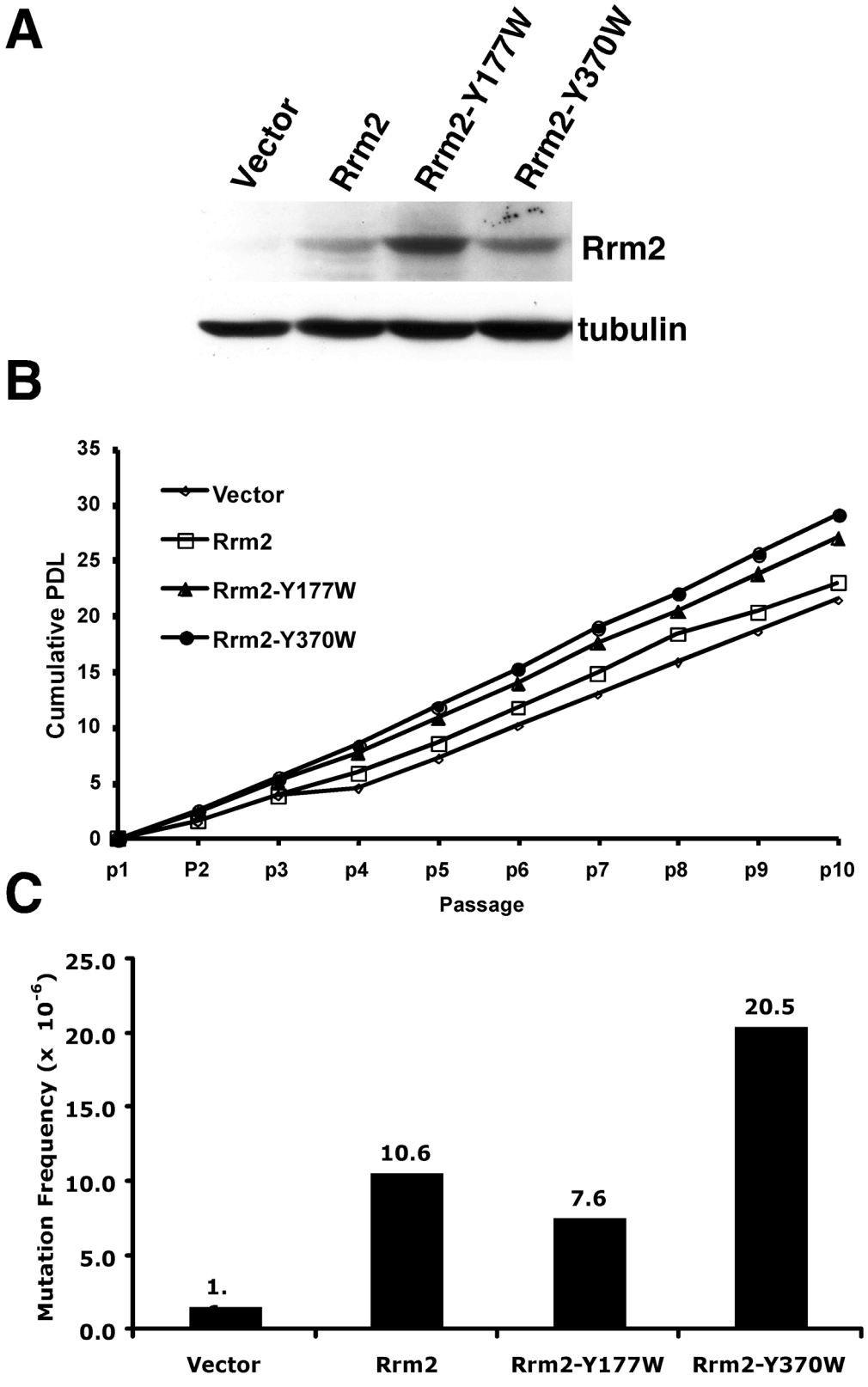
A
Vector
Rrm2
Rrm2-Y177W
Rrm2-Y370W
Rrm2
tubulin
B
Cumulative PDL
35
30
25
20
15
10
5
0
Vector
Rrm2
Rrm2-Y177W
Rrm2-Y370W
p1
P2
p3
p4
p5
p6
p7
p8
p9
p10
Passage
C
Mutation Frequency (x 10-6)
25.0
20.0
15.0
10.0
5.0
0.0
1.
10.6
7.6
20.5
Vector
Rrm2
Rrm2-Y177W
Rrm2-Y370W

### 3.4.4 Increased *Hprt* mutation rates in *Rrm2* mutant cells that are defective for RNR enzyme activity.

To test whether RNR-induced mutagenesis depends on RNR enzyme activity, we measured mutation frequency in *Rrm2* mutant cells, defective for RNR enzyme activity, using the *Hprt* mutation detection assay. Consistent with our previous results, a significantly increased mutation frequency was observed in wildtype *Rrm2* overexpressing cell pool ($10.6 \times 10^{-6}$) as compared to empty plasmid vector cells ($1.6 \times 10^{-6}$) (Fig. 3.4C). Notably, cell pools overexpressing *Rrm2-Y177W* or *Rrm2-Y370W* exhibited significantly increased mutation frequencies compared to control cells. Mutation frequency in cells overexpressing the *Rrm2-Y177W* mutant was lower than wildtype Rrm2 overexpressing cells, but significantly higher than vector ($7.6 \times 10^{-6}$ versus $1.6 \times 10^{-6}$). Since Rrm2-Y177W is defective for RNR enzyme activity but can still produce a transient tryptophan radical, this supports a model in which RNR-induced mutagenesis is independent of RNR enzyme activity and may instead be due to increased free radical production. Cells overexpressing Rrm2-Y370W showed the highest mutation frequency ($20.5 \times 10^{-6}$). The initial tyrosyl radical can still be produced in the Rrm2-Y370W mutant, but cannot be transferred to the Rrm1 subunit due to defects in the radical transfer path. Therefore, the high mutation frequency observed in cells overexpressing Rrm2-Y370W might reflect that initial tyrosyl radical produced in this mutant were leaked into cells and led to oxidative damage and increased mutagenesis. Together, these results indicate that Rrm2-induced mutagenesis is independent of RNR enzyme activity, and most likely depends on its radical production activity.

### 3.4.5 Increased ROS levels in *Rrm2* and *Rrm2* mutant cells.

To determine whether increased ROS levels account for the increased mutagenesis in wildtype *Rrm2* overexpressing cells. We first measured the levels of ROS in 3T3 cells overexpressing wildtype Rrm2 using carboxyl -2'-7-dichlorohydrofluorescein diacetate ($CH_3$-DCFDA) staining. $CH_3$-DCFDA can readily cross cell membranes and is hydrolyzed by intracellular esterase to non-fluorescent carboxyl -2'-7- dichlorohydrofluorescein ($CH_3$-DCFH) (Radisky et al., 2005). In the presence of ROS, $CH_3$-DCFH is oxidized, producing highly fluorescent molecule carboxyl -2'-7- dichlorofluorescein ($CH_3$-DCF). $CH_3$-DCF fluorescence is commonly used as a indicator of oxidative stress. As shown in Figure 3.5A, Rrm2 overexpressing cells exhibited an average 2.2 fold increase in ROS levels compared to empty vector cells($p<0.01$, t-test). Five independent Rrm2 overexpressing cell pools showed consistently increased ROS production. Consistent with previous reports that *H-ras* transformed 3T3 cells produce large amounts of the reactive oxygen species (Irani et al., 1997), *H-ras* transfected 3T3 cells were used as a positive control and showed a 5.1 fold increase in ROS levels compared to vector ($p<0.01$, t-test). Figure 3.5B shows the overlay of one representive experiment for $CH_3$-DCFDA intensity. These results indicate that increased ROS production contributes to Rrm2-induced mutagenesis. Although *Rrm2-Y177W* and *Rrm2-Y370W* mutants are defective for RNR enzyme activity, they can still produce a transient tryptophan radical or the initial tyrosyl radical, respectively. To further test whether increased mutagenesis in *Rrm2-Y177W* and *Rrm2-Y370W* mutant cells was due to increased ROS production, we measured intracellular ROS levels in cells overexpressing these mutants. As shown in Figure 3.5C, cells overexpressing *Rrm2-Y177W* showed a 2.7 fold increase in ROS levels compared to vector cells ($p<0.05$ t-test), suggesting that the *Rrm2-Y177W* mutant might cause mutagenesis through radical production and a possible oxidative damage mechanism. *Rrm2-Y370W* mutant cells exhibited the highest elevations in

Figure 3.5. Increased reactive oxygen species levels in Rrm2 and Rrm2 mutant overexpressing cells. (A) Intracelluar ROS levels were assessed by FACs analysis of $CH_3$-DCFDA fluorescence in *Rrm2* overexpressing 3T3 cell pools. *H-ras* transfected 3T3 cells used as a positive control. Each data point is the mean of 5 independent cell lines, with error bars representing the standard deviation. "*" symbol indicates that there is a statistically significant difference ($p < 0.05$) relative to control vector cells by student t –test. (B) Overlay of one representative experiment showing the distribution of $CH_3$-DCFDA fluorescence. (C) Intracellular ROS levels in 3T3 cells overexpressing *Rrm2, Rrm2-Y177W, Rrm2-Y370W* or empty plasmid vector assessed by FACs analysis of $CH_3$-DCFDA fluorescence. Each data point is mean of three independent experiments with error bars representing the standard deviations. "*" symbol indicates that there is a statistically significant difference ($p < 0.05$) relative to control vector cells by student t –test; "#" symbol indicates that p value is 0.051 by student t –test.

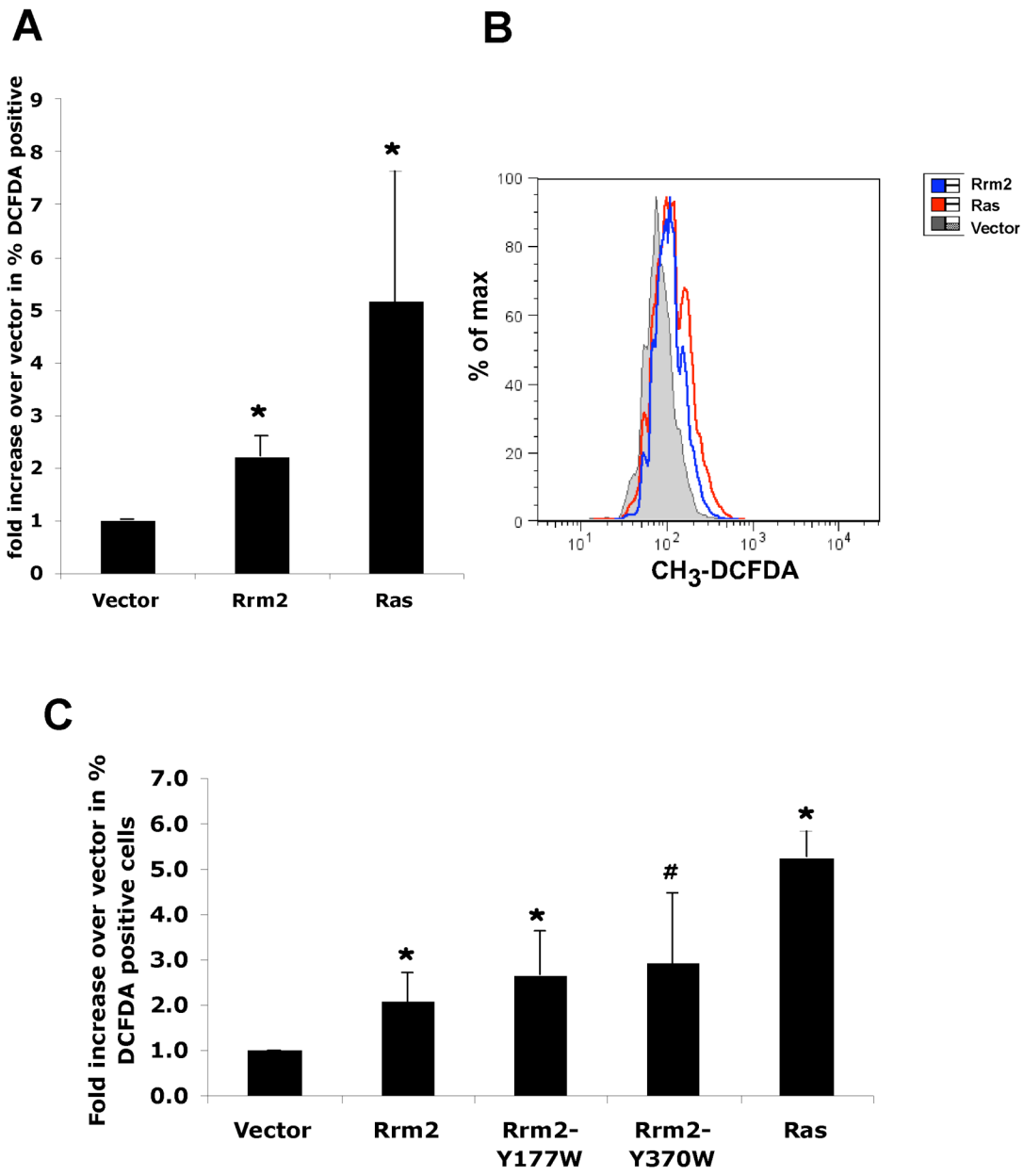
A
fold increase over vector in % DCFDA positive
0
1
2
3
4
5
6
7
8
9
*
*
Vector
Rrm2
Ras
B
% of max
0
20
40
60
80
100
$10^1$
$10^2$
$10^3$
$10^4$
$CH_3$-DCFDA
Rrm2
Ras
Vector
C
Fold increase over vector in % DCFDA positive cells
0.0
1.0
2.0
3.0
4.0
5.0
6.0
7.0
*
*
#
*
Vector
Rrm2
Rrm2-Y177W
Rrm2-Y370W
Ras

ROS production (2.9 fold increase compared to vector cells, p=0.051, t-test), which is in consistent with the highest *Hprt* mutation frequency observed in *Rrm2-Y370W* cells (Figure 3.4 C), further implicating elevated radical production, rather than increased RNR enzyme activity, as the major driving force of RNR-induced mutagenesis, and potentially, lung tumorigenesis.

### 3.4.6 Increased ROS levels in a Rrm2 mutant that is defective for radical production.

To directly test whether free radical formation is required for RNR-induced mutagenesis and lung tumorigenesis, we generated two additional *Rrm2* mutants to distinguish the role between RNR enzyme activity and radical production activity (Fig. 3.3).

A second mutation at the tyrosyl radical site, in which tyrosine residue is replaced by non-oxidizable phenylalanine, the *Rrm2-Y177F* mutant, has been shown to suppress the radical formation and completely destroy RNR enzyme activity (Potsch et al., 1999). A second mutation at the tyrosine 370 residue on the radical transfer path between the Rrm2 and Rrm1 subunit, in which tyrosine residue is replaced by non-oxidizable phenylalanine, *Rrm2-Y370F*, has been shown to be complete inactive for RNR enzyme activity, but the initial tyrosyl radical at residue 177 is intact (Rova et al., 1999). We generated *Rrm2-Y177F* and *Rrm2-Y370F* mutant constructs using site-directed mutagenesis and cloned them into same expression vector used for generating RNR overexpressing 3T3 cells and RNR transgenic mice. We then generated *Rrm2-Y177F* mutant and *Rrm2-Y370F* mutant overexpressing 3T3 cell pools as described in Material and Methods. Overexpression of individual Rrm2 mutant genes in these cells was confirmed by Western blot (Fig. 3.6A). The cells

overexpressing wildtype Rrm2, Rrm2-Y177F or Rrm2-Y370F mutants had similar proliferation rates as compared to cells expressing empty vector (Fig. 3.6B)

We predicted that cells overexpressing the *Rrm2-Y177F* mutant would not have increased ROS production, but cells overexpressing *Rrm2-Y370F* would, if increased ROS production in *Rrm2* overexpressing cells is dependent on radical production at the tyrosine Y177 site. Cells overexpressing wildtype *Rrm2* again showed a 2.3 fold increase in ROS levels compared to vector cells ($p=0.08$, t-test)(Fig. 3.6B). As we predicted, cells overexpressing *Rrm2-Y370F* mutant showed a 3.5 fold increase in ROS levels compared to that in vector cells ($p<0.05$, t-test). Surprisingly, cells overexpressing *Rrm2-Y177F*, defective for both enzyme activity and radical production, also showed increased ROS production (2.5 fold compared to vector cells, $p<0.05$, t-test). These data suggest that cells overexpressing *Rrm2-Y177F* mutant still cause increased oxidative stress, probably through other mechanisms, such as a dominant negative effect by binding to Rrm1 and indirectly inhibiting RNR function of providing dNTPs for mitochondria, causing mitochondria defect and increased oxidative stress. To test whether RNR-induced mutagenesis depends on the radical production activity, we are going to measure mutation frequency in Rrm2-Y177F mutant cells using *Hprt* mutation detection assay.

Figure 3.6. Increased reactive oxygen species levels in Rrm2 mutant overexpressing cells. (A) Western blot analysis of Rrm2 protein expression in 3T3 cells overexpressing *Rrm2-Y177F, Rrm2-Y370F* mutants. Total protein was extracted from the indicated cell lines and subjected to immunoblotting with antibodies specific to Rrm2. Membrane was re-probed for α-tubulin as a loading control. Samples were run on a single blot, which was then cropped to remove extraneous lanes. (B) Accumulated population doublings (PDL) of 3T3 cells overexpressing *Rrm2, Rrm2-Y177F, Rrm2-Y370F* or empty plasmid vector. Cells were cultured following a 3T3 culture schedule as described in Material and Methods. Plot shows the number of PDL. (C) Intracellular ROS levels in 3T3 cells overexpressing *Rrm2, Rrm2-Y177F, Rrm2-Y370F* or empty plasmid vector assessed by FACs analysis of $CH_3$-DCFDA fluorescence. Each data point is mean of three independent experiments with error bars representing the standard deviations. * Statistically significant difference ($p< 0.05$) relative to control vector cells by student t –test. # $p=0.08$; § $p=0.09$.

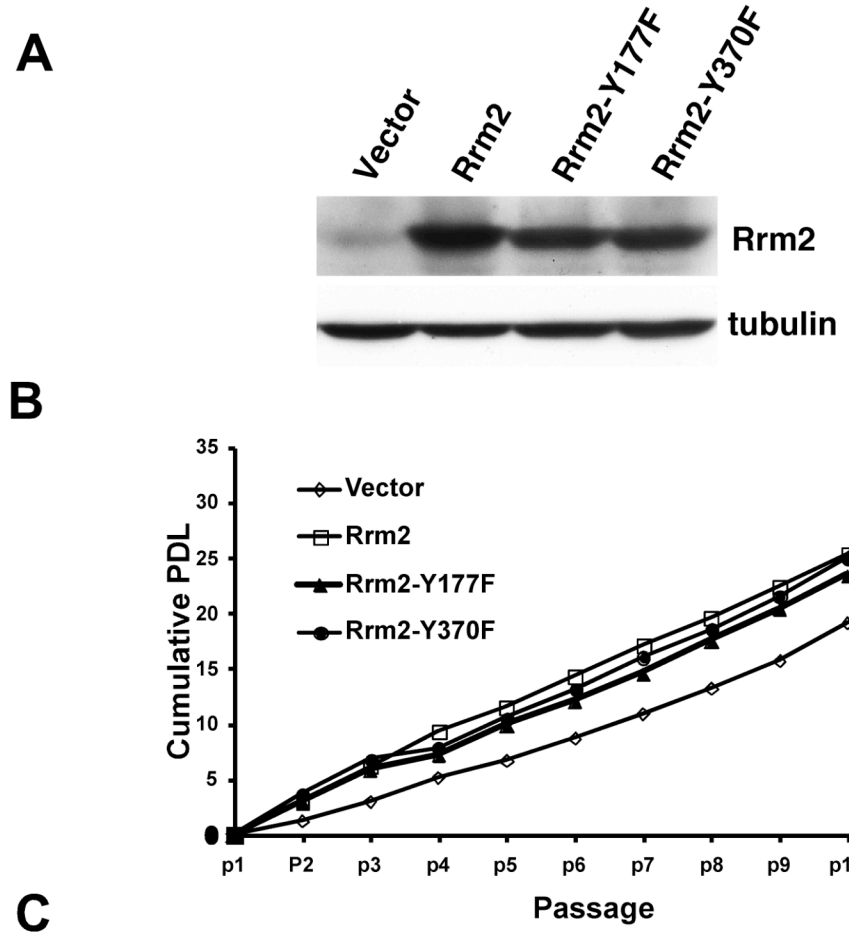
A
Vector
Rrm2
Rrm2-Y177F
Rrm2-Y370F
Rrm2
tubulin
B
Cumulative PDL
35
30
25
20
15
10
5
0
Vector
Rrm2
Rrm2-Y177F
Rrm2-Y370F
p1
P2
p3
p4
p5
p6
p7
p8
p9
p10
p11
Passage
C
Fold increase over vector in % DCFDA positive cells
6
5
4
3
2
1
0
#
*
*
§
Vector
Rrm2
Rrm2-Y177F
Rrm2-Y370F
Ras

## 3.5. **Discussion**

RNR overexpression is common in human cancers. However, up-regulation of RNR has long been thought of to act passively as a very downstream target of transforming pathway by solely providing dNTPs for cancer cell hyper-proliferation. Although deregulation of RNR has been shown to promote genetic instability in yeast and cell culture models (Caras and Martin, 1988; Chabes et al., 2003a; Reichard et al., 2000), the role of RNR deregulation in cancer initiation and progression in mouse models and human cancers had not been explored. We recently extended the analysis of RNR deregulation in transgenic mouse models and identified a novel oncogenic activity of RNR in lung specific tumorigenesis (Xu et al., 2008). We found that broadly overexpressing the small RNR subunits, *Rrm2* and *p53R2,* specifically causes lung carcinogenesis through a mutagenic mechanism. The key question we addressed in this study is what is the molecular mechanism of RNR-induced mutagenesis and lung tumorigenesis. Here we showed that RNR-induced mutagenesis and lung tumorigenesis were neither associated with detectable alterations in dNTP pool size/ratios, nor direct transforming activity. Interestingly, Rrm2 overexpressing cells exhibited significantly elevated ROS levels . Moreover, cells overexpressing mutant Rrm2 proteins, defective for RNR enzyme activity, exhibited enhanced mutagenesis and elevated ROS generation. Our results establish the causative role of RNR deregulation in elevated ROS production and enhanced mutagenesis, implying that free radical generation by RNR is sufficient for mutagenesis, which may be independent of RNR enzyme activity.

Although both p53R2 and Rrm2 have radical production activity, one *in vitro* study showed that p53R2 recombinant protein had anti-oxidant property (Xue et al.,

2006). It is possible that, unlike Rrm2, p53R2 might drive lung tumor development through a different unknown mechanism rather than oxidative stress, or p53R2 protein also produce free radical *in vivo* and drives lung tumorigenesis through oxidative stress. Mutagenic and carcinogenic analysis of p53R2 mutants that are defective for RNR enzyme activity or radical production activity will provide more insight into the role of oxidative stress in p53R2-induced lung tumorigenesis.

It is well known that free radicals let loose in the cell can cause oxidative damage to DNA, protein and lipids. RNR has long been conceived of an oxidant-generating enzyme, along with cytochrome c oxidase, NADPH oxidase and the cytochrome P450 system (O'Donnell et al., 1995). However, there is very little evidence directly demonstrating the oxidizing ability of RNR protein as an organic radical protein. One study reported that recombinant human RRM2 protein generated ROS *in vitro* in a cell free system, although recombinant p53R2 protein has been suggested to have antioxidant activity *in vitro* (Xue et al., 2006). Structural analysis of mouse Rrm2 protein showed that a hydrophobic channel to radical site in mouse Rrm2 is wider and makes the radical much more accessible to environment than *E.Coli* Rrm2 (Kauppi et al., 1996). Therefore, overexpression of mouse Rrm2 protein more likely cause increase oxidative stress due to the more accessible radicals. In our study, we provided the first direct evidence that overproduced ROS, probably at least partially due to overproduced free radicals in the R2 subunit of RNR, correlated with the enhanced mutagenesis caused by RNR overexpression. Since abundant evidence suggest that ROS plays an causative role in both human and mouse lung cancer development (Inoue et al., 1998; Le Marchand et al., 2002; Minowa et al., 2000; Sakumi et al., 2003; Tsuzuki et al., 2001; Xie et al., 2004), elevated ROS production and resultant enhanced mutagenesis due to RNR overexpression may explain why RNR transgenic mice, with widespread overexpression of RNR, specifically

developed lung but not other neoplasms at high frequency. The multiplicative increase in mutagenesis and lung carcinogenesis when combining RNR overexpression with mismatch repair deficiency also support increased ROS production as possible mechanisms since the mismatch repair system can suppresses the mutation accumulation due to oxidative DNA damage (Modrich, 2006; Slupphaug et al., 2003). ROS also have mitogenic effects on the cells and can play a direct role in neoplastic transformation (Irani et al., 1997). Cultured 3T3 cells overexpressing Mox1, a superoxide-generating oxidase, have transforming activity, exhibiting anchorage-independent growth and tumor formation in athymic mice (Suh et al., 1999).

To confirm that increased ROS production by overexpression of Rrm2 accounts for lung tumorigenesis, we are currently testing the effect of anti-oxidant treatment on Rrm2-induced lung tumorigenesis. N-acetylcysteine (NAC) is an aminothiol and synthetic precursor of intracellular cysteine and glutathione (GSH) and able to detoxify reactive free radicals through conjugation or reduction reaction. Anti-oxidant activity of NAC has been proposed to have antimutagenic and anticarcinogenic function (van Zandwijk, 1995). NAC has emerged as a most promising cancer chemopreventive agents, although 2-year supplement of NAC in lung cancer patients resulted in no benefit in terms of survival in clinic trials for NAC cancer prevention (van Zandwijk et al., 2000), which may be due to short period NAC intervention. In animal models, oral administration of NAC through diet has been found to prevent lung adenoma by carcinogens (De Flora et al., 1986). Our previous data showed that 100% of $Msh6^{-/-}Rrm2^{Tg}$ mice develop spontaneous lung neoplasms by 6 months of age. A mouse cohort consisting of $Msh6^{-/-}Rrm2^{Tg}$ mice and littermate controls are being established and treated with the anti-oxidant NAC in drinking water from the date of weaning to 6 months of age. This cohort will then be sacrificed

to assess whether NAC alleviates *Rrm2*-induced lung tumorigenesis. If NAC treatment can specifically reduce the lung tumor frequency, size and malignancy caused by *Rrm2* overexpression, these data will further strengthen the role of ROS production by the Rrm2 subunit in RNR-induced lung tumorigenesis. In addition, the role of ROS in RNR-induced lung tumorigenesis can also be confirmed by evaluating whether deficiency in base excision repair genes,*Ogg1* or *Mth1,* will accelerate RNR-induced lung tumor development by crossing RNR transgenic mice to *Ogg1* or *Mth1* knockout mice.

Whether free radical production is required for RNR-induced mutagenesis was not elucidated prior to our study. One assumption is that RNR overproduction leads to elevated dNTP pools, and this imbalance in dNTP pools accounts for RNR-induced mutagenesis. However, there is no convincing evidence for elevated dNTP pools caused by over-produced RNR enzyme in mammalian systems. Here we employed mutant Rrm2 proteins that have defective RNR enzyme activity to dissect the molecular mechanisms of RNR-induced mutagenesis and to distinguish the role of RNR enzyme activity and radical production activity in RNR-induced mutagenesis. Interestingly, cells overexpressing these mutants still exhibited a mutator phenotype, indicating that RNR induced mutagenesis is independent of RNR enzyme activity. Our observations imply that RNR overexpression drives lung specific tumorigenesis via increased ROS production and oxidative DNA damage, rather than via increased RNR enzyme activity. Consistent with this interpretation, mice overexpressing *Rrm1-D57N*, a mutant defective for dATP feedback inhibition and exhibiting hyperactive RNR enzyme activity, did not show obvious lung tumor predisposition as we observed in *Rrm2* and *p53R2* transgenic mice (Page JL and Weiss RS, unpublished data). These data support that RNR deregulation induces lung specific tumorigenesis independent of RNR enzyme activity and instead through increased free radical

production by overexpression of the small R2 subunit. Increased ROS levels in cells overexpressing wildtype *Rrm2* and *Rrm2-Y177W*, *Rrm2-Y370W* and *Rrm2-Y370F* mutants provide more direct evidence for this hypothesis. Further analysis of lung tumor development in transgenic mice overexpressing these Rrm2 mutants would confirm whether ROS-induced mutagenesis is responsible for lung carcinogenesis.

Surprisingly, cells overexpressing *Rrm2-Y177F*, which is defective for both RNR enzyme activity and tyrosyl radical production, still exhibited elevated ROS production. One possibility is that *Rrm2-Y177F* has a dominant negative effect through binding to the Rrm1 subunit to inhibit Rrm1 function. There is mounting evidence that Rrm1 and p53R2 form a complex to provide dNTPs for maintaining mitochondrial genome stability. Deficiency in p532R2 gene has been shown to cause severe mitochondrial DNA depletion in muscle (Bourdon et al., 2007). Thus, overexpressing *Rrm2-Y177F* may indirectly inhibit p53R2 function by competing with Rrm1 protein, causing mitochondrial dysfunction and a respiratory chain defect, and increased ROS production, which also raises the possibility that the *Rrm2* mutants that still can produce radicals but are defective for RNR enzyme activity might also have similar dominant negative effect. Analysis of mitochondrial function in Rrm2-Y177F mutant by Mitotracker (a probe specifically labeling mitochondria) staining, would clarify whether such a dominant negative mechanism occurs. The C-terminus of Rrm2 is involved in the binding of the R1 subunit (Nordlund and Eklund, 1993; Uppsten et al., 2006). Rrm2 mutants that are defective for both radical production and Rrm1 binding would circumvent this dominant negative effect.

The effect of RNR over-production on dNTP pool size in mammalian cells remains controversial. Various hydroxyurea-resistant cell lines containing a high level of overproduced R2 subunits exhibited no or only a modest increase in RNR activity and dNTP pools (Lin et al., 2007). In our study, we did not observe altered dNTP pool

size or ratios in RNR overexpressing 3T3 cells and RNR transgenic lung cells. These data support that mammalian cells have more strict dATP allosteric inhibition, which may be the major control of dNTP pool size. Therefore, overexpression of the small subunit of RNR may not lead to increased RNR enzyme activity due to feedback inhibition caused by increased dATP levels. However, we cannot rule out the possibility of a localized increase in dNTP pools due to subcellular dNTP compartmentalization, which is undetectable using currently available dNTP measurements. Moreover, other mechanisms, such as the control of other enzymes involved in de novo dNTP biosynthesis and the control of the salvage pathway of dNTP biosynthesis, may also play a role in keeping dNTP levels undisturbed in RNR overexpressing cells.

It has been proposed that Rrm2 has transforming activity based on the experiments showing that Rrm2 can cooperate with a variety of oncogenes to promote focus formation, anchorage-independent growth and tumor formation in syngeneic mice (Fan et al., 1998; Fan et al., 1996). In our study, we did not observe the enhanced focus formation when we co-transfected *Rrm2* with *H-ras* into 3T3 cells. This discrepancy may be due to different Rrm2 expressing constructs and different transformation methods; in our study, we used pCaggs expression constructs that place Rrm2 under the chicken β-actin promoter and cytomegalovirus enhancer regulatory sequence to get high levels of expression. We co-transfected H-ras with individual RNR genes, or vector (negative control) and c-Myc (positive control) into 3T3 cells. Previous studies used retrovirus expression constructs to overexpress Rrm2 and then transfected *H-ras* into established *Rrm2* expressing cells. Our results suggest that Rrm2 expressed from the pCaggs construct, cannot enhance *H-ras* induced focus formation. Thus, acute transforming activity probably does not account for RNR-induced mutagenesis and lung tumorigenesis.

Our findings not only elucidate the involvement of ROS production in *Rrm2*-induced mutagenesis, and potentially lung carcinogenesis, but also might have implications in the response of cancers to chemotherapeutic reagents. Inhibitors of Rrm2, such as hydroxyurea, have long been used as effective anti-cancer chemotherapy treatment. The molecular mechanism of hydroxyurea was identified long after its application; it has been thought to inhibit RNR enzyme activity through inactivation of the small R2 subunit by destruction of the tyrosyl free radical. Our findings suggest that anti-cancer effect of hydroxyurea might not be limited to the anti-proliferative effect of RNR inhibition, but may also be due to the inhibition of intracellular ROS production.

CHAPTER 4

## Summary and Future Directions

RNR plays an essential role in maintaining genomic stability by providing dNTPs, the basic building blocks of the genome, for DNA replication and repair. Abnormal expression of RNR has long been linked to human cancers, and studies in yeast and cultured cells show that deregulation of RNR is mutagenic. However the physiological effects of RNR deregulation in mammals have not been fully explored. The aim of this dissertation was to elucidate the physiological effect of RNR deregulation using transgenic mouse models (chapter 2) and to further dissect the molecular mechanisms of RNR-induced mutagenesis and lung tumorigenesis (chapter 3).

To determine the consequence of RNR deregulation in an animal model, we generated *Rrm1*, *Rrm2* and *p53R2* transgenic mice and obtained widespread, high level overexpression of the small RNR subunits, Rrm2 and p53R2, and the restricted overexpression of the large RNR subunit Rrm1 in transgenic mice. Notably, widespread overexpression of either small RNR subunit in mice specifically promotes lung tumorigenesis, with Rrm2 being more potent than p53R2 with respect to tumor size, multiplicity and malignancy. The lung neoplasms in $Rrm2^{Tg}$ and $p53R2^{Tg}$ mice histopathologically and immunohistochemically mimic human lung cancer, particularly lung adenocarcinomas. These finding raise the possibility that increased RNR expression may have a role in human lung tumorigenesis.

To investigate the mechanism by which RNR deregulation causes lung tumorigenesis, we generated RNR overexpressing 3T3 cells and found that RNR overexpression is mutagenic in cultured cells. To evaluate a role for mutagenesis in

RNR-induced lung carcinogenesis, we investigated whether combining RNR deregulation with a defect in the mismatch repair system would synergistically increase mutagenesis and tumorigenesis. We found that mismatch repair deficiency synergized with RNR overexpression to greatly increase mutagenesis and carcinogenesis. Our data support that mismatch repair normally suppresses the mutations induced by RNR de-regulation and further confirmed that RNR-induced lung tumorigenesis through a mutagenic mechanism.

A mutagenic mechanism implies that RNR overexpression triggers mutation accumulations in oncogenes or tumor suppressor genes, driving lung tumorigenesis. K-ras is frequently mutated in both human lung cancers and mouse lung cancers. We explored whether activating mutations of K-ras is involved in RNR-induced lung tumorigenesis and found that mutated *K-ras* is central to *Rrm2*- and *p53R2*-induced lung tumorigenesis.

A key question from this study is what is the molecular mechanism for mutagenesis and lung tumorigenesis induced by *Rrm2* and *p53R2* overexpression. One possibility is that RNR overexpression leads to altered dNTP levels that impair replication fidelity and trigger mutations in growth regulatory genes. A second possibility is that the small RNR subunit has direct transforming activity, driving lung tumorigenesis. Alternatively, free radical production by Rrm2 or p53R2 contributes to cell transformation through oxidative stress induced mutagenesis. Thus, we propose the initial model for lung tumorigenesis by RNR overexpression based on our findings in chapter 2 (Fig. 4.1). This model postulates that overexpression of the small RNR subunit leads to mutagenesis, through either altered dNTP levels and/or increased oxidative stress due to overproduced free radicals. The mutagenic effect of RNR overexpression results in mutations in growth regulatory genes, such as K-ras, driving lung neoplasm initiation

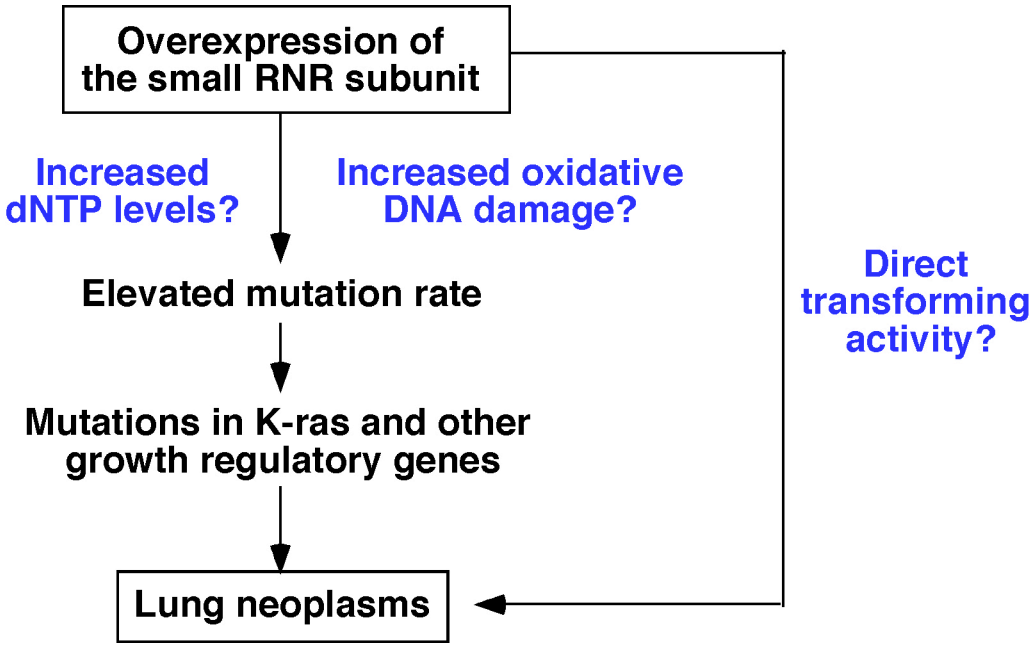


Figure 4.1. Initial model for RNR overexpression and lung cancer. Overexpression of the small RNR subunit leads to mutagenesis through either altered dNTP levels and/or increased oxidative stress due to overproduced free radicals. The mutagenic effect of RNR overexpression results in mutations in growth regulatory genes, such as K-ras, driving lung neoplasm initiation and /or progression. Alternatively, the small RNR subunit has direct transforming activity to transform normal lung cells into malignant cancer cells.

and /or progression. Alternatively, the small RNR subunit could have direct transforming activity through an unknown mechanism to transform normal lung cells into malignant cancer cells.

In chapter 3, we performed a series of experiments to address whether altered dNTP levels, RNR transforming activity, or increased oxidative stress are involved in RNR-induced mutagenesis and lung tumorigenesis.

RNR overexpression was not associated with detectable changes in dNTP levels or ratios in RNR overexpressing 3T3 cells and transgenic lung tissue, suggesting that RNR overexpression-induced mutagenesis and lung tumorigenesis might be not involved in altered dNTP levels or ratios. Moreover, RNR did not show direct transforming activity, nor enhanced transforming activity when co-transfected with *H-ras*, suggesting that RNR induced mutagenesis and lung carcinogenesis might not involve the direct transforming activity of RNR.

To determine whether radical production activity is involved in RNR-induced mutagenesis, we generated two Rrm2 mutant cell pools. The *Rrm2-Y177W* mutant, with a mutation at the tyrosyl radical site, has been shown to be defective for enzyme activity and to only produce a transient tryptophan radical. The *Rrm2-Y370W* mutant, with a mutations in the radical transfer path between Rrm2 and Rrm1 subunits, only has 1.7% of RNR enzyme activity compared to the wildtype Rrm2 protein. Both mutants are defective for RNR enzyme activity, but can still produce a transient tryptophan radical or the initial tyrosyl radical, respectively. Interestingly, cells overexpressing either mutant still exhibited enhanced mutagenesis, suggesting that Rrm2-induced mutagenesis likely is independent of RNR enzyme activity, but rather depends on its radical production activity.

Rrm2 overexpressing cells showed significantly higher intracellular ROS levels than control cells. Moreover, cells overexpressing Rrm2 mutants, also showed

increased ROS levels in agreement with their enhanced mutagenesis. Although it is possible that these Rrm2 mutants, which are able to produce radical but defective for RNR enzyme activity, also have dominant negative effect and cause mitochondrial defects and associated oxidative stress, these results highlight the importance of radical production, rather than RNR enzyme activity, as the major driving force of RNR induced mutagenesis, and potentially lung tumorigenesis.

Based on these findings, I propose a model for RNR-induced lung tumorigenesis as shown in Fig. 4.2. Overexpression of the small RNR subunit leads to mutagenesis through increased oxidative stress, likely due to overproduction of free radicals. The mutagenic effect of RNR overexpression results in mutations in growth regulatory genes, such as K-ras, driving lung neoplasm formation.

Ongoing experiments, testing whether anti-oxidant treatment will alleviate Rrm2-induced lung tumorigenesis in a mouse model, will further strengthen the role of oxidative stress in RNR-induced mutagenesis and lung tumorigenesis. In addition, analysis of mutations in p53R2 radical production site and radical transfer sites would provide more information about the role of the radical property of the small RNR subunit in mutagenesis and tumorigenesis. p53R2 shares 80% homology with Rrm2. The dinuclear iron center, the tyrosyl radical site, and the radical transfer pathway are all conserved between Rrm2 and p53R2. However, recombinant p53R2 protein has been suggested to have anti-oxidant activity in vitro (Xue et al., 2006).Analysis of similar mutants at tyrosyl radical site and radical transfer pathway of p53R2 would confirm that Rrm2 and p53R2 utilize the same mutagenic mechanism, such as increased ROS production by overproduced free radicals. Finally, analysis of whether repair of oxidative DNA damage by the base excision repair pathway suppresses RNR induced lung tumorigenesis by crossing RNR transgenic mice to mice defective for

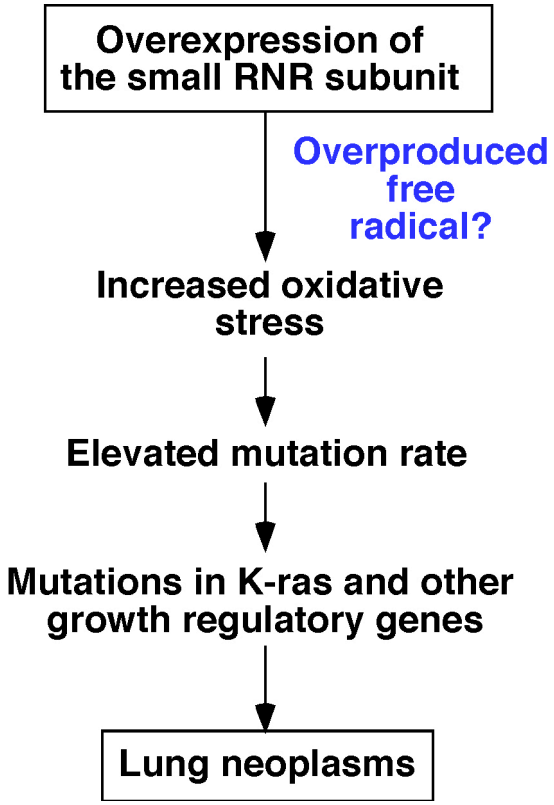


Figure 4.2. Current model for mechanisms of RNR overexpression and lung cancer. Overexpression of the small RNR subunit leads to mutagenesis through increase oxidative stress, possibly due to overproduced free radicals, and thereby enhanced mutagenesis. The mutagenic effect of RNR overexpression results in mutations in growth regulatory genes, such as K-ras, driving lung neoplasm formation.

repairing oxidative DNA damage would establish the significance of oxidative DNA damage in RNR-induced lung tumorigenesis.

This novel lung cancer model based on RNR overexpression holds great promise for further dissection of the molecular mechanisms of lung cancer initiation and progression. Interesting questions that can be addressed using this novel lung cancer model in future studies include 1) Are bronchioalveolar stem cells (BASCs), the putative lung cancer stem cells, more sensitive to RNR-induced mutagenesis and does BASCs expansion occur during early stage of RNR-induced lung tumorigenesis? To address this question, BASCs can be isolated from RNR transgenic mice at different development stage and mutation frequency of RNR overexpression BASCs cells can be measured using Hprt assay. 2) What are the other growth regulatory genes in addition to *K-ras* that are mutated and involved in RNR-induced lung tumors? Genetic alterations of other growth regulatory genes can be identified by sequence capture microarray analysis in RNR-induced lung tumors. 3) Are alterations in *RRM2* and *p53R2* genes (mutations or gene amplification) involved in human lung carcinogenesis? This question can be addressed by sequencing and in situ hybridization of human *RRM2* and *p53R2* genes in human lung cancer samples.

Aside from dissecting the mechanisms of lung cancer development, this novel mouse lung cancer model also can be used to test putative chemopreventive or chemotherapeutic agents in lung cancer prevention and treatment. It also has value as a model of lung cancer for imaging studies for micro-CT and multiphoton microscope, such as for computational assessment of lung tumor growth rate, tumor progression, and regression using micro-CT technology.

-

# BIBLIOGRAPHY

Akerblom, L., Ehrenberg, A., Graslund, A., Lankinen, H., Reichard, P., and Thelander, L. (1981). Overproduction of the free radical of ribonucleotide reductase in hydroxyurea-resistant mouse fibroblast 3T6 cells. Proc Natl Acad Sci U S A *78*, 2159-2163.

Alani, E., Cao, L., and Kleckner, N. (1987). A method for gene disruption that allows repeated use of URA3 selection in the construction of multiply disrupted yeast strains. Genetics *116*, 541-545.

Amara, F. M., Sun, J., and Wright, J. A. (1996). Defining a novel cis-element in the 3'-untranslated region of mammalian ribonucleotide reductase component R2 mRNA. cis-trans-interactions and message stability. J Biol Chem *271*, 20126-20131.

Angel, P., Imagawa, M., Chiu, R., Stein, B., Imbra, R. J., Rahmsdorf, H. J., Jonat, C., Herrlich, P., and Karin, M. (1987). Phorbol ester-inducible genes contain a common cis element recognized by a TPA-modulated trans-acting factor. Cell *49*, 729-739.

Bates, S. R., Gonzales, L. W., Tao, J. Q., Rueckert, P., Ballard, P. L., and Fisher, A. B. (2002). Recovery of rat type II cell surfactant components during primary cell culture. Am J Physiol Lung Cell Mol Physiol *282*, L267-276.

Bebenek, K., Roberts, J. D., and Kunkel, T. A. (1992). The effects of dNTP pool imbalances on frameshift fidelity during DNA replication. J Biol Chem *267*, 3589-3596.

Bepler, G., Gautam, A., McIntyre, L. M., Beck, A. F., Chervinsky, D. S., Kim, Y. C., Pitterle, D. M., and Hyland, A. (2002). Prognostic significance of molecular genetic aberrations on chromosome segment 11p15.5 in non-small-cell lung cancer. J Clin Oncol *20*, 1353-1360.

Bepler, G., Sharma, S., Cantor, A., Gautam, A., Haura, E., Simon, G., Sharma, A., Sommers, E., and Robinson, L. (2004). RRM1 and PTEN as prognostic parameters for overall and disease-free survival in patients with non-small-cell lung cancer. J Clin Oncol *22*, 1878-1885.

Bjorklund, S., Skog, S., Tribukait, B., and Thelander, L. (1990). S-phase-specific expression of mammalian ribonucleotide reductase R1 and R2 subunit mRNAs. Biochemistry *29*, 5452-5458.

Blasco, M. A., Lee, H. W., Hande, M. P., Samper, E., Lansdorp, P. M., DePinho, R. A., and Greider, C. W. (1997). Telomere shortening and tumor formation by mouse cells lacking telomerase RNA. Cell *91*, 25-34.

Bourdon, A., Minai, L., Serre, V., Jais, J. P., Sarzi, E., Aubert, S., Chretien, D., de Lonlay, P., Paquis-Flucklinger, V., Arakawa, H.*, et al.* (2007). Mutation of RRM2B, encoding p53-controlled ribonucleotide reductase (p53R2), causes severe mitochondrial DNA depletion. Nat Genet *39*, 776-780.

Burton, T. R., Kashour, T., Wright, J. A., and Amara, F. M. (2003). Cellular signaling pathways affect the function of ribonucleotide reductase mRNA binding proteins: mRNA stabilization, drug resistance, and malignancy (Review). Int J Oncol *22*, 21-31.

Caras, I. W., and Martin, D. W., Jr. (1988). Molecular cloning of the cDNA for a mutant mouse ribonucleotide reductase M1 that produces a dominant mutator phenotype in mammalian cells. Mol Cell Biol *8*, 2698-2704.

Ceppi, P., Volante, M., Novello, S., Rapa, I., Danenberg, K. D., Danenberg, P. V., Cambieri, A., Selvaggi, G., Saviozzi, S., Calogero, R.*, et al.* (2006). ERCC1 and RRM1 gene expressions but not EGFR are predictive of shorter survival in advanced non-small-cell lung cancer treated with cisplatin and gemcitabine. Ann Oncol *17*, 1818-1825.

Chabes, A., Domkin, V., Larsson, G., Liu, A., Graslund, A., Wijmenga, S., and Thelander, L. (2000). Yeast ribonucleotide reductase has a heterodimeric iron-radical-containing subunit. Proc Natl Acad Sci U S A *97*, 2474-2479.

Chabes, A., Georgieva, B., Domkin, V., Zhao, X., Rothstein, R., and Thelander, L. (2003a). Survival of DNA damage in yeast directly depends on increased dNTP levels allowed by relaxed feedback inhibition of ribonucleotide reductase. Cell *112*, 391-401.

Chabes, A., and Stillman, B. (2007). Constitutively high dNTP concentration inhibits cell cycle progression and the DNA damage checkpoint in yeast Saccharomyces cerevisiae. Proc Natl Acad Sci U S A *104*, 1183-1188.

Chabes, A., and Thelander, L. (2000). Controlled protein degradation regulates ribonucleotide reductase activity in proliferating mammalian cells during the normal cell cycle and in response to DNA damage and replication blocks. J Biol Chem *275*, 17747-17753.

Chabes, A. L., Bjorklund, S., and Thelander, L. (2004). S Phase-specific transcription of the mouse ribonucleotide reductase R2 gene requires both a proximal repressive E2F-binding site and an upstream promoter activating region. J Biol Chem *279*, 10796-10807.

Chabes, A. L., Pfleger, C. M., Kirschner, M. W., and Thelander, L. (2003b). Mouse ribonucleotide reductase R2 protein: a new target for anaphase-promoting complex-Cdh1-mediated proteolysis. Proc Natl Acad Sci U S A *100*, 3925-3929.

Chan, A. K., Litchfield, D. W., and Wright, J. A. (1993). Phosphorylation of ribonucleotide reductase R2 protein: in vivo and in vitro evidence of a role for p34cdc2 and CDK2 protein kinases. Biochemistry *32*, 12835-12840.

Chang, L., Zhou, B., Hu, S., Guo, R., Liu, X., Jones, S. N., and Yen, Y. (2008). ATM-mediated serine 72 phosphorylation stabilizes ribonucleotide reductase small subunit

p53R2 protein against MDM2 to DNA damage. Proc Natl Acad Sci U S A *105*, 18519-18524.

Chen, F. Y., Amara, F. M., and Wright, J. A. (1994). Defining a novel ribonucleotide reductase r1 mRNA cis element that binds to an unique cytoplasmic trans-acting protein. Nucleic Acids Res *22*, 4796-4797.

Chen, M., Rahman, L., Voeller, D., Kastanos, E., Yang, S. X., Feigenbaum, L., Allegra, C., Kaye, F. J., Steeg, P., and Zajac-Kaye, M. (2007a). Transgenic expression of human thymidylate synthase accelerates the development of hyperplasia and tumors in the endocrine pancreas. Oncogene *26*, 4817-4824.

Chen, S. H., Smolka, M. B., and Zhou, H. (2007b). Mechanism of Dun1 activation by Rad53 phosphorylation in Saccharomyces cerevisiae. J Biol Chem *282*, 986-995.

Chiba, I., Takahashi, T., Nau, M. M., D'Amico, D., Curiel, D. T., Mitsudomi, T., Buchhagen, D. L., Carbone, D., Piantadosi, S., Koga, H., and et al. (1990). Mutations in the p53 gene are frequent in primary, resected non-small cell lung cancer. Lung Cancer Study Group. Oncogene *5*, 1603-1610.

Cooperman, B. S., and Kashlan, O. B. (2003). A comprehensive model for the allosteric regulation of Class Ia ribonucleotide reductases. Adv Enzyme Regul *43*, 167-182.

De Flora, S., Astengo, M., Serra, D., and Bennicelli, C. (1986). Inhibition of urethan-induced lung tumors in mice by dietary N-acetylcysteine. Cancer Lett *32*, 235-241.

Deng, Z. L., Xie, D. W., Bostick, R. M., Miao, X. J., Gong, Y. L., Zhang, J. H., and Wargovich, M. J. (2005). Novel genetic variations of the p53R2 gene in patients with colorectal adenoma and controls. World J Gastroenterol *11*, 5169-5173.

Desany, B. A., Alcasabas, A. A., Bachant, J. B., and Elledge, S. J. (1998). Recovery from DNA replicational stress is the essential function of the S-phase checkpoint pathway. Genes Dev *12*, 2956-2970.

Droge, W. (2002). Free radicals in the physiological control of cell function. Physiol Rev *82*, 47-95.

Edelmann, W., Yang, K., Umar, A., Heyer, J., Lau, K., Fan, K., Liedtke, W., Cohen, P. E., Kane, M. F., Lipford, J. R.*, et al.* (1997). Mutation in the mismatch repair gene Msh6 causes cancer susceptibility. Cell *91*, 467-477.

Eklund, H., Uhlin, U., Farnegardh, M., Logan, D. T., and Nordlund, P. (2001). Structure and function of the radical enzyme ribonucleotide reductase. Prog Biophys Mol Biol *77*, 177-268.

Elford, H. L., Freese, M., Passamani, E., and Morris, H. P. (1970). Ribonucleotide reductase and cell proliferation. I. Variations of ribonucleotide reductase activity with tumor growth rate in a series of rat hepatomas. J Biol Chem *245*, 5228-5233.

Elledge, S. J., and Davis, R. W. (1990). Two genes differentially regulated in the cell cycle and by DNA-damaging agents encode alternative regulatory subunits of ribonucleotide reductase. Genes Dev *4*, 740-751.

Elledge, S. J., Zhou, Z., Allen, J. B., and Navas, T. A. (1993). DNA damage and cell cycle regulation of ribonucleotide reductase. Bioessays *15*, 333-339.

Engstrom, Y., Eriksson, S., Jildevik, I., Skog, S., Thelander, L., and Tribukait, B. (1985). Cell cycle-dependent expression of mammalian ribonucleotide reductase. Differential regulation of the two subunits. J Biol Chem *260*, 9114-9116.

Engstrom, Y., and Rozell, B. (1988). Immunocytochemical evidence for the cytoplasmic localization and differential expression during the cell cycle of the M1 and M2 subunits of mammalian ribonucleotide reductase. Embo J *7*, 1615-1620.

Engstrom, Y., Rozell, B., Hansson, H. A., Stemme, S., and Thelander, L. (1984). Localization of ribonucleotide reductase in mammalian cells. Embo J *3*, 863-867.

Eriksson, S., Graslund, A., Skog, S., Thelander, L., and Tribukait, B. (1984). Cell cycle-dependent regulation of mammalian ribonucleotide reductase. The S phase-correlated increase in subunit M2 is regulated by de novo protein synthesis. J Biol Chem *259*, 11695-11700.

Fan, H., Huang, A., Villegas, C., and Wright, J. A. (1997). The R1 component of mammalian ribonucleotide reductase has malignancy-suppressing activity as demonstrated by gene transfer experiments. Proc Natl Acad Sci U S A *94*, 13181-13186.

Fan, H., Villegas, C., Huang, A., and Wright, J. A. (1998). The mammalian ribonucleotide reductase R2 component cooperates with a variety of oncogenes in mechanisms of cellular transformation. Cancer Res *58*, 1650-1653.

Fan, H., Villegas, C., and Wright, J. A. (1996). Ribonucleotide reductase R2 component is a novel malignancy determinant that cooperates with activated oncogenes to determine transformation and malignant potential. Proc Natl Acad Sci U S A *93*, 14036-14040.

Fenwick, R. G. (1985). The HGPRT system. In Molecular Cell Genetics, M. Gottesman, ed. (New York: Wiley), pp. 333-373.

Filatov, D., Bjorklund, S., Johansson, E., and Thelander, L. (1996). Induction of the mouse ribonucleotide reductase R1 and R2 genes in response to DNA damage by UV light. J Biol Chem *271*, 23698-23704.

Gautam, A., and Bepler, G. (2006). Suppression of lung tumor formation by the regulatory subunit of ribonucleotide reductase. Cancer Res *66*, 6497-6502.

Gautam, A., Li, Z. R., and Bepler, G. (2003). RRM1-induced metastasis suppression through PTEN-regulated pathways. Oncogene *22*, 2135-2142.

Gazdar, A. F. (2007). DNA repair and survival in lung cancer--the two faces of Janus. N Engl J Med *356*, 771-773.

Goeze, A., Schluns, K., Wolf, G., Thasler, Z., Petersen, S., and Petersen, I. (2002). Chromosomal imbalances of primary and metastatic lung adenocarcinomas. J Pathol *196*, 8-16.

Goswami, P. C., Sheren, J., Albee, L. D., Parsian, A., Sim, J. E., Ridnour, L. A., Higashikubo, R., Gius, D., Hunt, C. R., and Spitz, D. R. (2000). Cell cycle-coupled variation in topoisomerase IIalpha mRNA is regulated by the 3'-untranslated region. Possible role of redox-sensitive protein binding in mRNA accumulation. J Biol Chem *275*, 38384-38392.

Graff, P., Amellem, O., Andersson, K. K., and Pettersen, E. O. (2002). Role of ribonucleotide reductase in regulation of cell cycle progression during and after exposure to moderate hypoxia. Anticancer Res *22*, 59-68.

Guittet, O., Hakansson, P., Voevodskaya, N., Fridd, S., Graslund, A., Arakawa, H., Nakamura, Y., and Thelander, L. (2001). Mammalian p53R2 protein forms an active ribonucleotide reductase in vitro with the R1 protein, which is expressed both in resting cells in response to DNA damage and in proliferating cells. J Biol Chem *276*, 40647-40651.

Hakansson, P., Dahl, L., Chilkova, O., Domkin, V., and Thelander, L. (2006a). The Schizosaccharomyces pombe replication inhibitor Spd1 regulates ribonucleotide reductase activity and dNTPs by binding to the large Cdc22 subunit. J Biol Chem *281*, 1778-1783.

Hakansson, P., Hofer, A., and Thelander, L. (2006b). Regulation of mammalian ribonucleotide reduction and dNTP pools after DNA damage and in resting cells. J Biol Chem *281*, 7834-7841.

Herrick, J., and Sclavi, B. (2007). Ribonucleotide reductase and the regulation of DNA replication: an old story and an ancient heritage. Mol Microbiol *63*, 22-34.

Ho, S. N., Hunt, H. D., Horton, R. M., Pullen, J. K., and Pease, L. R. (1989). Site-directed mutagenesis by overlap extension using the polymerase chain reaction. Gene *77*, 51-59.

Hoeijmakers, J. H. (2001). Genome maintenance mechanisms for preventing cancer. Nature *411*, 366-374.

Huang, A., Fan, H., Taylor, W. R., and Wright, J. A. (1997). Ribonucleotide reductase R2 gene expression and changes in drug sensitivity and genome stability. Cancer Res *57*, 4876-4881.

Inoue, M., Osaki, T., Noguchi, M., Hirohashi, S., Yasumoto, K., and Kasai, H. (1998). Lung cancer patients have increased 8-hydroxydeoxyguanosine levels in peripheral lung tissue DNA. Jpn J Cancer Res *89*, 691-695.

Irani, K., Xia, Y., Zweier, J. L., Sollott, S. J., Der, C. J., Fearon, E. R., Sundaresan, M., Finkel, T., and Goldschmidt-Clermont, P. J. (1997). Mitogenic signaling mediated by oxidants in Ras-transformed fibroblasts. Science *275*, 1649-1652.

Jakubczak, J. L., Merlino, G., French, J. E., Muller, W. J., Paul, B., Adhya, S., and Garges, S. (1996). Analysis of genetic instability during mammary tumor progression using a novel selection-based assay for in vivo mutations in a bacteriophage lambda transgene target. Proc Natl Acad Sci U S A *93*, 9073-9078.

Johansson, E., Hjortsberg, K., and Thelander, L. (1998). Two YY-1-binding proximal elements regulate the promoter strength of the TATA-less mouse ribonucleotide reductase R1 gene. J Biol Chem *273*, 29816-29821.

Johnson, L., Mercer, K., Greenbaum, D., Bronson, R. T., Crowley, D., Tuveson, D. A., and Jacks, T. (2001). Somatic activation of the K-ras oncogene causes early onset lung cancer in mice. Nature *410*, 1111-1116.

Jordan, A., and Reichard, P. (1998). Ribonucleotide reductases. Annu Rev Biochem *67*, 71-98.

Kashlan, O. B., and Cooperman, B. S. (2003). Comprehensive model for allosteric regulation of mammalian ribonucleotide reductase: refinements and consequences. Biochemistry *42*, 1696-1706.

Kauppi, B., Nielsen, B. B., Ramaswamy, S., Larsen, I. K., Thelander, M., Thelander, L., and Eklund, H. (1996). The three-dimensional structure of mammalian ribonucleotide reductase protein R2 reveals a more-accessible iron-radical site than Escherichia coli R2. J Mol Biol *262*, 706-720.

Ke, P. Y., Kuo, Y. Y., Hu, C. M., and Chang, Z. F. (2005). Control of dTTP pool size by anaphase promoting complex/cyclosome is essential for the maintenance of genetic stability. Genes Dev *19*, 1920-1933.

Kelekar, A., and Cole, M. D. (1987). Immortalization by c-myc, H-ras, and Ela oncogenes induces differential cellular gene expression and growth factor responses. Mol Cell Biol *7*, 3899-3907.

Keohavong, P., DeMichele, M. A., Melacrinos, A. C., Landreneau, R. J., Weyant, R. J., and Siegfried, J. M. (1996). Detection of K-ras mutations in lung carcinomas: relationship to prognosis. Clin Cancer Res *2*, 411-418.

Kimura, T., Takeda, S., Sagiya, Y., Gotoh, M., Nakamura, Y., and Arakawa, H. (2003). Impaired function of p53R2 in Rrm2b-null mice causes severe renal failure through attenuation of dNTP pools. Nat Genet *34*, 440-445.

Kolberg, M., Strand, K. R., Graff, P., and Andersson, K. K. (2004). Structure, function, and mechanism of ribonucleotide reductases. Biochim Biophys Acta *1699*, 1-34.

Kotova, I., Chabes, A. L., Lobov, S., Thelander, L., and Bjorklund, S. (2003). Sequences downstream of the transcription initiation site are important for proper initiation and regulation of mouse ribonucleotide reductase R2 gene transcription. Eur J Biochem *270*, 1791-1801.

Kunz, B. A. (1988). Mutagenesis and deoxyribonucleotide pool imbalance. Mutat Res *200*, 133-147.

Kunz, B. A., and Kohalmi, S. E. (1991). Modulation of mutagenesis by deoxyribonucleotide levels. Annu Rev Genet *25*, 339-359.

Kunz, B. A., Kohalmi, S. E., Kunkel, T. A., Mathews, C. K., McIntosh, E. M., and Reidy, J. A. (1994). Deoxyribonucleoside triphosphate levels: a critical factor in the maintenance of genetic stability. Mutat Res *318*, 1-64.

Lau, P. J., Flores-Rozas, H., and Kolodner, R. D. (2002). Isolation and characterization of new proliferating cell nuclear antigen (POL30) mutator mutants that are defective in DNA mismatch repair. Mol Cell Biol *22*, 6669-6680.

Le Marchand, L., Donlon, T., Lum-Jones, A., Seifried, A., and Wilkens, L. R. (2002). Association of the hOGG1 Ser326Cys polymorphism with lung cancer risk. Cancer Epidemiol Biomarkers Prev *11*, 409-412.

Lea, D. E., and Coulson, C. A. (1949). The distribution of numbers of mutants in bacterial populations. J Genet *49*, 264-285.

Lee, Y. D., and Elledge, S. J. (2006). Control of ribonucleotide reductase localization through an anchoring mechanism involving Wtm1. Genes Dev *20*, 334-344.

Lee, Y. D., Wang, J., Stubbe, J., and Elledge, S. J. (2008). Dif1 is a DNA-damage-regulated facilitator of nuclear import for ribonucleotide reductase. Mol Cell *32*, 70-80.

Lin, Z. P., Belcourt, M. F., Carbone, R., Eaton, J. S., Penketh, P. G., Shadel, G. S., Cory, J. G., and Sartorelli, A. C. (2007). Excess ribonucleotide reductase R2 subunits coordinate the S phase checkpoint to facilitate DNA damage repair and recovery from replication stress. Biochem Pharmacol *73*, 760-772.

Lin, Z. P., Belcourt, M. F., Cory, J. G., and Sartorelli, A. C. (2004). Stable suppression of the R2 subunit of ribonucleotide reductase by R2-targeted short interference RNA sensitizes p53(-/-) HCT-116 colon cancer cells to DNA-damaging agents and ribonucleotide reductase inhibitors. J Biol Chem *279*, 27030-27038.

Linnoila, R. I., Mulshine, J. L., Steinberg, S. M., and Gazdar, A. F. (1992). Expression of surfactant-associated protein in non-small-cell lung cancer: a discriminant between biologic subsets. J Natl Cancer Inst Monogr, 61-66.

Liu, C., Powell, K. A., Mundt, K., Wu, L., Carr, A. M., and Caspari, T. (2003). Cop9/signalosome subunits and Pcu4 regulate ribonucleotide reductase by both checkpoint-dependent and -independent mechanisms. Genes Dev *17*, 1130-1140.

Liu, X., Zhou, B., Xue, L., Shih, J., Tye, K., Qi, C., and Yen, Y. (2005). The ribonucleotide reductase subunit M2B subcellular localization and functional importance for DNA replication in physiological growth of KB cells. Biochem Pharmacol *70*, 1288-1297.

Lui, W. O., Tanenbaum, D. M., and Larsson, C. (2001). High level amplification of 1p32-33 and 2p22-24 in small cell lung carcinomas. Int J Oncol *19*, 451-457.

Ma, X. J., Salunga, R., Tuggle, J. T., Gaudet, J., Enright, E., McQuary, P., Payette, T., Pistone, M., Stecker, K., Zhang, B. M.*, et al.* (2003). Gene expression profiles of human breast cancer progression. Proc Natl Acad Sci U S A *100*, 5974-5979.

Maciag, A., and Anderson, L. M. (2005). Reactive oxygen species and lung tumorigenesis by mutant K-ras: a working hypothesis. Exp Lung Res *31*, 83-104.

Mahler, J. F., Stokes, W., Mann, P. C., Takaoka, M., and Maronpot, R. R. (1996). Spontaneous lesions in aging FVB/N mice. Toxicol Pathol *24*, 710-716.

Mann, G. J., Graslund, A., Ochiai, E., Ingemarson, R., and Thelander, L. (1991). Purification and characterization of recombinant mouse and herpes simplex virus ribonucleotide reductase R2 subunit. Biochemistry *30*, 1939-1947.

Mann, G. J., Musgrove, E. A., Fox, R. M., and Thelander, L. (1988). Ribonucleotide reductase M1 subunit in cellular proliferation, quiescence, and differentiation. Cancer Res *48*, 5151-5156.

Marsischky, G. T., Filosi, N., Kane, M. F., and Kolodner, R. (1996). Redundancy of Saccharomyces cerevisiae MSH3 and MSH6 in MSH2-dependent mismatch repair. Genes Dev *10*, 407-420.

Mathews, C. K. (2006). DNA precursor metabolism and genomic stability. Faseb J *20*, 1300-1314.

Miller, A. B., Altenburg, H. P., Bueno-de-Mesquita, B., Boshuizen, H. C., Agudo, A., Berrino, F., Gram, I. T., Janson, L., Linseisen, J., Overvad, K.*, et al.* (2004). Fruits and vegetables and lung cancer: Findings from the European Prospective Investigation into Cancer and Nutrition. Int J Cancer *108*, 269-276.

Mills, N. E., Fishman, C. L., Rom, W. N., Dubin, N., and Jacobson, D. R. (1995). Increased prevalence of K-ras oncogene mutations in lung adenocarcinoma. Cancer Res *55*, 1444-1447.

Minowa, O., Arai, T., Hirano, M., Monden, Y., Nakai, S., Fukuda, M., Itoh, M., Takano, H., Hippou, Y., Aburatani, H.*, et al.* (2000). Mmh/Ogg1 gene inactivation results in accumulation of 8-hydroxyguanine in mice. Proc Natl Acad Sci U S A *97*, 4156-4161.

Modrich, P. (2006). Mechanisms in eukaryotic mismatch repair. J Biol Chem *281*, 30305-30309.

Morrison, A., Johnson, A. L., Johnston, L. H., and Sugino, A. (1993). Pathway correcting DNA replication errors in Saccharomyces cerevisiae. Embo J *12*, 1467-1473.

Muller, W. J., Sinn, E., Pattengale, P. K., Wallace, R., and Leder, P. (1988). Single-step induction of mammary adenocarcinoma in transgenic mice bearing the activated c-neu oncogene. Cell *54*, 105-115.

Nakabeppu, Y., Tsuchimoto, D., Ichinoe, A., Ohno, M., Ide, Y., Hirano, S., Yoshimura, D., Tominaga, Y., Furuichi, M., and Sakumi, K. (2004). Biological significance of the defense mechanisms against oxidative damage in nucleic acids caused by reactive oxygen species: from mitochondria to nuclei. Ann N Y Acad Sci *1011*, 101-111.

Nakano, K., Balint, E., Ashcroft, M., and Vousden, K. H. (2000). A ribonucleotide reductase gene is a transcriptional target of p53 and p73. Oncogene *19*, 4283-4289.

Nikitin, A. Y., Alcaraz, A., Anver, M. R., Bronson, R. T., Cardiff, R. D., Dixon, D., Fraire, A. E., Gabrielson, E. W., Gunning, W. T., Haines, D. C.*, et al.* (2004). Classification of proliferative pulmonary lesions of the mouse: recommendations of the mouse models of human cancers consortium. Cancer Res *64*, 2307-2316.

Niwa, H., Yamamura, K., and Miyazaki, J. (1991). Efficient selection for high-expression transfectants with a novel eukaryotic vector. Gene *108*, 193-199.

Nordlund, P., and Eklund, H. (1993). Structure and function of the Escherichia coli ribonucleotide reductase protein R2. J Mol Biol *232*, 123-164.

Nordlund, P., and Reichard, P. (2006). Ribonucleotide reductases. Annu Rev Biochem *75*, 681-706.

O'Donnell, V. B., Spycher, S., and Azzi, A. (1995). Involvement of oxidants and oxidant-generating enzyme(s) in tumour-necrosis-factor-alpha-mediated apoptosis: role for lipoxygenase pathway but not mitochondrial respiratory chain. Biochem J *310 ( Pt 1)*, 133-141.

Parada, L. F., Tabin, C. J., Shih, C., and Weinberg, R. A. (1982). Human EJ bladder carcinoma oncogene is homologue of Harvey sarcoma virus ras gene. Nature *297*, 474-478.

Pei, J., Balsara, B. R., Li, W., Litwin, S., Gabrielson, E., Feder, M., Jen, J., and Testa, J. R. (2001). Genomic imbalances in human lung adenocarcinomas and squamous cell carcinomas. Genes Chromosomes Cancer *31*, 282-287.

Pitterle, D. M., Kim, Y. C., Jolicoeur, E. M., Cao, Y., O'Briant, K. C., and Bepler, G. (1999). Lung cancer and the human gene for ribonucleotide reductase subunit M1 (RRM1). Mamm Genome *10*, 916-922.

Pontarin, G., Ferraro, P., Hakansson, P., Thelander, L., Reichard, P., and Bianchi, V. (2007). p53R2-dependent ribonucleotide reduction provides deoxyribonucleotides in quiescent human fibroblasts in the absence of induced DNA damage. J Biol Chem *282*, 16820-16828.

Pontarin, G., Fijolek, A., Pizzo, P., Ferraro, P., Rampazzo, C., Pozzan, T., Thelander, L., Reichard, P. A., and Bianchi, V. (2008). Ribonucleotide reduction is a cytosolic process in mammalian cells independently of DNA damage. Proc Natl Acad Sci U S A *105*, 17801-17806.

Potsch, S., Lendzian, F., Ingemarson, R., Hornberg, A., Thelander, L., Lubitz, W., Lassmann, G., and Graslund, A. (1999). The iron-oxygen reconstitution reaction in protein R2-Tyr-177 mutants of mouse ribonucleotide reductase. Epr and electron nuclear double resonance studies on a new transient tryptophan radical. J Biol Chem *274*, 17696-17704.

Probst, H., Schiffer, H., Gekeler, V., and Scheffler, K. (1989). Oxygen dependent regulation of mammalian ribonucleotide reductase in vivo and possible significance for replicon initiation. Biochem Biophys Res Commun *163*, 334-340.

Radisky, D. C., Levy, D. D., Littlepage, L. E., Liu, H., Nelson, C. M., Fata, J. E., Leake, D., Godden, E. L., Albertson, D. G., Nieto, M. A.*, et al.* (2005). Rac1b and reactive oxygen species mediate MMP-3-induced EMT and genomic instability. Nature *436*, 123-127.

Rahman, I. (2003). Oxidative stress, chromatin remodeling and gene transcription in inflammation and chronic lung diseases. J Biochem Mol Biol *36*, 95-109.

Rahman, L., Voeller, D., Rahman, M., Lipkowitz, S., Allegra, C., Barrett, J. C., Kaye, F. J., and Zajac-Kaye, M. (2004). Thymidylate synthase as an oncogene: a novel role for an essential DNA synthesis enzyme. Cancer Cell *5*, 341-351.

Reenan, R. A., and Kolodner, R. D. (1992). Characterization of insertion mutations in the Saccharomyces cerevisiae MSH1 and MSH2 genes: evidence for separate mitochondrial and nuclear functions. Genetics *132*, 975-985.

Reichard, P. (1988). Interactions between deoxyribonucleotide and DNA synthesis. Annu Rev Biochem *57*, 349-374.

Reichard, P., Eliasson, R., Ingemarson, R., and Thelander, L. (2000). Cross-talk between the allosteric effector-binding sites in mouse ribonucleotide reductase. J Biol Chem *275*, 33021-33026.

Riboli, E., and Norat, T. (2003). Epidemiologic evidence of the protective effect of fruit and vegetables on cancer risk. Am J Clin Nutr *78*, 559S-569S.

Rodenhuis, S., Slebos, R. J., Boot, A. J., Evers, S. G., Mooi, W. J., Wagenaar, S. S., van Bodegom, P. C., and Bos, J. L. (1988). Incidence and possible clinical significance of K-ras oncogene activation in adenocarcinoma of the human lung. Cancer Res *48*, 5738-5741.

Rova, U., Adrait, A., Potsch, S., Graslund, A., and Thelander, L. (1999). Evidence by mutagenesis that Tyr(370) of the mouse ribonucleotide reductase R2 protein is the

connecting link in the intersubunit radical transfer pathway. J Biol Chem *274*, 23746-23751.

Sakumi, K., Tominaga, Y., Furuichi, M., Xu, P., Tsuzuki, T., Sekiguchi, M., and Nakabeppu, Y. (2003). Ogg1 knockout-associated lung tumorigenesis and its suppression by Mth1 gene disruption. Cancer Res *63*, 902-905.

Shao, J., Zhou, B., Chu, B., and Yen, Y. (2006). Ribonucleotide reductase inhibitors and future drug design. Curr Cancer Drug Targets *6*, 409-431.

Shao, J., Zhou, B., Zhu, L., Qiu, W., Yuan, Y. C., Xi, B., and Yen, Y. (2004). In vitro characterization of enzymatic properties and inhibition of the p53R2 subunit of human ribonucleotide reductase. Cancer Res *64*, 1-6.

Sherman, P. A., and Fyfe, J. A. (1989). Enzymatic assay for deoxyribonucleoside triphosphates using synthetic oligonucleotides as template primers. Anal Biochem *180*, 222-226.

Slupphaug, G., Kavli, B., and Krokan, H. E. (2003). The interacting pathways for prevention and repair of oxidative DNA damage. Mutat Res *531*, 231-251.

Smeds, J., Kumar, R., and Hemminki, K. (2001). Polymorphic insertion of additional repeat within an area of direct 8 bp tandem repeats in the 5'-untranslated region of the p53R2 gene and cancer risk. Mutagenesis *16*, 547-550.

Snyder, R. D. (1984). The role of deoxynucleoside triphosphate pools in the inhibition of DNA-excision repair and replication in human cells by hydroxyurea. Mutat Res *131*, 163-172.

Snyder, R. D. (1985). Effects of nucleotide pool imbalances on the excision repair of ultraviolet-induced damage in the DNA of human diploid fibroblasts. Basic Life Sci *31*, 163-173.

Souglakos, J., Boukovinas, I., Taron, M., Mendez, P., Mavroudis, D., Tripaki, M., Hatzidaki, D., Koutsopoulos, A., Stathopoulos, E., Georgoulias, V., and Rosell, R. (2008). Ribonucleotide reductase subunits M1 and M2 mRNA expression levels and clinical outcome of lung adenocarcinoma patients treated with docetaxel/gemcitabine. Br J Cancer *98*, 1710-1715.

Stubbe, J. (1994). Protein structure. Controlling radical reactions. Nature *370*, 502.

Suh, Y. A., Arnold, R. S., Lassegue, B., Shi, J., Xu, X., Sorescu, D., Chung, A. B., Griendling, K. K., and Lambeth, J. D. (1999). Cell transformation by the superoxide-generating oxidase Mox1. Nature *401*, 79-82.

Tanaka, H., Arakawa, H., Yamaguchi, T., Shiraishi, K., Fukuda, S., Matsui, K., Takei, Y., and Nakamura, Y. (2000). A ribonucleotide reductase gene involved in a p53-dependent cell-cycle checkpoint for DNA damage. Nature *404*, 42-49.

Thelander, L., and Berg, P. (1986). Isolation and characterization of expressible cDNA clones encoding the M1 and M2 subunits of mouse ribonucleotide reductase. Mol Cell Biol *6*, 3433-3442.

Tsuzuki, T., Egashira, A., Igarashi, H., Iwakuma, T., Nakatsuru, Y., Tominaga, Y., Kawate, H., Nakao, K., Nakamura, K., Ide, F.*, et al.* (2001). Spontaneous tumorigenesis in mice defective in the MTH1 gene encoding 8-oxo-dGTPase. Proc Natl Acad Sci U S A *98*, 11456-11461.

Uhlin, U., and Eklund, H. (1994). Structure of ribonucleotide reductase protein R1. Nature *370*, 533-539.

Uppsten, M., Farnegardh, M., Domkin, V., and Uhlin, U. (2006). The first holocomplex structure of ribonucleotide reductase gives new insight into its mechanism of action. J Mol Biol *359*, 365-377.

Uramoto, H., Sugio, K., Oyama, T., Hanagiri, T., and Yasumoto, K. (2006). P53R2, p53 inducible ribonucleotide reductase gene, correlated with tumor progression of non-small cell lung cancer. Anticancer Res *26*, 983-988.

van Zandwijk, N. (1995). N-acetylcysteine (NAC) and glutathione (GSH): antioxidant and chemopreventive properties, with special reference to lung cancer. J Cell Biochem Suppl *22*, 24-32.

van Zandwijk, N., Dalesio, O., Pastorino, U., de Vries, N., and van Tinteren, H. (2000). EUROSCAN, a randomized trial of vitamin A and N-acetylcysteine in patients with head and neck cancer or lung cancer. For the EUropean Organization for Research and Treatment of Cancer Head and Neck and Lung Cancer Cooperative Groups. J Natl Cancer Inst *92*, 977-986.

Weinberg, G., Ullman, B., and Martin, D. W., Jr. (1981). Mutator phenotypes in mammalian cell mutants with distinct biochemical defects and abnormal deoxyribonucleoside triphosphate pools. Proc Natl Acad Sci U S A *78*, 2447-2451.

Weiss, R. S., Enoch, T., and Leder, P. (2000). Inactivation of mouse Hus1 results in genomic instability and impaired responses to genotoxic stress. Genes Dev *14*, 1886-1898.

Wheeler, L. J., Rajagopal, I., and Mathews, C. K. (2005). Stimulation of mutagenesis by proportional deoxyribonucleoside triphosphate accumulation in Escherichia coli. DNA Repair (Amst) *4*, 1450-1456.

Wijnhoven, S. W., Kool, H. J., van Oostrom, C. T., Beems, R. B., Mullenders, L. H., van Zeeland, A. A., van der Horst, G. T., Vrieling, H., and van Steeg, H. (2000). The relationship between benzo[a]pyrene-induced mutagenesis and carcinogenesis in repair-deficient Cockayne syndrome group B mice. Cancer Res *60*, 5681-5687.

Wong, M. P., Fung, L. F., Wang, E., Chow, W. S., Chiu, S. W., Lam, W. K., Ho, K. K., Ma, E. S., Wan, T. S., and Chung, L. P. (2003). Chromosomal aberrations of primary lung adenocarcinomas in nonsmokers. Cancer *97*, 1263-1270.

Wright, J. A., Chan, A. K., Choy, B. K., Hurta, R. A., McClarty, G. A., and Tagger, A. Y. (1990). Regulation and drug resistance mechanisms of mammalian ribonucleotide reductase, and the significance to DNA synthesis. Biochem Cell Biol *68*, 1364-1371.

Wu, X., and Huang, M. (2008). Dif1 controls subcellular localization of ribonucleotide reductase by mediating nuclear import of the R2 subunit. Mol Cell Biol *28*, 7156-7167.

Xie, Y., Yang, H., Cunanan, C., Okamoto, K., Shibata, D., Pan, J., Barnes, D. E., Lindahl, T., McIlhatton, M., Fishel, R., and Miller, J. H. (2004). Deficiencies in mouse Myh and Ogg1 result in tumor predisposition and G to T mutations in codon 12 of the K-ras oncogene in lung tumors. Cancer Res *64*, 3096-3102.

Xu, X., Page, J. L., Surtees, J. A., Liu, H., Lagedrost, S., Lu, Y., Bronson, R., Alani, E., Nikitin, A. Y., and Weiss, R. S. (2008). Broad overexpression of ribonucleotide reductase genes in mice specifically induces lung neoplasms. Cancer Res *68*, 2652-2660.

Xue, L., Zhou, B., Liu, X., Qiu, W., Jin, Z., and Yen, Y. (2003). Wild-type p53 regulates human ribonucleotide reductase by protein-protein interaction with p53R2 as well as hRRM2 subunits. Cancer Res *63*, 980-986.

Xue, L., Zhou, B., Liu, X., Wang, T., Shih, J., Qi, C., Heung, Y., and Yen, Y. (2006). Structurally dependent redox property of ribonucleotide reductase subunit p53R2. Cancer Res *66*, 1900-1905.

Yamaguchi, T., Matsuda, K., Sagiya, Y., Iwadate, M., Fujino, M. A., Nakamura, Y., and Arakawa, H. (2001). p53R2-dependent pathway for DNA synthesis in a p53-regulated cell cycle checkpoint. Cancer Res *61*, 8256-8262.

Yanamoto, S., Kawasaki, G., Yoshitomi, I., and Mizuno, A. (2003). Expression of p53R2, newly p53 target in oral normal epithelium, epithelial dysplasia and squamous cell carcinoma. Cancer Lett *190*, 233-243.

Yao, R., Zhang, Z., An, X., Bucci, B., Perlstein, D. L., Stubbe, J., and Huang, M. (2003). Subcellular localization of yeast ribonucleotide reductase regulated by the DNA replication and damage checkpoint pathways. Proc Natl Acad Sci U S A *100*, 6628-6633.

You, M., Candrian, U., Maronpot, R. R., Stoner, G. D., and Anderson, M. W. (1989). Activation of the Ki-ras protooncogene in spontaneously occurring and chemically induced lung tumors of the strain A mouse. Proc Natl Acad Sci U S A *86*, 3070-3074.

Zhang, L. H., Vrieling, H., van Zeeland, A. A., and Jenssen, D. (1992). Spectrum of spontaneously occurring mutations in the hprt gene of V79 Chinese hamster cells. J Mol Biol *223*, 627-635.

Zhang, Z., An, X., Yang, K., Perlstein, D. L., Hicks, L., Kelleher, N., Stubbe, J., and Huang, M. (2006). Nuclear localization of the Saccharomyces cerevisiae ribonucleotide reductase small subunit requires a karyopherin and a WD40 repeat protein. Proc Natl Acad Sci U S A *103*, 1422-1427.

Zhao, X., Chabes, A., Domkin, V., Thelander, L., and Rothstein, R. (2001). The ribonucleotide reductase inhibitor Sml1 is a new target of the Mec1/Rad53 kinase cascade during growth and in response to DNA damage. Embo J *20*, 3544-3553.

Zhao, X., Muller, E. G., and Rothstein, R. (1998). A suppressor of two essential checkpoint genes identifies a novel protein that negatively affects dNTP pools. Mol Cell *2*, 329-340.

Zhao, X., and Rothstein, R. (2002). The Dun1 checkpoint kinase phosphorylates and regulates the ribonucleotide reductase inhibitor Sml1. Proc Natl Acad Sci U S A *99*, 3746-3751.

Zheng, Z., Chen, T., Li, X., Haura, E., Sharma, A., and Bepler, G. (2007). DNA synthesis and repair genes RRM1 and ERCC1 in lung cancer. N Engl J Med *356*, 800-808.

Zhou, B., Mo, X., Liu, X., Qiu, W., and Yen, Y. (2001). Human ribonucleotide reductase M2 subunit gene amplification and transcriptional regulation in a homogeneous staining chromosome region responsible for the mechanism of drug resistance. Cytogenet Cell Genet *95*, 34-42.

Zhou, B. S., Ker, R., Ho, R., Yu, J., Zhao, Y. R., Shih, J., and Yen, Y. (1998a). Determination of deoxyribonucleoside triphosphate pool sizes in ribonucleotide reductase cDNA transfected human KB cells. Biochem Pharmacol *55*, 1657-1665.

Zhou, B. S., Tsai, P., Ker, R., Tsai, J., Ho, R., Yu, J., Shih, J., and Yen, Y. (1998b). Overexpression of transfected human ribonucleotide reductase M2 subunit in human cancer cells enhances their invasive potential. Clin Exp Metastasis *16*, 43-49.

Zhou, Z., and Elledge, S. J. (1993). DUN1 encodes a protein kinase that controls the DNA damage response in yeast. Cell *75*, 1119-1127.